Ironmaking Process using Carbon Deposition by Chemical Vapor Infiltration (CVI) Method

(化学気相浸透(CVI)法による炭素析出を用いる製鉄プロセス)

Laboratory of Energy Media

Rochim Bakti CAHYONO

Hokkaido University

2015

Contents

Abstract

The consumption of iron and steel would increase in the near future to meet the rapid economic growth of several countries such as China, Indonesia, India, and Brazil. However, the iron and steel industry is facing serious problems related to limited resources, energy, and environment simultaneously due to high dependency on high-grade ore and coking coal. A proper strategy should be devised to explore innovative methods for substituting the conventional raw materials and energy resources.

The chemical vapor infiltration (CVI) ironmaking process consists of integrated pyrolysis-tar decomposition over a porous low-grade ore. This process was proposed to solve the aforementioned problems by effective utilization of low-grade coal and biomass. Tar that may cause operational problems such as pipe plugging, condensation, and tar aerosol formation is also resolved in this process. In this thesis, the proposed CVI system is comprehensively examined by discussing several important parameters such as various porous materials, different carbon sources, optimum temperature, kinetic analysis, and product microstructure. In addition, the overall evaluation of the proposed system is discussed on the basis of an exergy analysis to confirm the benefits of the system. The thesis consists of six chapters in which first and last chapters describe general introduction and conclusions, respectively.

Chapter 2 describes a detailed evaluation of the CVI ironmaking process using a low-grade ore as a carbon storage medium and catalyst for tar decomposition. The low-grade ore showed a significant effect on the tar decomposition process by enhancing carbon deposition and total gas product formation. The tar amount obtained from pyrolysis was strongly affected on carbon deposition. The bituminous, a high-grade coal produced the highest carbon deposition due to large tar product composition. A larger amount of combined water within the low-grade

ore resulted in pore size less than 4 nm, which was suitable for carbon deposition. The highest amount of carbon deposition was obtained when pyrolysis and tar decomposition were conducted at 800°C and 600°C, respectively. A higher temperature of tar decomposition resulted in lower carbon deposition owing to the gasification process. However, sintering started at 800°C and it significantly diminished the BET surface area of iron ore. Indirect reduction simultaneaously occurred with the decomposition process thereby producing Fe_3O_4 at 600°C and FeO at 800°C. The reduction of the CVI ore began at 750°C, while that of the reference, mixture of Fe_3O_4 and coke started at 1100°C. The CVI ore exhibited higher reactivity owing to nanoscale contact between the iron ore and carbon.

In chapter 3, the kinetic analysis and carbon deposition phenomenon of tar decomposition over the low-grade ore are examined to understand the CVI process. Both the kinetic constant and deactivation factor are evaluated successfully using a simple proposed model within the ranges 0.13–0.55 s^{-1} and 1.72–2.53 s^{-1}, respectively, at 500–700°C with the activation energy of 44.86 kJ/mol. The deactivation factor exhibited a similar tendency as the amount of carbon deposition within iron ore pores.

Chapter 4 includes a study of the characteristics of the CVI product related with the microstructure of the porous ore and distribution of carbon deposition. On the basis of TEM images, a layered structure containing ~3-nm-diameter pores was observed after dehydration owing to the removal of the hydroxide (OH) group from FeOOH. This pore size was deemed appropriate for tar decomposition and resultant carbon deposition. EDS results confirmed that carbon distribution was highest near the outer surface and decreased gradually with increasing depth in the inner section of ore. In addition to the ore structure, the type of carbon deposition was also successfully evaluated using Raman spectroscopy. The carbon deposition by the CVI

process within ore pores was categorized as amorphous carbon (a:C), with an sp3 content of 19–21%.

Chapter 5 describes the exergy analysis and presents a feasibility study on the applications of the CVI process in the ironmaking industry. The CVI process significantly increases the exergy content of iron ore. On the basis of 3.86 %mass carbon deposition (experimental value) and production of 1000 kg metallic Fe, the exergy loss of the proposed system was found to decrease by about 16.7% compared to that of conventional systems through the recovery of both chemical and thermal tar exergy. When the CVI ore was sent to a sinter plant, the amount of deposited carbon was sufficient to completely replace coke breeze in which the ratio of the CVI ore is above 70% of the total input ore. The total enthalpy of the CVI ore originated from the reoxidation of Fe_3O_4 and deposited carbon. The application of the CVI ore in a sinter plant would result in an extensive decrease of the coke breeze and CO_2 emissions.

On the basis of these results, it could be concluded that the proposed CVI ironmaking process offers promising benefits by alleviating the problems related to resource, energy, and environment simultaneously.

Chapter 1

General Introduction

1.1 Steel consumption and production

Iron and steel are the main constituents of many products used in modern daily life not only final product for direct consumption but also as raw material in further processing industry. Generally, the steel consumption has been highly considered to be linked to the economic growth which greatly affects other development activity such as construction, industrial equipment, transportation and daily consumption [1-5]. The steel consumption per capita has been used as barometer of the economic development and prosperity indicator of each country.

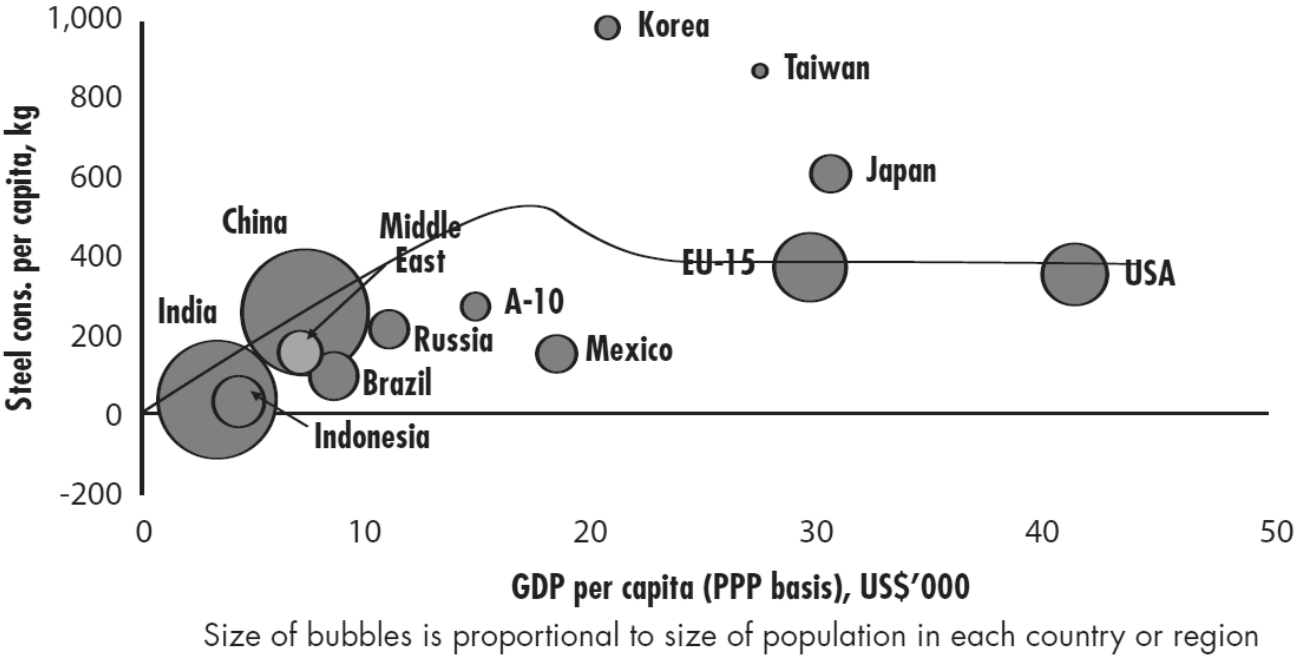

Fig. 1-1 Steel consumption and GDP per capita in selected countries [6-7]

Fig. 1-1 shows the relationship between steel consumption and income per capita in the selected countries in the world [6-7]. Obviously, the position of several developed industrial countries like USA, Japan and EU-15 is different with other countries that still developing theirs industrial sector. It means that steel consumption before industrialization both per capita or in absolute amount is lower compared to developed country. When the industrialization is started within the countries like China, Brazil, India and Indonesia, the steel consumption would be very intensive to construct the infrastructures such as ports, bridges, roads, airports, railways and industrial equipment. In case of Indonesia situation, the combination of large population, 220 million and low level of steel consumption per capita would force the increasing of steel consumption in this nation at least over the next decade [8-10].

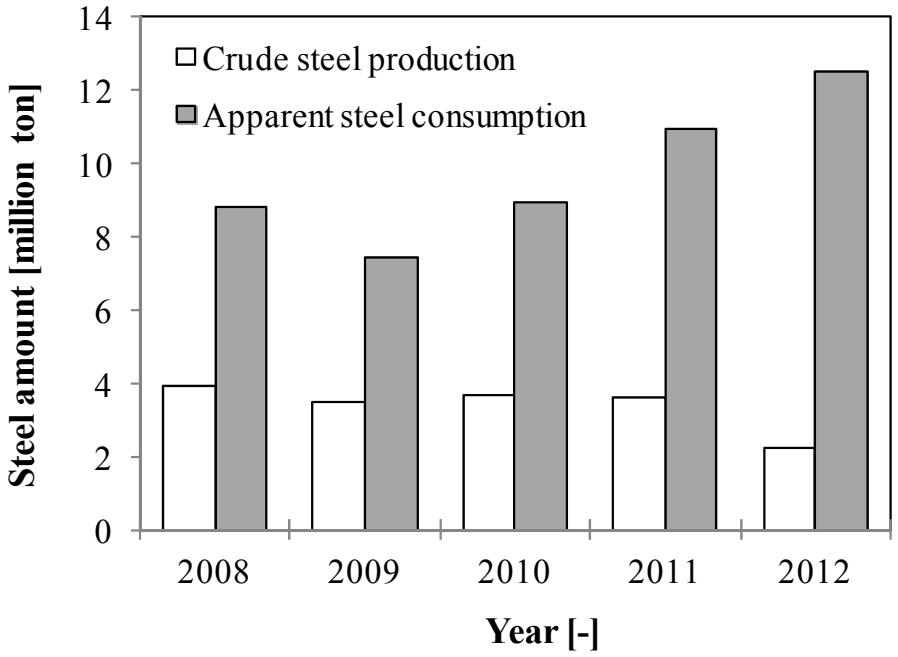

Data source: South East Asia Iron and Steel Institute (SEAISI) [11] and World steel association [12]

Fig. 1-2 Steel consumption and domestic production in Indonesia

This country owns essential natural resources such as low grade coal, natural gas, oil, biomass and low grade iron ore which are highly required for being developed country. Indonesia is one of the key players in the world as top exporter of coal and natural gas [13-15]. By good governance and human development program from the government, Indonesia would be potential industrial country in near future. In addition to consumption, the iron and steel industry in Indonesia is quite limited both amount and capacity to supply the steel demand such as Krakatau Steel, Krakatau POSCO and Krakatau Osaka Steel [16]. Fig. 1-2 shows the domestic crude steel production and apparent steel consumption in Indonesia. The consumption is rising due to good economic situation and industrialization while the domestic production is stable. The large gap between production and domestic production forces this country to import the steel product from prospective steel producers which come from Japan, China and Korea. Indonesia government issues some regulations related to natural resources, oil and gas that states explicitly for giving the priority of using those materials in domestic industry [17]. This condition would initiates rapid development for production sector in Indonesia especially iron and steel industry. Similar to Indonesia, other countries such as China, India and Brazil are also in the early step of industrialization. Therefore, the production of iron and steel would boost to meet the excessive consumption for rapid economic growth not only in Indonesia but also China, India and Brazil.

Nowadays, the worldwide iron and steel is produced by two main methods i.e. primary and secondary routes with the production sharing of 65% and 35%, respectively [18-19]. The primary consists of three steps: raw material preparation, ironmaking and steelmaking that use several materials such as iron ore, coking coal, limestone and small amount of recycled steel. In the preparation step, the coking coal is converted to coke in the coke oven facility by heating up the material in limited oxygen atmosphere. In addition, fine ore, limestone and coke breeze are

fed to sinter plant or pelletizing facility to produce sinter and pellet, respectively. Furthermore, the coke, sinter/pellet and limestone flux are sent to the top of blast furnace for reduction process and producing pig iron. By flowing heated air from the bottom, several reaction occur inside the blast furnace at temperature about 500-1700^{o}C as follow:

$$2C + O_2 \rightarrow 2CO \quad (1.1.1)$$

$$3Fe_2O_3 + CO \rightarrow Fe_3O_4 + CO_2 \quad (1.1.2)$$

$$Fe_3O_4 + CO \rightarrow FeO + CO_2 \quad (1.1.3)$$

$$FeO + CO \rightarrow Fe + CO_2 \quad (1.1.4)$$

$$FeO + C \rightarrow Fe + CO \quad (1.1.5)$$

The blast furnace ironmaking process produces pig iron and emits the wastes such as the blast furnace gas (BFG) and slag containing mainly CO_2 and flux material, respectively.

The pig iron is treated in the steelmaking process for producing raw steel material. Based on the principal process, the primary steel production could be divided into three basic different processes with a brief description as follow [20-22]:

a. Blast furnace (BF) – basic oxygen furnace (BOF)

   In the BOF process, the 70–90% melted pig iron and 10–30% steel scrap are charged into reactor vessel for steel production. The scrap is added to reduce the reactor temperature. The industrial oxygen is bown into the mixture and reacts with carbon inside iron through exothermic reaction. The process generates CO2 and decrease carbon content within product. This process contributes 66% of the worldwide steel production [23-24]

b. Blast furnace (BF) – open hearth furnace (OHF)

   The main role in OHF process is burning out the excess carbon and other impurities within pig iron to produce high quality of steel. This technology is applied in the beginning of steelmaking industry. Currently, the most OHF steelmaking industry was

closed due to fuel inefficiency and limited resources. Only small numbers are still exist in the East Europe such as Ukraine and supply around 3% of world steel production [23-24].

c. Direct reduction (DR) – electric arc furnace (EAF)

The fundamental process in EAF process is relied on scrap, not reducing of iron oxide. In the integrated process, the EAF process may be stand-alone operation due to raw material limitation. The EAF process proceeds by charging 100% recycled steel scrap melted by electrical energy using carbon electrodes. The carbon's role is not as dominant as it is in the blast furnace-OHF/BOF processes. This technology delivers about 6% of global steel production [23-24].

1.2 Ironmaking problems: Resource, Energy and Enviroment

The iron and steel production is highly depending on the nonrenewable material and fossil fuel as energy source. By excessive worldwide demand of iron and steel material in near future, this industry faces serious problems related to the resources, energy and environment.

a. Resources: coking coal and high grade iron ore

In order to produce 1 ton of pig iron, the typical ironmaking industry requires 525 kg of coking coal, 1390 kg of high grade ore and 120 kg of limestone [25-26]. The increasing of the steel production would force high demand of high grade iron ore and coking coal which in turn increasing their price in the market as shown in Fig. 1-3 (a). The price of high grade ore containing total Fe more than 60%mass is rising from 40 USD/ton in 2003 to 100 USD/ton in 2011[27].

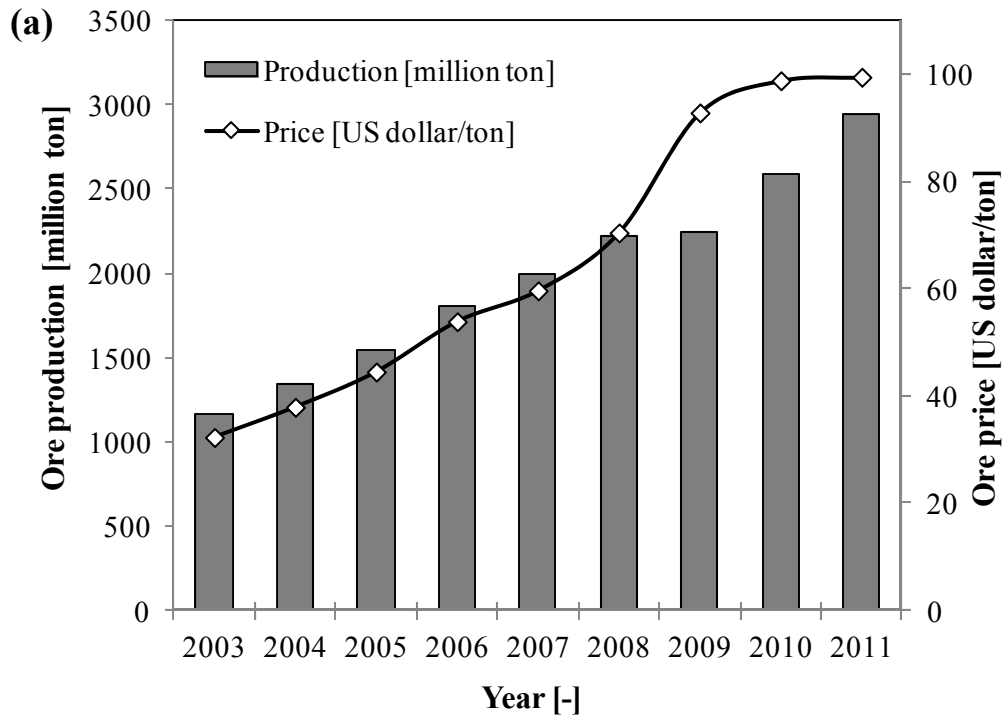

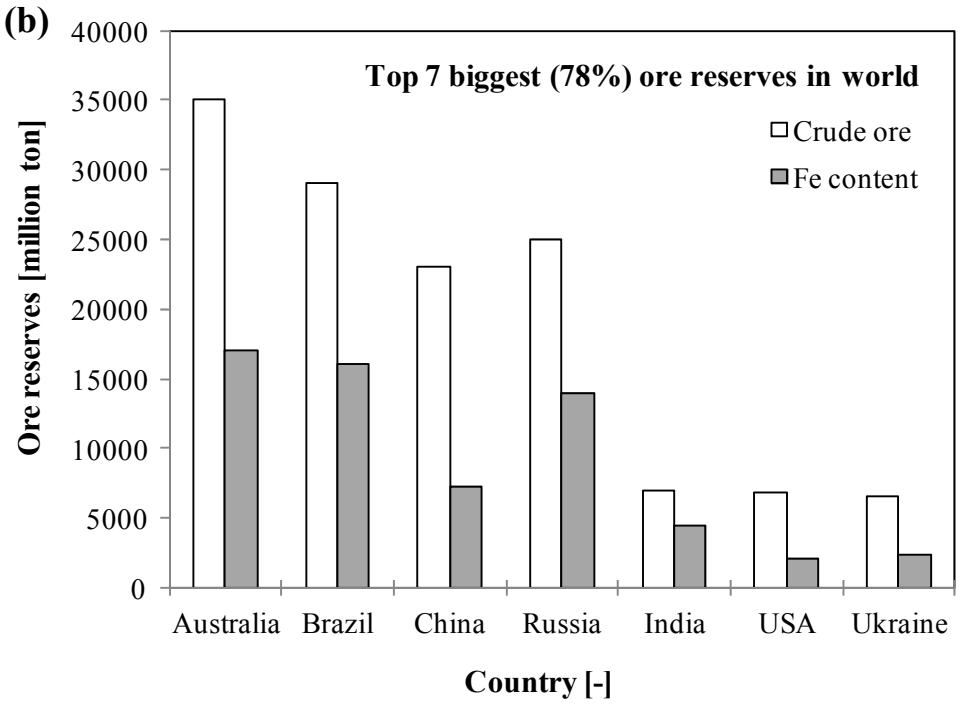

Data source: US Geological Survey (USGS) [28]

Fig. 1-3 (a) Iron ore production and price in the world, (b) The worldwide reserves of iron ore in the top 7 biggest countries.

The production of high grade iron ore is also increasing to realize the demand of steel company in the world which prefers to use it. Therefore, the alternative iron ore is highly necessitated to stabilize the price and to keep the sustainability of ironmaking industry. One of the promising candidates is low grade iron ore contains less than 60%mass of total Fe. The material is still available abundantly but ineffectively used due to the difficulty in the ore preparation as shown in the Fig. 1-3 (b). The reserves of iron ore in the world mostly contain of small of Fe content which originate from China, USA and Ukraine. When low-grade iron ores such as goethite ore are sent to a sinter machine or blast furnace, a large amount of energy is required to dehydrate the ore due to high content of combined water (CW).

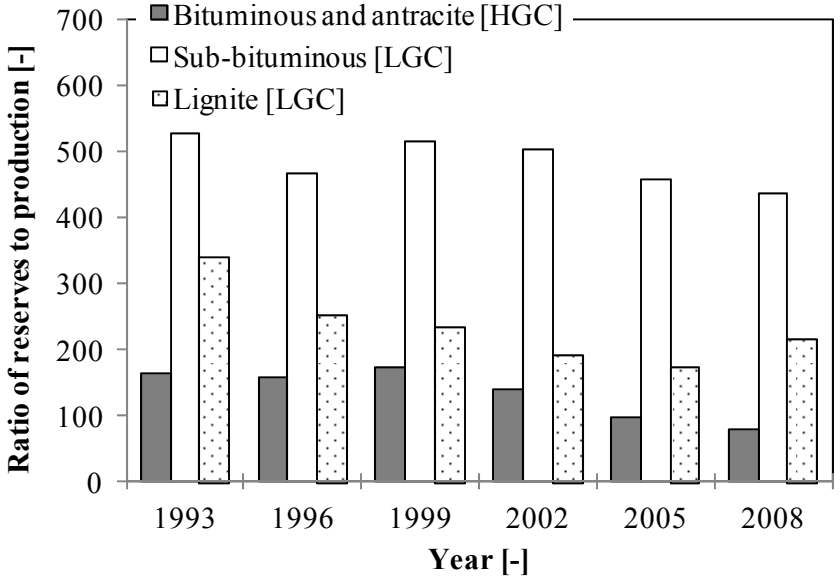

Data source: the institute of energy economics Japan (IEEJ) [29] and world energy council [30]

Fig. 1-4 The ratio of reserves to production for high grade coal (HGC) and low grade coal (LGC) in the world.

Beside high grade ore, the steel production is also excessively dependent on the coke which is produced from high rank coal such as bituminous. Approximately 71% of total steel was produced by iron ore reducing with coke and coal in the blast furnace [31-34]. The coke

plays important rules in blast furnace operation such as energy source, reducing agent of iron ore and to maintain bed permeability [35-37]. The price of coking coal is increasing due to the high consumption rate and limited resources. Fig. 1-4 shows the ratio of reserves to production of various coals in the world. The higher ratio indicates large availability and limited utilization. Obviously, the high grade coal hold lower ratio compared to low grade coal for both sub-bituminous and lignite. Therefore, to reduce the cost of energy for the raw material, low grade coal such as lignite and sub-bituminous coals which are cheaper and abundantly than high grade coal, should be used in the ironmaking process. In addition, utilization of biomass should also be introduced as much as possible in ironmaking industry to replace the coking coal. It is well known that many advantage of biomass utilization are carbon natural, renewable and abundant resources.

b. Energy: high consumption and less recovery

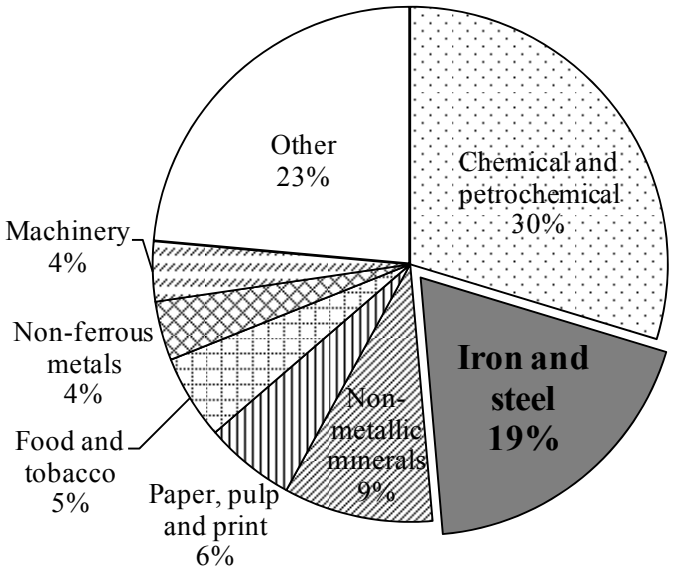

Data source: International Energy Agency (IEA) [38]

Fig. 1-5 the sharing of final energy consumption in the industry sector worldwide

High temperature process forces the steel industry as one of the most energy-intensive industries in the world which accounts for about 24 EJ per year, 19% of global industrial energy uses as shown in Fig. 1-5 [39-40]. The energy intensive of this industry largely depends on technology and which processes are used such as BF-OHF, BF-BOF, or EAF. The energy consumption of the ironmaking process contributes around 70% of the total energy consumption of iron and steel industry which blast furnace and coking processes expend largest part, 39% and 11.9% of energy, respectively [41]. It means that ironmaking system plays important role for any energy saving in this industry especially blast furnace and coking facilities.

In addition to energy consumption, the ironmaking industry faces other problem related to energy efficiency and recovery. The energy efficiency is linked to several parameters such as production capacity, technology and raw material quality. It is well known that large production capacity and advanced technology result higher energy efficiency. As biggest steel producer in the world, China owns steel industry with predominant of small production capacity. It cause that the energy efficiency of China's ironmaking industry is lower than in industrialized country such as US, Europe and Japan, for example 726 kg of coal equivalent per ton steel (kg-ce/t) in China compared to 646 kg-ce/t in developed country [42]. During iron and steel production, various level of waste heat is generated such as high temperature of slag, combustion gas which only small of the waste heat is recovered [43-44]. Several actions have been taken to improve energy efficiency during the process, such as process development and hot-slag energy recovery [45-46].

c. Environment: CO2 emission and handling waste

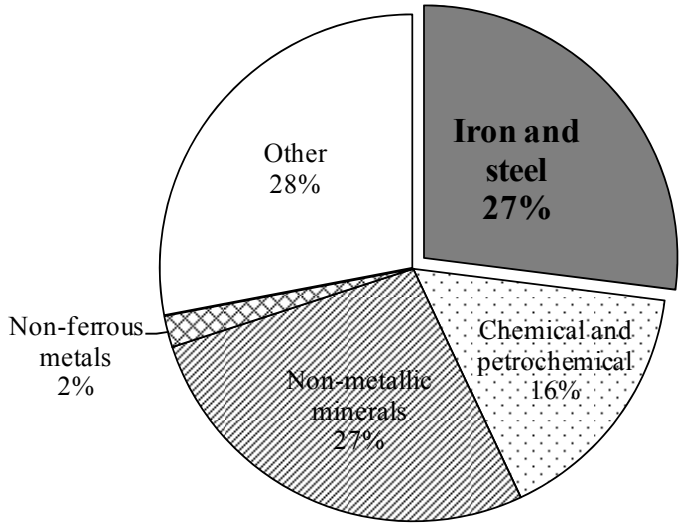

Total direct CO_2 emission : 9.7 Gt/year (36% world CO_2)

Data source: International Energy Agency (IEA) [38]

Fig. 1-6 the direct CO2 emission by industrial sector worldwide

The highly intensity of fossil fuels utilization causes this industry as biggest contributors to CO_2 emissions, it accounts as 27% of industrial CO2 emission or 4.6% of the total global as shown in Fig. 1-6 [47]. In order to produce 1 ton crude steel by iron ore reduction, this industry emits about average 2152 kg of CO2 [48]. CO2 emissions from iron and steel production are produced by the combustion of fossil fuels, the use of electrical energy, and the use of coal and lime as feedstock to reduce iron oxide to iron and later as an additive to strengthen steel. Several programs have been initiated worldwide to reduce fossil fuel utilization and CO_2 emissions, such as ULCOS in the EU, COURSE50 in Japan, and AISI in the USA [49-51]. In addition, a simple way to resolve emission concerns is to use biomass resources in the ironmaking industry.

1.3 Chemical Vapor Infiltration (CVI) method

Chemical Vapor Infiltration (CVI) is a unique process which matrix material is infiltrated into porous material using reactive gas at elevated temperature to form fiber-reinforced composites. This method is widely used to deposit solid materials like carbon, silicon carbide, boron nitride within porous material by the vapor decomposition for producing carbon-carbon composite as well as ceramic matrix composites [52-55]. CVI is an extension of Chemical Vapor Decomposition (CVD). The CVD involves the deposition onto a surface material while CVI implies the deposition within the porous material. Based on the figure in the literature [54], the CVI process typically consists of several steps as follow:

1. Gas penetration into the boundary layer from bulk gas
2. Gas diffusion into the pores of porous material
3. Gas adsorption onto the inner surface of the pore
4. Chemical reactions occurs and coating forms on the porous material
5. Desorption of gas by-products from the surface
6. Diffusion outwards of gas by-products
7. Gas by-product return to the bulk gas via boundary layer

Basically, the CVI process can be categorized into several groups based on the controlling parameter with a brief description as follow:

a. **Isothermal/isobaric CVI process**

   The reactant gas is supplied to the porous material at uniform pressure and temperature. In this process, the reaction is very slow due to small diffusion rate of reactant.

b. **Temperature gradient (TG-CVI)**

Temperature gradient occurs along the porous material at the gas vapor starts to diffuse from the hotter surface to cooler surface at the other side. The reactant gas decomposes mainly in the hotter surface due to high decomposition rate in elevated temperature.

c. **Thermal gradient-forced flow (F-CVI)**

Temperature gradient within porous material is achieved by heating the above part while the bottom part is cooled. Forced flows are determined by the difference in the pressure of the input and exhaust gases. By temperature difference and forced flow, the diffusion and decomposition of reactant gas are increased so that the densification time could be reduced.

d. Pulsed flow (P-CVI)

In this process, the gas pressure in the surrounding of porous material alters quickly. The CVI process occurs in several cycles which the changing of pressure is repeatable. In each cycle, the reactant gas is removed from CVI reactor and followed by its filling again.

Based on the typical process above, the material produced by CVI process would own several advantages compared to other composite production process such as [57-59]:

1. Low residual stress due to low infiltration temperature
2. Large, complex shape product could be produced in a near-net shape
3. Enhanced mechanical properties, corrosion resistance and thermal shock resistance
4. Various matrices can be fabricated
5. Very low fiber damage

Generally, it is well known that the reaction rate is closely related to the distance between reactants. The high reaction rate is resulted when the distance of those reactants is ultimate close each other. In case of ironmaking process, the reduction of iron ore to metallic iron highly depend on the distance of ore and carbon source as shown in Fig. 1-7 [60].

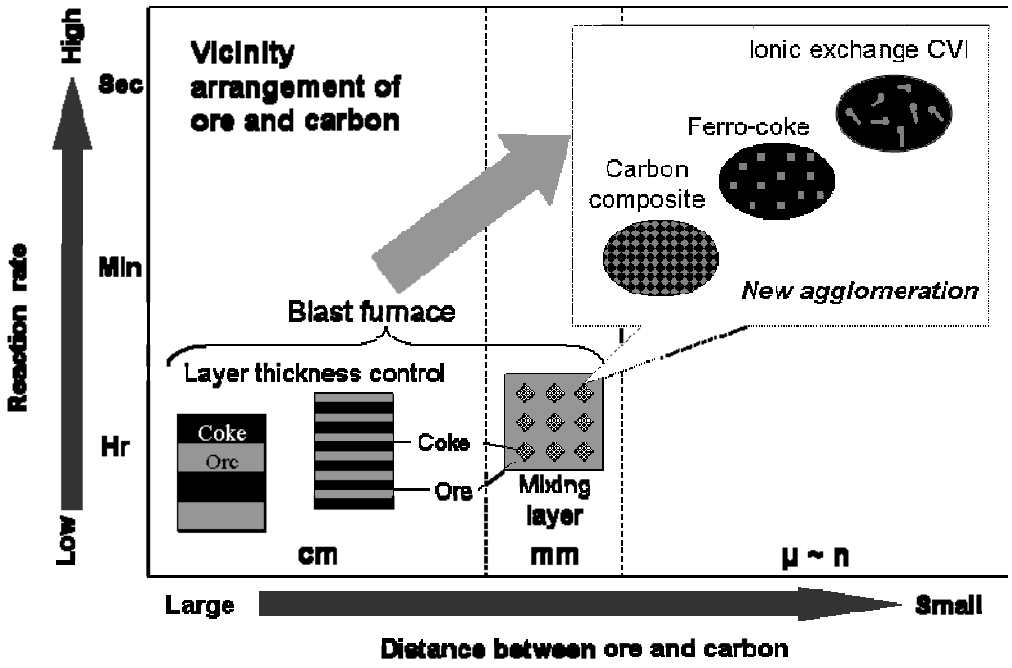

Fig. 1-7 Relationship between reaction rate and arrangement of iron ore and carbon

In the existing blast furnace operation, the iron ore and coke is adjusted to be layer by layer arrangement, thus the distance between iron ore and coke is about centimeter order which results low rate of reduction reaction. The new agglomeration processes are proposed such as carbon composite, ferro-coke and ionic exchange to reduce the distance between ore and carbon. As mentioned in the previous section, the CVI process can produce iron ore composite that the carbon deposits within pore of iron ore within nanometer order. Therefore, the reduction reaction of this composite is expected to be significant increased compared to conventional system.

1.4 Pyrolysis and tar decomposition

Pyrolysis is the rapid thermal decomposition of organic compounds in the absence of oxygen to produce char, liquid and gas. The product distribution depends on the solid fuel composition, heating rate and final temperature [61]. The typical pyrolysis process consists of several steps such as: softening, devolatilization-swelling, ignition-soot formation, gasification and fragmentation when the temperature is increased [62]. Based on the temperature and purpose, pyrolysis can be categorized into three groups [63]:

1. Slow pyrolysis

   The heating rate is quite slow, 0.1-2^{o}C/s and long residence time inside the reactor (hour). The main purpose is to produce solid product with high carbon content.

2. Fast pyrolysis

   In this process, the heating rate is quite fast, typically higher than 2^{o}C/s. The residence time of solid fuels within the reactor is very fast, in second order. Due to rapid devolatilization, the liquid product, tar is main target of this process.

3. Gasification

   The temperature process is quite high for carbon gasification which depends on the solid fuel characteristic. The major product is gas compared to the other group product.

Solid fuel is converted to char, tar, and gas through pyrolysis process in the ironmaking industry. Char is the main product used as a reducing agent, while tar vapor and gas are by-products generated during the process containing high amounts of carbon and energy. In the pyrolysis process, tar material may cause operational problems such as pipe plugging, condensation, and tar aerosol formation [64-66]. Complete conversion of tar into a major portion of the gaseous product inside the reactor system has been the most important engineering subject [67-69] since

it can greatly enhance the process efficiency and reduce the implementation/operating cost of the process. Several methods have been proposed for removing tar component to increase the gasification process such as absorption-adsorption and catalytic decomposition [70-71]. Chemical conversion through catalytic decomposition is more attractive because tar components can be converted into valuable products [72]. It is well known that complete decomposition of tar over several metal catalysts such as Ni, Pt, Rh, and Pd are promising method [73-76]. Nickel catalysts in various types have been obtained to be highly effective for tar decomposition process in coal or biomass pyrolysis. For example, the NiMo catalyst removed almost 100% of tar material which contains mostly of methylnaphthalene hydrocarbon at 500^{o}C [77]. However, there is still very serious problem related with catalyst deactivation due to carbon deposition. Aznar et al observes that the catalyst activity of typical nickel A is drop into 54% during 35 h experiment time [78]. Beside carbon deposition, high cost for raw material and regeneration method are another problems related to the conventional metal catalyst.

In order to solve their problem, different approach was proposed using certain material as catalyst that can still be used after the loss of activity. An example is the utilization of charcoal in the biomass pyrolysis for tar decomposition simultaneously and producing higher gas product [79-81]. The carbon deposition within charcoal resulted by tar decomposition increases total carbon content as well as heating value of charcoal. Therefore, the inactive iron ore catalyst could be excellent raw material in the ironmaking industry.

1.5 Scope of the present work

As a key industry in the world economic growth, the iron and steel industry is simultaneously facing crucial problems such as resource, energy and environment. Several candidates of raw materials are available to solve those problems such as utilization of low grade coal, biomass, and low rank iron ore which are abundantly and low price. In addition, carbon cycling and heat recovery technologies should be introduced as much as possible within the ironmaking industry. The proposed system in advanced is extremely required to apply these raw material and technologies simultaneously to ironmaking process

In order to solve the problems above, the following system which based on the CVI process of tar decomposition is proposed through this thesis.

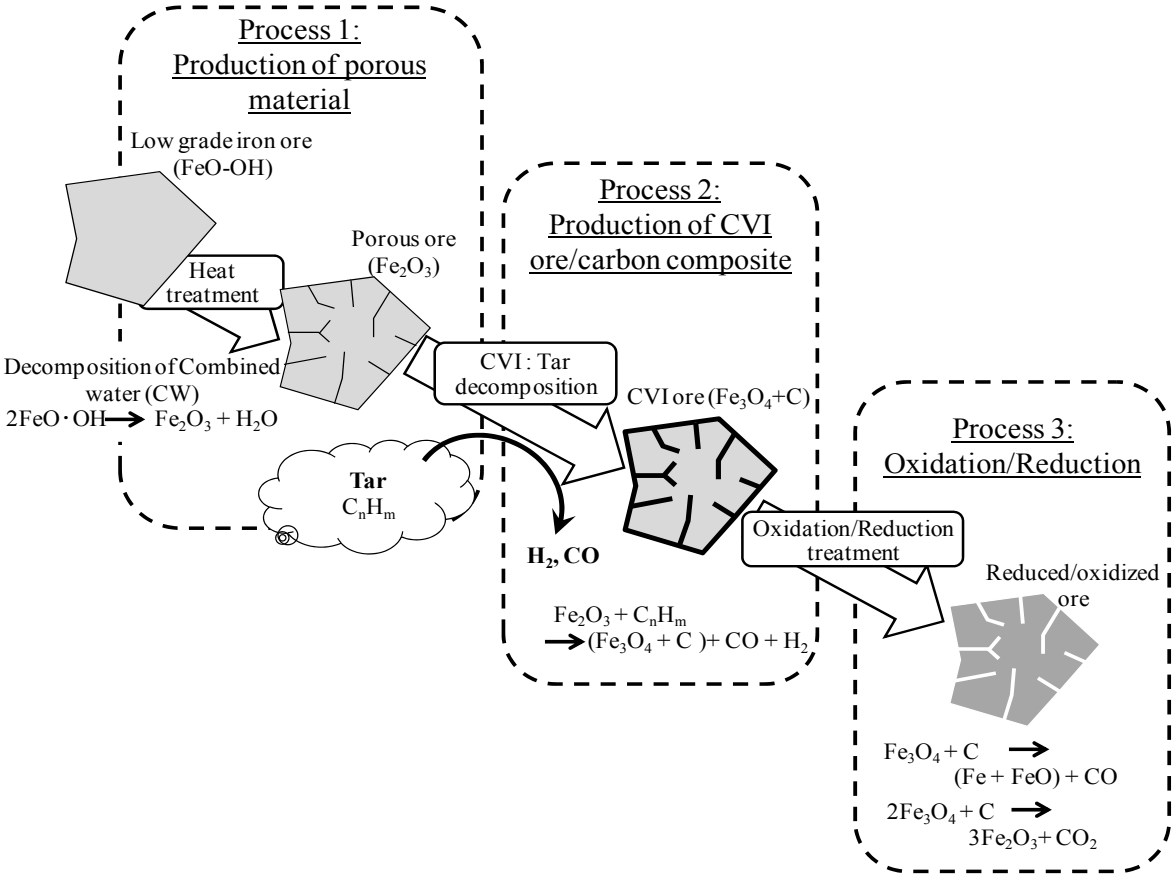

Fig. 1-8 The schematic diagram of CVI ironmaking

Fig. 1-8 shows the schematic diagram of the proposed process which is termed CVI ironmaking and consists of three main steps:

1. **Production of porous material**

   The low grade irons ore such as goethite and limonite (FeOOH) is still abundantly available but ineffectively used because of its high amount of combined water (CW). This is disadvantage due to large amount of energy required to remove CW but can generate porous material. In this step, the iron ore is subjected for dehydration process with slow heating rate at 450^{o}C in air atmosphere.

   $$2FeOOH(s) \leftrightarrow Fe_2O_3(s) + H_2O(g) \qquad (1.1)$$

   This process produces porous iron ore which could be utilized as carbon storage and catalyst of tar decomposition.

2. **Production of iron/carbon composite**

   The volatile matter, tar and pyrolysis gas are introduced to a porous iron ore for tar decomposition by CVI process. The tar vapor infiltrates and decomposes into gas and carbon within pore material according to the following reaction

   $$\text{Tar} \rightarrow H_2 + CO + CO_2 + CH_4 + \text{other light hydrocarbons} + C \qquad (1.2)$$

   When the gas product returns to gas bulk, the carbon will be deposited within iron ore pores to produce CVI ore. Because of the carbon deposited within pores, the distance between carbon and iron atoms was ultimately close.

3. **Reduction/Oxidation of CVI product**

   The CVI product contenting carbon deposition acts as a reducing agent or supplementary fuels in the next ironmaking process. In the case of reduction process, this material is expected to own higher reactivity due to shorter distance between carbon and iron atoms than that in a conventional blast furnace operation. This material is highly considered for supplementary fuels in sintering plant to reduce the usage of coke breeze.

The critical step in CVI ironmaking is the second step which produces of iron/carbon composite through CVI process. Therefore, this thesis would comprehensively examine in this step and characterize the product. In addition, the total evaluation of the proposed system is studied by energy analysis. The content of this thesis is divided into seven chapters as follow:

Chapter 1 presents the general introduction of this study.

Chapter 2 describes detail evaluation of CVI process using low grade ore as carbon storage and catalyst of tar decomposition. Several parameters are investigated such as different quality of solid fuels as carbon source, temperature and combined water content within the ore. The purpose of this chapter was also to obtain the optimum temperatures for both the pyrolysis and tar decomposition to produce highest carbon deposition. Moreover, the reactivity of CVI product in the reduction process was also examined.

In the chapter 3, the kinetic analysis of tar decomposition over low grade ore was evaluated and compared to other material in related experiment. In addition, the effect of carbon deposition within iron ore pores on tar decomposition was also discussed to further understand of CVI ironmaking process.

Chapter 4 studies the characteristic of the CVI product related to the microstructure of porous ore and distribution of carbon deposition. This section also assessed the type of carbon deposition

during the proposed process over porous iron ore, with various solid fuels used as a carbon source

Chapter 5 describes the feasibility study on the application and exergy analysis of CVI process in the ironmaking industry. The exergy analysis for producing of CVI ore using proposed system was discussed and compared to conventional method. In addition, the study of CVI ore utilization in sinter plants was discussed in terms of energy consumption and coke breeze usage.

Chapter 6 summarizes the results of this thesis as a general conclusion

References

[1] MC. Robert. Metal use and the world economy. Resources Policy 22 (1996): 183–196.

[2] B. Rehiasz. Polish steel consumption, 1974–2008. Resources Policy 31 (2006): 37–49.

[3] L. Warell and A. Olsson. Trends and developments in the Intensity of steel use: An Econometric Analysis. Securing the future and 8th ICARD, June 23-26 (2009). Skelleftea, Sweden

[4] KS. Huh. Steel consumption and economic growth in Korea: Long-term and short-term evidence. Resource policy 36 (2011): 107-113

[5] S. Ghosh. Steel consumption and economic growth: evidence from India. Resources policy 31 (2006): 7-11

[6] S. Sengupta and H. Beddows. The benefits of intergarted steel production in the Middle East. Direct from MIDREX 4th (2007): 3-6

[7] M. Walsh. Overview and outlook of global steel production. Steel Logistics conference (2007). London. Hatch Beddows.

[8] World Bank Data. 2013. http://data.worldbank.org/country/indonesia

[9] Badan Perencanaan Pembangunan Nasional, Badan Pusat Statistik, United Nations Population Funds. Indonesia population projection 2010-2035. Jakarta 2013.

[10] P. Crompton. Forecasting and consumption in South-East Asia. Resources Policy 31 (1999): 37–49.

[11] South East Asia Iron and Steel Institute (SEAISI). Apparent steel consumption of total steel products. Selangor Malaysia (2012)

[12] World steel association. Steel statistical yearbook 2012. Worldsteel Committee on Economic Studies. Brussels (2013)

[13] World Coal Associations. Global availability of coal. London (2011)

[14] International Energy Agency (IEA). World Energy Outlook. OECD/IEA. France (2011)

[15] MH. Hasan, TM Mahlia, H. Nur. A review on energy scenario and sustainable energy in Indoensia. Renewable and Sustainable Energy Reviews 16 (2012): 2316– 2328

[16] The structure and prospects of the Indonesia steel industry. 75th Steel Committee Meeting. OECD. Paris (2013)

[17] H. Nugroho, G. Hardjakoesoema, J. Setiawan, A. Hakim, M. Moechtar. Gas energy pricing in Indoneesia for promoting the sustainable economic growth. 19th World Energy Congress, Sidney, Australia (2004).

[18] World Steel Association, 2011. Steel statistical yearbook 2011

[19] International Energy Agency (IEA). Worldwide trends in energy use and efficiency: key insights from IEA indicator analysis (2008): 30-31

[20] M. Yellishetty, PG. Ranjith, A. Tharumarajah. Iron ore and steel production trends and material flow in the world: is this really sustainable? Resources, conservation and recycling 54 (2010): 1084-1094

[21] J. Farla and K. Blok. The quality of energy intensity indicators for international comparison in the iron and steel industry. Energy policy 29 (2001): 523-543

[22] L. Price, J. Sinton, E. Worrell, D. Phylipsen, H. Xiulian, L. Ji. Energy use and carbon dioxide emissions from steel production in China. Energy 27 (2002): 429-446

[23] E. Worrell, L. Prince, N. Martin, J. Farla, R. Schaeffer. Energy intensity in the iron and steel industry: a comparasion of physical and economic indicators. Energy policy 25 (1997): 727-744

[24] M. Larsson, C. Wang, J. Dahl. Development of a method for analyzing energy, environmental and economic efficiency for an integrated steel plant. Applied themal engineering 26 (2006): 1353-1361

[25] T. Akiyama and JI. Yagi. Methodology to evaluate reduction limit of carbon dioxide emission and minimum energy consumption for ironmaking. ISIJ International 38 (1998): 896-903

[26] H. Nogami, JI. Yagi, RS. Sampaio. Exergy analysis of charcoal charging operation of blast furnace. ISIJ International 44 (2004): 1646-1652

[27] F. Flues,D. Rübbelke, S. Vögele. Energy efficiency and industrial output: The case of the iron and steel industry. ZEW Discussion Papers No. 13-101 (2013)

[28] US. Geoligical survey. Iron ore. USGS, mineral commodity summaries (2003-2011)

[29] K. Morita. Coal trends: trends in coal supply, demand and prices as seem from statistics, is it true that economic development in Asia is impossible without low grade coal? IEEJ 13 (2013). November issue.

[30] World energy council. Survey of energy resources. London (1993-2008)

[31] M. Kirschen, K. Badr, H. Pfeifer, Influence of direct reduced iron on the energy balance of the electric arc furnace in steel industry, Energy 36 (2011) 6146–6155.

[32] World Steel Association. Fact sheet energy. (2008)

[33] World Coal Institute. The Coal Resaource : A comphrensive overview of coal. London (2005)

[34] J. Kopfle and R. Hunter. DRI in steel production: direct reduction's role in the world steel industry. Ironmaking and Steelmaking 35 (2008): 254-259.

[35] Diez, M.A., Alvarez, R., Barriocanal, C. Coal for metallurgical coke production: predictors of coke quality and future requirements for cokemaking. International Journal of Coal Geology, 2002; 50: 389-412.

[36] S. Watakabe, L. Takeda, H. Nishimura, S. Goto, N. Nishimura, T. Uchida, M. Kiguchi. Development of high ratio mixed charging technique to the blast furnace. ISIJ International 46 (2006): 513–522

[37] S. Matsuhashi, H. Kurosawa, S. Natsui, T. Kon, S. Ueda, R. Inoue, T. Ariyama. Evaluation of coke mixed charging based on packed bed structure and gas permeability changes in blast furnace by DEM-CFD model. ISIJ International 52 (2012); 1990–1999

[38] International Energy Agency (IEA). Worldwide trends in energy use and efficiency: key insights from IEA indicator analysis (2008): 30-31

[39] International Energy Agency (IEA). Tracking industrial energy efficiency and CO2 emissions. Head of Communication and Information Office OECD/IEA Paris (2007): 95.

[40] C. Xu and D. Cang. A brief overview of low CO2 emission technologies for iron and steelmaking. Journal of iron and steel research international 17 (2010): 1-7

[41] ZC. Guo and ZX. Fu. Current situation of energy consumption and measures taken for energy saving in the iron and steel industry in China. Energy 35 (2010): 4356-4360

[42] H. Li, W. Bao, C. Xiu, Y. Zhang. Energy conservation and circular economy in China's process industries. Energy 35 (2010): 4273-4281

[43] G. Ma, J. Cai, W. Zeng, H. Dong. Analytical research on waste heat recovery and utilization of China's iron and steel industry. Energy Procedia 14 (2012): 1022-1028

[44] Wright, J.K., Taylor, I.F., Philip, D.K. A review of progress of the development of new ironmaking technologies. Minerals Engineering, 1991; 4: 983-1001.

[45] Ziebik, A., Lampert, K., Szega, M. Energy analysis of blast-furnace system operating with the Corex process and CO_2 removal. Energy, 2008; 33: 199-205.

[46] H. Zhang, H. Wang, X. Zhu, YJ. Qiu, K. Li, R. Chen, Q. Liao. A review of waste heat recovery technologies towards molten slag in steel industry. Applied energy 112 (2013): 956-966

[47] D. Gielen. CO2 removal in the iron and steel industry. Energy conversion and management 44 (2003): 1027-1037

[48]C. Hu, L. Chen, C. Zhang, Y. Qi, R. Yin. Emission mitigation of CO2 in the steel industry: current status and future scenarios. Journal of iron and steel research international 13 (2006): 38-42

[49] J. Fu, G. Tang, R. Zhao, and W. Hwang. Carbon reduction programs and key technologies in global steel industry. Journal of Iron and Steel Research International 21 (2014): 275-281

[50] P. Wooders. Energy-intensive industries: decision making for a low-carbon future, the case of steel . The International Institute for Sustainable Development (2002).

[51] S. Wu, J. Xu, JI. Yagi, X. Guo, L. Zhang. Prediction of pre-reduction shaft furnace with top gas recycling technology aiming to cut down CO2 emission. ISIJ International 51 (2011): 1344–1352

[52] S. Vaidyaraman, WJ. Lackey, GB. Freeman, PK. Agrawal, MD. Langman. Fabrication of carbon-carbon composites by forced flow-thermal gradient chemical vapor infiltration. J. Mater. Res. 10 (1995): 1469-1477

[53] Y. Xu, L. Zhang, L. Cheng, D. Yan. Microstructure and mechanical properties of three-dimensional carbon/silicon carbide composites fabricated by chemical vapor infiltration. Carbon 36 (1998): 1051-1056

[54] DA. Streitwieser, N. Popovska, H. Gerhard, G. Emig. Application of the chemical vapor infiltration and reaction (CVI-R) technique for the preparation of highly porous biomorphic SiC ceramics derived from paper. Journal of the European ceramic society 26 (2005): 817-828

[55] Y. Katoh, L. Snead, T. Nozawa, T. Hinoki, A. Kohyama, N. Igawa, T. Taguchi. Mechanical properties of chemically vapor-infiltrated silicon carbide structural composites with thin carbon interphases for fusion and advanced fission applications. Materials Transactions 46 (2005): 527-535

[56] Y. Xu and XT. Yan. Chemical vapour deposition: an integrated engineering design for advanced materials. Spinger-Verlag London limited (2010). 165-210

[57] Y. Xu and L. Zhang. Three-dimensional carbon/silicon carbide composites prepared by chemical vapor infiltration. J. Am. Ceram. Soc. 80 (1997): 1897-1900

[58] Y. Xu, L. Cheng, L. Zhang. Carbon/silicon carbide composites preparted by chemical vapor infiltration with silicon melt infiltration. Carbon 37 (1999): 1179-1187

[59] P. Delhaes. Chemical vapor deposition and infiltration processes of carbon materials. Carbon 40 (2002): 641-657

[60] Private communication with Prof. Masakata Shimizu, Kyushu University.

[61] H. Hu, Q. Zhou, S. Zhu, B. Meyer, S. Krzack, G. Chen. Product distribution and sulfur behavior in coal pyrolysis. Fuel Processing Technology 85 (2004) : 849– 861

[62] PR. Solomon, TH. Fletcher, RJ. Pugmire. Progress in coal pyrolysis. Fuel 72 (1993): 587-597

[63] RC. Brown. Thermochemical processing of biomass: conversion to fuels, chemicals, and power. Wiley Series in Renewable Resources. John Wiley and Sons (2011)

[64] J. Han and H. Kim. The reduction and control technology of tar during biomass gasification/pyrolysis: An overview. Renewable and sustainable energy reviews 12 (2008): 397-416

[65] C. Myren, C. Hornell, E. Bjornbom, K. Sjostrom, Catalytic tar decomposition of biomass pyrolysis gas with a combination of dolomite and silica, Biomass and Bioenergy 23 (2002): 217–227.

[66] S. Hosokai, K. Norinaga, T. Kimura, M. Nakano, CZ. Li, JI. Hayashi. Reforming of volatiles from the biomass pyrolysis over charcoal in a sequence of coke deposition and steam gasification of coke. Energy and Fuel25 (2011): 5387-5393.

[67] Milne T, Evans RJ. Biomass gasifier tars: their nature, formation, and conversion. National Renewable Energy Laboratory Report NREL/TP-570-25357 (1998)

[68] R. Zhang, R.B. Brown, A. Suby, K. Cummer, Catalytic destruction of tar in biomass derived producer gas, Energy Conversion and Management 45 (2004) 995–1014.

[69] Devi L, Ptasinski KJ, Janssen FJJG. A review of the primary measures for tar elimination in biomass gasification processes. Biomass Bioenergy 2003;24:125–40.

[70] A. Samsudin and ZA. Zainal. Tar reduction in biomass producer gas via mechanical, catalytic and thermal methods: A review. Renewable and sustainable energy reviews 15 (2011): 2355-2377

[71] A. Paethanom, S. Nakahara, M. Kobayashi, P. Prawisudha, K. Yoshikawa, Performance of tar removal by absorption and adsorption for biomass gasification, Fuel Processing Technology 104 (2012) 144 – 154.

[72] H. Noichi, A. Uddin, E. Sasoka, Stem reforming of naphthalene as model biomass tar over iron-alumunium and iron-zirconium oxide catalyst catalysts, Fuel Processing Technology 91 (2010) 1609 – 1616.

[73] Y. Shen and K. Yoshikawa. Recent progresses in catalytic tar elimination during biomass gasification or pyrolysis: A review. Renewable and Sustainable Energy Reviews 21 (2013): 371–392

[74] P. Lu, Z. Yuan, C. Wu, L. Ma, Y. Chen, N. Tsubaki, Bio-syngas production from biomass catalytic gasification, Energy Conversion and Management 48 (2007) 1132–1139.

[75] P.A. Simell, J.O. Hepola, A.O.I. Krause, Effects of gasification gas components on tar and ammonia decomposition over hot gas cleanup catalysts, Fuel 76 (1997) 1117–1127.

[76] M. Asadullah, T. Miyazawa, S.I. Ito, K. Kunimori, M. Yamada, K. Tomishige, Gasification of different biomasses in a dual-bed gasifier system combined with novel catalysts with high energy efficiency, Appl Catal A: Gen. 267 (2004) 95–102.

[77] B. Dou, J. Gao, X. Sha, SW. Baek. Catalytic cracking of tar component from high temperature fuel gas. Applied Thermal Engineering 23 (2003): 2229-2239.

[78] MP. Aznar, MA. Caballero, J. Gil, JA. Martin, J. Corella. Commercial steam reforming catalysts to improve biomass gasification with steam-oxygen mixtures: 2. Catalytic tar removal. Ind. Eng. Chem. Res 37 (1998): 2668-2680.

[79] ZY. Abu El-Rub, EA. Bramer, G. Brem. Experimental comparison of biomass chars with other catalysts for tar reduction. Fuel 87 (2008): 2243–2252.

[80] S. Hosokai, K. Kumabe, M. Ohshita, K. Norinaga, CZ. Li, JI. Hayashi. Mechanism of decomposition of aromatics over charcoal and necessary condition for maintaining its activity. Fuel 87 (2008): 2914–2922.

[81] T. Kimura, M. Nakano, S. Hosokai, K. Norinaga, CZ. Li, JI. Hayashi. Steam reforming of biomass tar over charcoal in a coke-deposition/steam-reforming sequence. Proceedings of CHEMECA 2009, Perth, CD-ROM Edition; (2009).

Chapter 2

Carbon deposition through CVI process over low grade iron ore

2.1 Introduction

The iron and steel industry is highly dependent on metallurgical coke, which is produced from coking coal, high-grade bituminous, and has crucial roles as an energy source, reducing agent, and maintaining bed permeability in blast furnace operation [1, 2]. Approximately 71% of total steel was produced by reducing of iron ore with coke and coal in the blast furnace [3]. High growing of this industry needs great availability of metallurgical coke which rising of coking coal price. In order to ensure the energy security for iron and steel industry, a proper strategy should be taken by researchers to explore several innovative methods to substitute the conventional reducing agents. Srivastava et al. used woody biomass as a reducing agent by combining it with magnetite ore to produce pellets. This material successfully produced pig iron by high-temperature (1475°C) reduction [4]. Other researchers have used carbon sources such as steelmaking wastes, tar sludge, and oil from steel-rolling mills to fabricate briquettes of materials as replacements for conventional reducing agents [5]. A hydrothermal method using an autoclave (0.1 MPa) has been used to improve the properties of low-grade sub-bituminous coal, which can be used as coking coal [6]. The treatment can greatly increase the strength and reactivity of sub-bituminous coal. Non-coking coal is upgraded to metallurgical coke by blending with biomass materials such as bagasse pitch, coconut shell, coconut waste, molasses, and sawdust [7]. Beside wooden biomass, low grade coal such as lignite and sub-bituminous which are large resource and cheaper price, are promising candidate to replace coke usage. Utilization of wooden biomass also

offers possibility to apply renewable energy and reduce the CO_2 emission of steelmaking industry.

Pyrolysis is main process in the iron and steel industry for converting solid fuels to produce char, tar and gas. Char is the main product used as a reducing agent while tar vapor and gas are by-products containing high amounts of carbon and energy. It is well known that the amount of volatile matter produced by biomass and low grade coals, such as lignite coal and sub-bituminous coal, during the pyrolysis process is higher (25–65 %mass) than that produced by high grade coal[8]. The tar material is mainly composed of condensable organic materials and may cause operational problems such as pipe plugging, condensation, and tar aerosol formation [9, 10]. Catalytic tar decomposition is one of promising method to avoid such problems and increase the efficiency of pyrolysis process [11, 12]. Several materials were studied by a number of researchers as potential catalyst such as Ni, Pt, Rh, and Pd [13-16]. Nickel based catalysts are very active in tar decomposition but deactivation of catalyst by carbon deposition is main problem [17]. Furthermore, the disposal of inactive nickel catalysts is toxic and a potential of environmental problem. Another option of tar decomposition is to apply a catalyst or catalyst-like solid that can be used as material or fuel even after loss of activity, as example tar decomposition over charcoal. After reaction, charcoal and deposited carbon could be utilized as fuels and reducing agent [18].

The effective utilization of low grade ore should be introduced in modern iron and steel industry to substitute high grade ore which shortage resources and expensive. However, when low grade iron ores such as goethite ore are sent to a sinter machine, a large amount of energy is required to dehydrate the ore due to high content of combined water (CW). On the other hand, dehydration of CW is attractive for producing porous materials within the ore: nanocracks are

initiated and propagated during the dehydration process and nanopores that can be used as valuable reaction sites are produced within the ore [20]. Udin et.al reported that iron oxide shows good catalytic activity in tar decomposition process to produce valuable gasses and specific surface area of ore is main factor to maintain the catalyst activity [21].

By using both the carbon reduction agent and porous low grade ore, a new concept of ironmaking was proposed to turn the demerits into merits. The integrated pyrolysis-tar decomposition over porous low grade ore by CVI process was proposed to solve the tar problem, reduction agent and limited amount of high grade iron ore. The tar component, produced by pyrolysis, decomposed over low grade ore into valuable gas and carbon. Furthermore, the solid carbon deposited within pores iron ore and acted as a reducing agent in the ironmaking process. The porous low grade iron ore has role as decomposition catalyst and carbon storage that inactive catalyst with carbon deposition could be attractive material in ironmaking process. The proposed system could be great candidate for decreasing high usage of coking coal as reducing agent and effective utilization of low grade ore, simultaneously. Therefore, the purpose of this study was to evaluate in detail the utilization of low grade ore as tar decomposition catalyst and carbon storage through the proposed system, CVI ironmaking process.

It well known that the product distribution of pyrolysis process is highly depends on the characterization of solid fuel [22-25]. The fuel owns high content of fixed carbon produces large amount of char as solid product. Generally, the biomass fuel with lower amount of fixed carbon generates smaller char and larger volatile matter contained gas and tar products compared to coal [27]. In the first part of result and discussion, section 2.3.1, the comparative analysis of various solid fuels as carbon source on tar decomposition was examined to explore the possibility of CVI ironmaking. In addition, the effect of tar decomposition on overall product of pyrolysis process

was also discussed in term of energy efficiency. In the next section, 2.3.2, the study would be focused on the temperature effect of tar decomposition and carbon deposition. The gas compositions rely on the characteristic of raw material, heating rate, particle size and temperature [26-28]. Detailed information related the carbon deposition conditions such as temperature and reduction behaviors are necessary to confirm the phenomena involved during proposed system. Low grade coals such as sub-bitumitous coal and lignite coal were used in this experiment due to available abundantly and limited utilization in the iron and steel industry. The reactivity of iron ore containing carbon, CVI ore on reduction reaction was also investigated and compared to conventional system in this section. The optimum temperatures for both pyrolysis and decomposition process were discussed in last section, 2.3.3 for maximizing the carbon deposition within iron ore. The proposed system is a two-stage process involving pyrolysis in the upstream part and tar decomposition over porous low-grade ore in the downstream part. It is well known that pyrolysis and tar decomposition are highly dependent on temperature. In the pyrolysis process, the thermal cracking of coal at elevated temperatures produces large amounts of volatile matter and enhances tar conversion in the decomposition process to produce deposited carbon and gases [29-30]. In contrast, a high-activity tar component at elevated temperatures promotes gas production rather than carbon deposition within a porous ore. Coal pyrolysis and tar decomposition therefore show opposite behaviours in carbon deposition within porous ores. Specific temperature conditions for each process should be determined to obtain maximum carbon deposition within porous ore. The processes over two different low-grade iron ores with different contents of combined water (CW) were also evaluated to understand the main factors in the carbon deposition process.

2.2 Material and experiment method

2.2.1 Materials

Different qualities of solid fuels were examined in the experiments as carbon source for tar decomposition as listed in the Table 2-1. Based on the proximate and ultimate analysis, bituminous coal as high grade coal showed high quality fuel due to large carbon content. In order to avoid the effect of particle size, each solid fuel were crushed and sieved to approximately 250–500 μm.

Table 2-1 Proximate and ultimate analysis of coal raw materials

Sample	Proximate analysis [%mass]			Ultimate analysis [%mass]				
	FC	Volatile	Ash	C	H	N	O[a]	S
Bituminous (BIT)	66.9	24.4	8.7	80.2	5.3	1.8	12.8	05
Lignite (LIGN)	47.2	50.9	1.9	68.5	5.0	0.6	25.6	0.3
Sub-bituminous (SBIT)	49.0	48.4	2.6	71.6	5.0	1.0	22.3	0.1
Palm kernel shell (PKS)	24.2	65.4	10.4	49.5	5.7	0.8	44.0	0.0

FC: fixed carbon; [a]: calculated by difference.

Table 2-2 shows the main properties of low grade pisolate ore that used in these experiments. Because of small amount of total iron, the utilization of this ore was limited in currently ironmaking industry. Large amount of combined water was attractive to create porous material for carbon deposition. The ore was crushed and sieved to obtain a sample with similar particle sizes ranging from 0.95 to 2 mm.

Table 2-2 Properties of ore samples

Low grade ore	PS[a] [mm]	TFe[b] [%mass]	CW[c] [%mass]	SA[d] [m^2/g]
Pisolite (P) ore	0.95–2	49.73	5.90	11.83
Robe-river (R) ore	0.95–2	57.20	7.60	17.15
Hamersley (H) ore	0.95–2	58.22	8.62	23.20

[a]PS: particle size; [b]TFe: total iron; [c]CW: combined water; [d]SA: Brunauer–Emmett–Teller surface area.

Tar decomposition and carbon deposition required high surface area for reaction site and carbon storage, respectively. In order to increase surface area and create porous material, the ore was dehydrated at 450°C with heating rate of 3°C/min and a holding time of 1 h in air atmosphere. Thermogravity (TG) experiments of the ore sample reported that CW would decompose at 350°C. Therefore, the dehydration of ore at 450°C was adequate to fully dissipate of CW from the ore pore and created porous material. In order to evaluate dehydration process, several properties such as surface area, average pore volume, and pore size distribution were measured before and after the experiment using a Brunauer-Emmett-Teller (BET) analyzer.

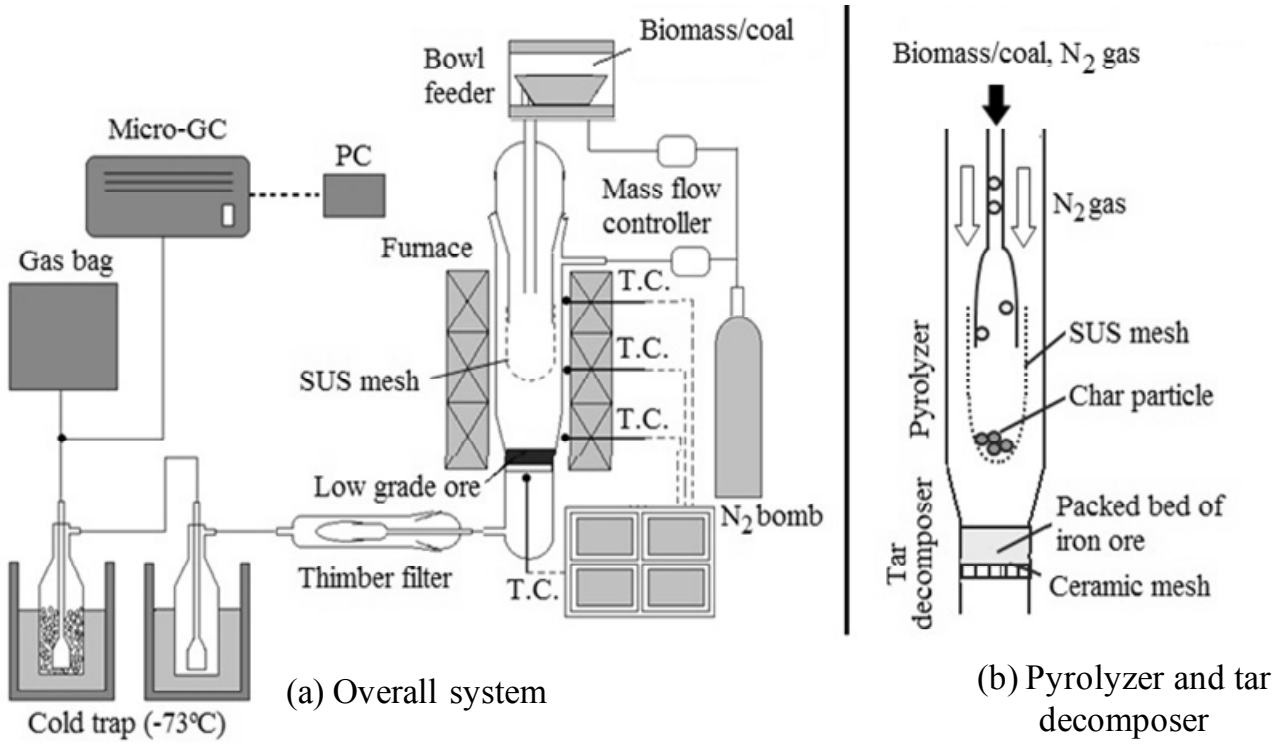

(a) Overall system

(b) Pyrolyzer and tar decomposer

Fig. 2-1 Experimental apparatus for pyrolysis, tar decomposition, and carbon deposition. Case 1: no iron ore; case 2: 3 g of iron ore. Solid fuels were charged at a flow rate of 0.1 g/min for 40 min under N_2 flow rate of 250 mL/min. (T.C.: temperature controller, PC: personal computer, GC: gas chromatography)

2.2.2 Experimental methods

2.2.2.1 Pyrolysis and tar decomposition (CVI process)

A quartz reactor tube as showed in Fig. 2-1 was used in these experiments with an inner diameter and height of 30 mm and 550 mm, respectively. In order to maintain the experiment temperature, the electrical furnace was equipped with six thermocouples and temperature controller. Experiments were performed at atmospheric pressure with a total N_2 flow of 250 mL/min. The solid fuel was continuously charged into the reactor using a bowl feeder at a rate of 0.1 g/min for 40 min after stable temperature. Fast pyrolysis happened inside the reactor and produced char, tar vapor and gases. Char product was collected with SUS 404 while tar vapor and gases poured to the bottom of reactor. The effect of iron ore on tar decomposition was evaluated by performing experiments without iron ore (case 1) and 3 g of iron ore (case 2) inside the reactor. In case 2, tar vapor and gases were introduced to iron ore for tar decomposition and carbon deposition. The generated gas and remaining tar were removed from the bottom and allowed to flow through a cold trap which was maintained at –73°C by adding liquid N_2 for separation between tar vapor and gases. A gas chromatograph (GC) analyzer and micro GC were employed to detect H_2, CO, CO_2, and light hydrocarbon gases. The ore structure and compound were characterized using XRD analysis while BET analyzer was used to examine the changing of surface area, average pore diameter and pore size distribution. The carbon content within iron ore was measured using CHN elemental analyzer to examine carbon deposition. Based on these experimental results, the effect of solid fuels on tar decomposition and carbon deposition were discussed.

2.2.2.2 The reactivity on reduction reaction of iron ore-deposited carbon, CVI ore

In order to evaluate the reactivity in reduction reaction, the iron ore contained carbon namely CVI ore was investigated by the thermogravimetric method. A mixture of the reagent Fe_3O_4 and metallurgical coke was used as a reference of conventional system for comparison. The sample was heated at the rate of 50°C/min until 1200°C by flowing argon at the high flow rate of 500 NmL/min to ensure that only direct reduction occurred in this process. This means that the gas products of the reduction reaction which were CO and CO_2 never contributed or affected the iron reduction reaction. In order to evaluate the reaction mechanism, the final product was characterized by XRD analysis and the amount of carbon was determined.

2.2.2.3 Optimum temperature of pyrolysis and tar decomposition (CVI process)

The optimum temperature of CVI process was evaluated using similar apparatus but the procedure was modified slightly to adapt the temperature control. The electrical furnace was equipped with six thermocouples and a temperature controller at the top, middle, and bottom. The pyrolysis and tar decomposition temperature were precisely controlled and monitored by the top and bottom controllers, respectively. The temperature of the middle controller was fixed at the average of the top and bottom temperatures. In order to obtain the optimum temperature of the pyrolysis process, we examined different temperatures (500–800°C), with a constant temperature for tar decomposition (600°C). Subsequently, the optimum pyrolysis was used to find the optimum of tar decomposition by examination different temperatures (400-800^{o}C). A comparison of two different iron ores was performed under the optimum conditions for both the pyrolysis and tar decomposition temperatures.

2.3 Result and discussion

2.3.1 Tar decomposition and carbon deposition from various solid fuels

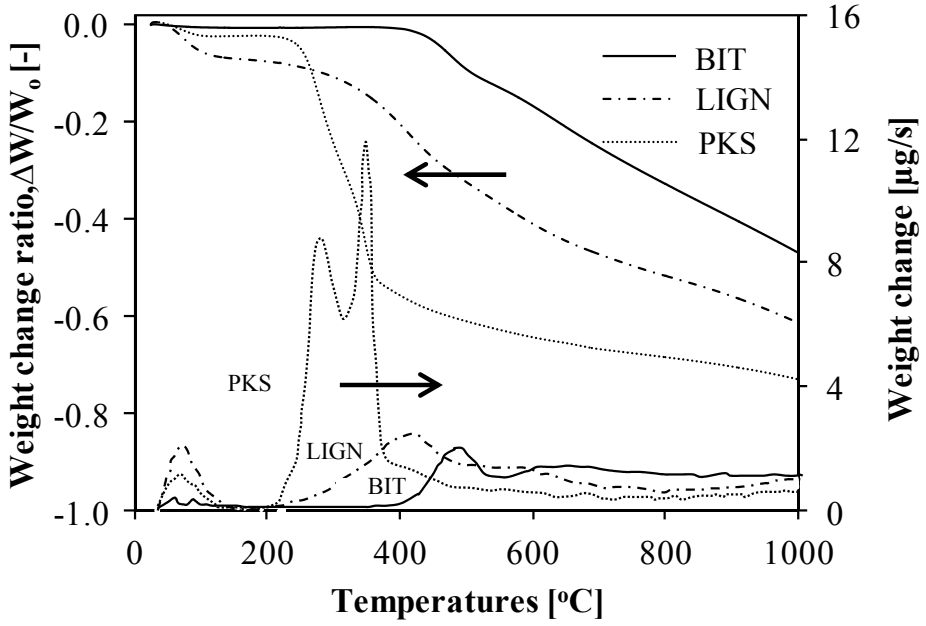

Fig. 2-2 TG/DTG profiles of various solid fuels studied during pyrolysis process at N_2 atmosphere. Sample weight: 10 mg, particle size: 250–500 µm and heating rate: 50^{o}C/min

Fig. 2-2 shows the pyrolysis characteristic of each solid fuel using TG-DTA in N_2 atmosphere that helpful to understand the pyrolysis behavior. BIT evidenced smallest total weight loss compared to other fuels due to high content of fixed carbon. It means that BIT would produce high char and small volatile matter (tar and gas). It was noted that small weight loss up to 200^{o}C because of moisture evaporation. High oxygen content as moisture of biomass PKS caused large weight loss in this area. The thermal decomposition was started at 240 – 400 ^{o}C that referred to PKS, LIGN and BIT respectively. In this area, high weight loss occurred as a result of volatile matter decomposition. Thermal decomposition of PKS was consist two peaks that correspond to decomposition of cellulose and lignin that had different decomposition temperature. Meantime, only one peak appeared in the LIGN and BIT decomposition due to

mainly carbon content. These results were useful information to optimize the pyrolysis temperature and carbon deposition during integrated pyrolysis-tar decomposition process. At equal pyrolysis temperature, PKS would produce smallest char and largest volatile matter compared to other fuels.

Fig. 2-3 shows the product distribution of the pyrolysis without tar decomposition process (case 1) of different solid fuels. Obviously, the BIT produced largest char product while the PKS is smallest, it agreed with the TG/DTG data. This result corresponds to the characteristic of original fuel which BIT owned highest fixed carbon compared to other fuels. In addition to char product, the BIT also generated largest portion of tar among the tested solid fuels. By similar experiment condition, this tar product would be raw material for tar decomposition when the porous ore was placed in fixed bed reactor (case 2). Therefore, the BIT was expected to have more carbon deposition within ore pores due to highest raw material of tar decomposition.

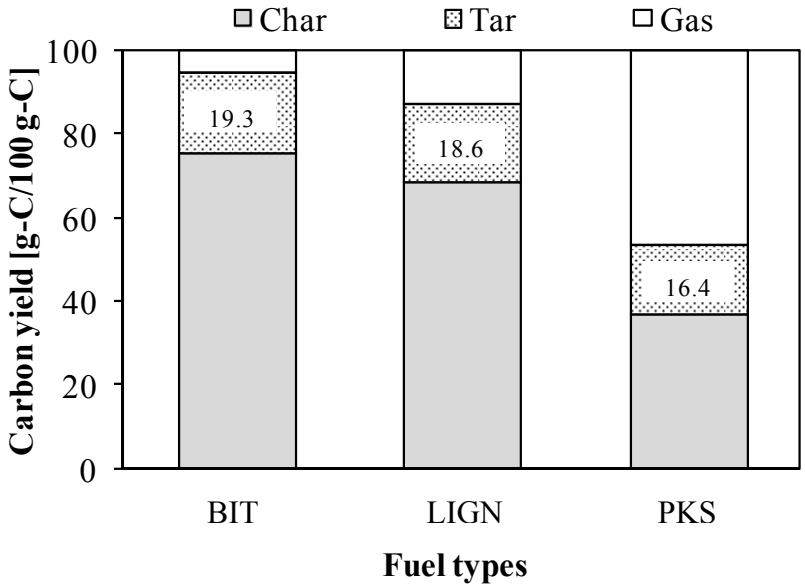

Fig. 2-3 Product distribution of the pyrolysis of various solid fuels at 600°C without tar decomposition treatment (case 1: no iron ore).

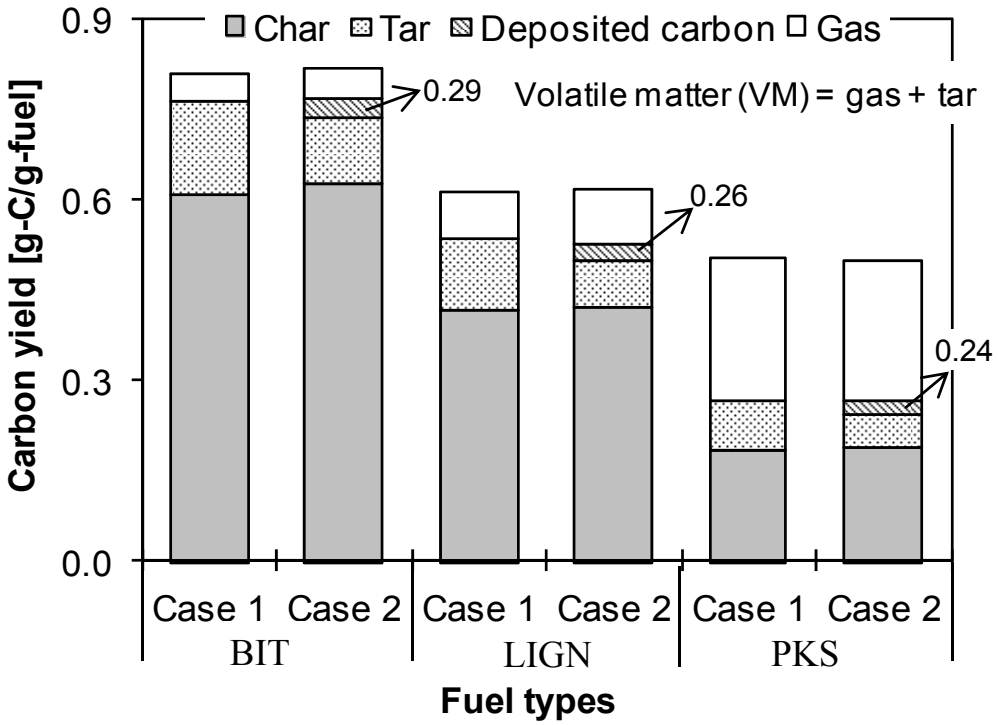

Fig. 2-4 Product distribution of the pyrolysis of various solid fuels at 600°C. Case 1: no iron ore; case 2: 3 g of iron ore.

Fig. 2-4 shows the effect of iron ore on carbon product distribution of each solid fuel during pyrolysis process, total carbon was calculated in basis of mass-input fuel. BIT produced highest total carbon due to large fixed carbon in raw material. In the case 1, PKS resulted smallest tar amount while BIT was highest. Large volatile matter in PKS raw material was easier to convert in the gases form due to low decomposition temperature. The effect of iron ore on the pyrolysis product could be examined by comparison of case 1 and case 2. The introduction of iron ore into pyrolysis process decreased the amount of tar and converted to gases and deposited carbon through catalytic tar decomposition (2.1).

$$\text{Tar} \rightarrow H_2 + CO + CO_2 + CH_4 + \text{other light hydrocarbons} + C \qquad (2.1)$$

Heavy and light hydrocarbons of tar decomposed over iron ore surface and pore to produce carbon and gases. Beside carbon storage, iron ore also played important rule as catalyst in the tar decomposition. Each solid fuel produced specific amount of tar that become raw material for tar decomposition. This condition caused different result of carbon deposition; high quantity of tar in BIT generated larger carbon deposition compared to other fuels. Therefore, carbon deposition required huge amount of tar from pyrolysis process. The solid fuels that produced great amount of tar would be suitable for carbon deposition.

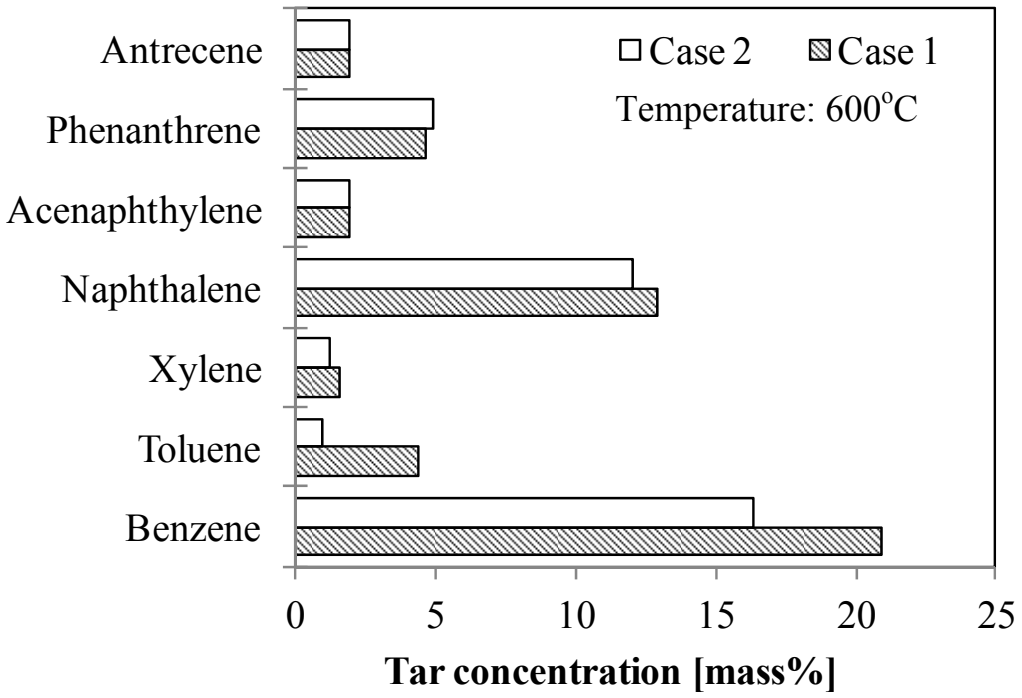

Fig. 2-5 Change of LIGN tar composition due to decomposition process over porous low grade ore. Case 1: no iron ore; case 2: 3 g of iron ore

Fig. 2-5 shows the changing of tar composition as a result of decomposition process over low grade ore in the experiments. As known, the tar material composed of various hydrocarbons with different structures. By placed the porous ore in the fixed bed rector as catalyst (case 2), the

amount of tar component decreased compared to experiment without porous ore (case 1). The data validated the product distribution in Fig 2-4 that the tar decomposition occurred to produce additional gas and deposited carbon within ore pores. Based on this result, the porous low grade ore played important role not only carbon storage but also promoting the decomposition process.

In order to evaluate the effectiveness of carbon deposition through tar decomposition, ratio of deposited carbon was calculated. This ratio described the possibility of reacted tar as deposited carbon. Fig. 2-6 shows the correlation between reacted tar and ratio of deposited carbon in each solid fuel. BIT resulted highest reacted tar due to huge amount of tar raw material from pyrolysis process but the ratio of deposited carbon was smallest. Tar component was converted to gases and carbon through catalytic process.

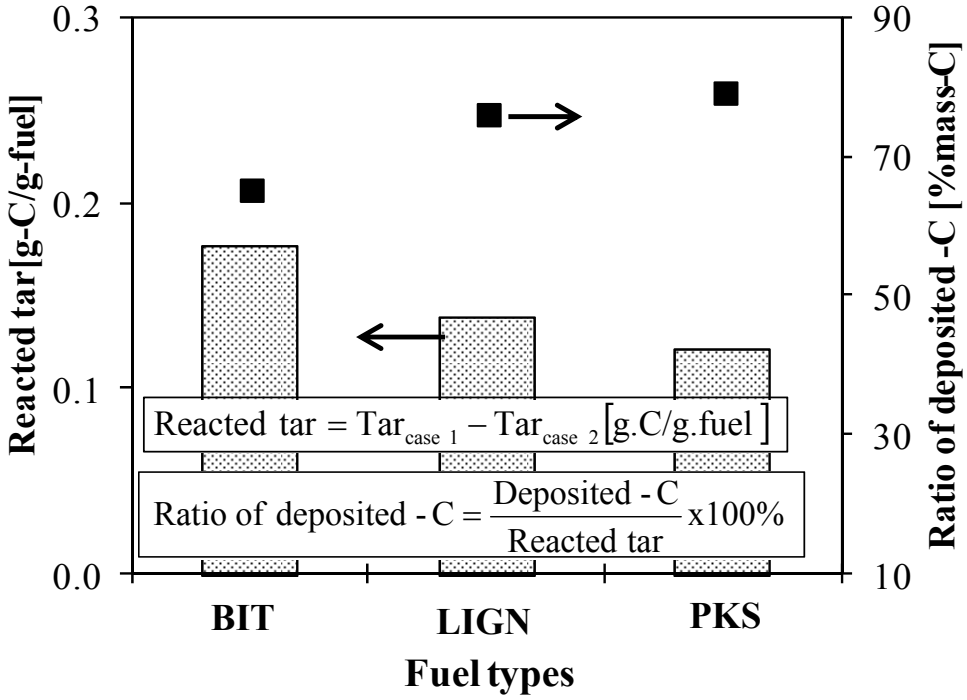

Fig. 2-6 Effect of various fuels on reacted tar and ratio of deposited-C within porous iron ore. Case 1: no iron ore; case 2: 3 g of iron ore

Several factors affected the catalyst activity such as available area, catalyst components and tar components. Simultaneously with tar decomposition, tar carbon deposited within pore ore and consumed available area and pore volume during the process. Thus, reducing area and volume caused small possibility of carbon deposition. Ratio of deposited carbon was increased at small reacted of tar due to high availability of volume for deposition

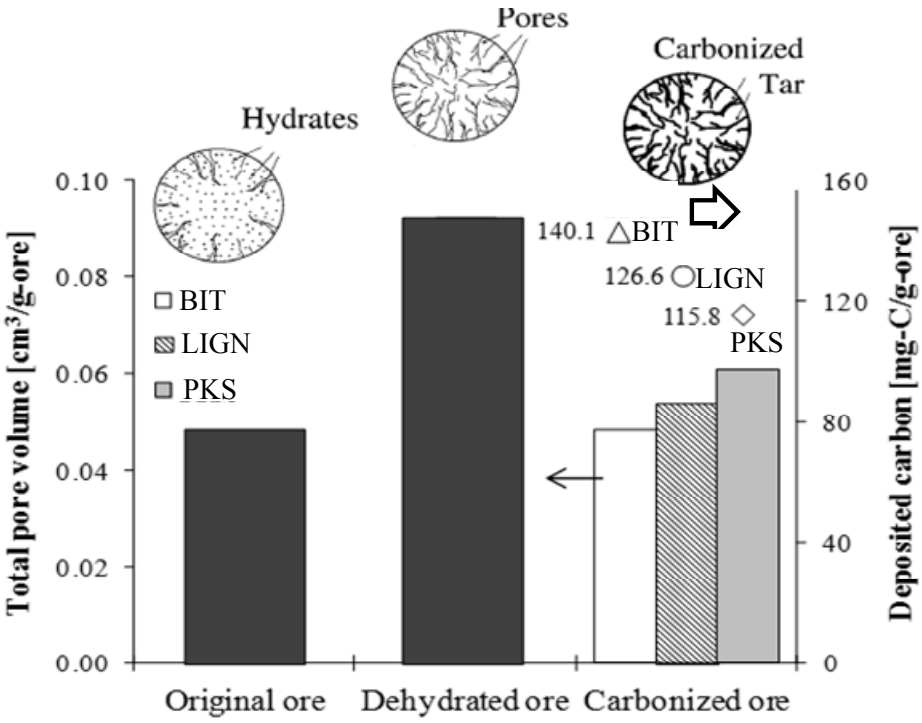

Fig. 2-7 Change in total pore volume of iron ore and the amount of deposited carbon during experiments at 600°C.

Fig. 2-7 shows the change of total pore volume of iron ore in each experiment steps. Tar decomposition and carbon deposition required large surface area and pore volume as reaction site and carbon storage. Dehydration of combined water (CW) at 450°C was effective to increase the pore volume almost twice from original ore. CW within iron ore decomposed and evaporated

during heating-up through (2.2). The remaining site of CW was vacant and enhanced pore volume.

$$2FeOOH \rightarrow Fe_2O_3 + H_2O \qquad (2.2)$$

Tar carbon deposited within pores ore and reduced the total pore volume after decomposition process. It was clearly that the reducing pore volume of BIT was highest due to large carbon deposition. The diminishing of pore volume was proportional with the amount of deposited carbon. Thus, tar carbon deposited effectively within iron pore which was reveled with large decreasing of pore volume at high carbon deposition. However, the remaining pore volume after decomposition process was still a half of dehydrated ore. This condition promoted the study for optimization of pyrolysis and tar decomposition condition to increase amount of carbon deposition.

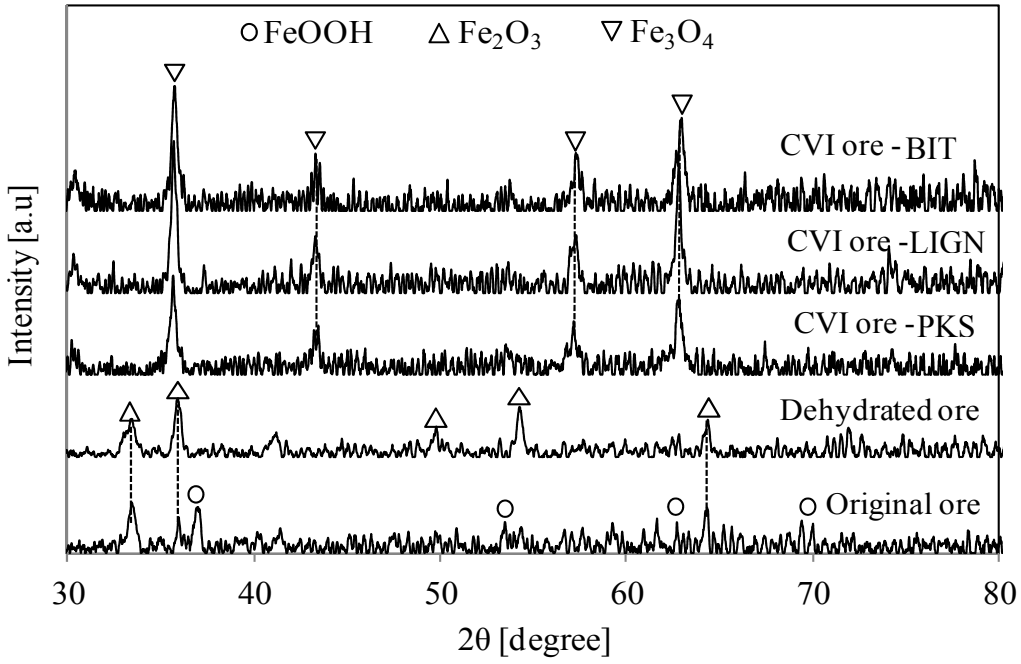

Fig. 2-8 Change of XRD pattern of iron ore for each experiment steps in the pyrolysis-tar decomposition process (case 2). Case 1: no iron ore; case 2: 3 g of iron ore

XRD analysis was proceeded to investigate the transforming of iron compound in each experiment steps as seen in Fig. 2-8. Dehydration process was done perfectly and converted all FeOOH to Fe_2O_3. This step created porous material that suitable for tar decomposition and carbon deposition. All Fe_2O_3 reduced and altered to Fe_3O_4 after the experiment for all solid fuels. The reducing gases such as H_2 and CO were generated during pyrolysis process and indirect reduction simultaneously occurred with tar decomposition. The larger gas product from PKS pyrolysis was insufficient to produce FeO during indirect reduction due to thermodynamic limitation. Therefore, the ore product of tar decomposition contained not only deposited carbon but also semi reduced ore (Fe_3O_4).

2.3.2 Effect of temperature on low grade coal-tar decomposition for enhancing reactivity

2.3.2.1 Effect of temperature of product distribution

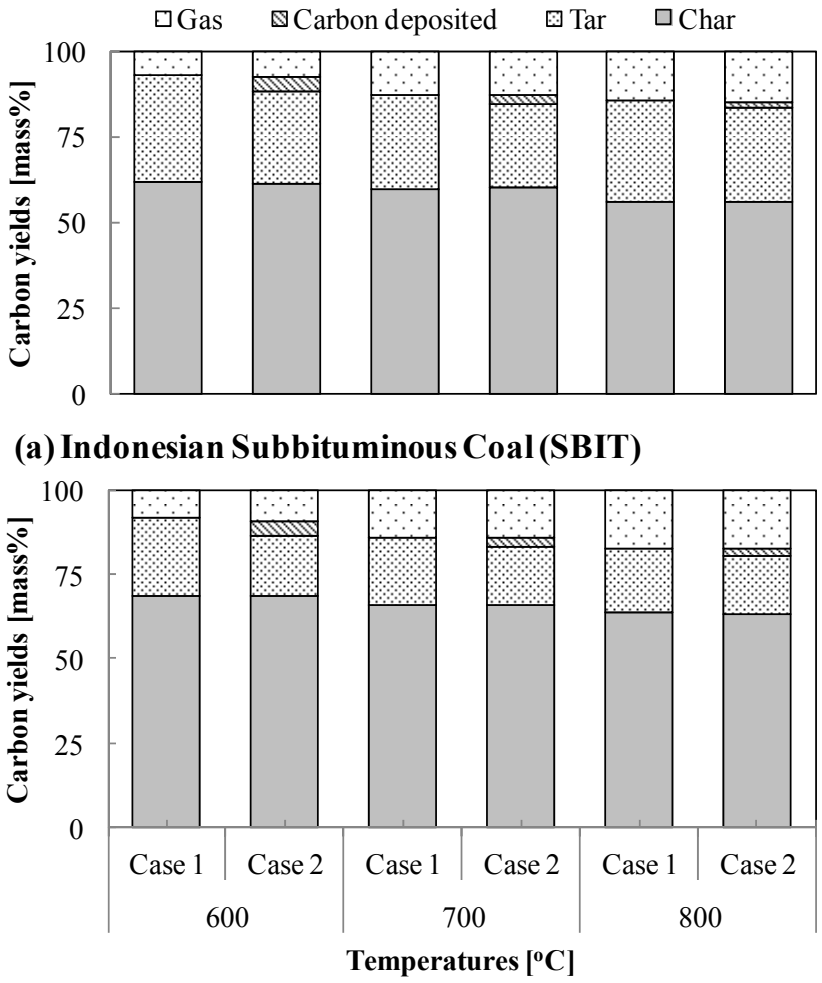

Fig. 2-9 Effect of pisolite iron ore on product distribution due to pyrolysis of two low-grade coals at different temperatures: (a) subbituminous coal from Indonesia (SBIT) and (b) Australian lignite coal (LIGN). Case 1: No iron ore (Pyrolysis), case 2: Fixed bed of 3 g of iron ore (Pyrolysis-Tar decomposition) for 40 min under the a N_2 flow rate of 250 mL/min.

Fig. 2-9 shows the effect of pisolate iron ore on the distribution of pyrolysis products of LIGN and SBIT at different temperatures. The amount of char product obtained in case 1 and case 2 was similar for both coals, which shows the reproducibility of these experiments. As previous section, the introduction of iron ore to pyrolysis products that contain tar vapor and gas caused decomposition of tar through (2.1). The tar components that were heavy and light hydrocarbons decomposed and cracked within the iron ore pores to form gases and carbon, thus resulting in a less amount of tar and higher amount of the total gas product. Simultaneously with tar decomposition, the carbon product of tar decomposition also infiltrated and deposited within the pores of the iron ore, as deposited tar carbon. This data agreed with the result reported by Udin et al. that iron oxide promoted catalytic tar decomposition [21]. The catalyst that contained metal oxides prevented the formation of stable chemical structures and derived the weakening of C–C bonds inside the hydrocarbon molecule; the activation energy of the reaction decreased, and thus, the hydrocarbon decomposed into gases, lighter hydrocarbons, and carbon [31]. Thus, besides carbon storage, the iron ore also showed activity in the catalytic tar decomposition process.

The effect of temperature on the pyrolysis and tar decomposition was also shown in the Fig. 2-9. It was well known that the amount of char product decreased at high pyrolysis temperatures while the amount of volatile matter (tar and gases) increased. When tar conversion was calculated from the ratio of tar decomposition to original pyrolysis tar (case 1), it was seen that tar conversion decreased at high temperatures for both types of coal. The product distribution of char and volatile matter (including tar and gas) in the pyrolysis process greatly depended on the temperature. Thermal cracking, decarboxylation, and depolymerization were preferred at high temperatures [32]. For both coal raw materials, carbon deposition within ore

pores was declined at high temperatures. The tar components were more active and easier to decompose into gas phase material. Therefore, high temperature will be suitable for the gas product whereas the deposition of a large amount of carbon will be realized at low temperatures.

Fig. 2-10 shows the effect of iron ore on gas composition of LIGN pyrolysis process at different temperatures. In case 2, there were several reactions occurred simultaneously inside the reactor such tar decomposition, indirect reaction, and gas reforming.

$$3Fe_2O_3 + CO \rightarrow 2Fe_3O_4 + CO_2 \quad (2.3)$$

$$3Fe_2O_3 + H_2 \rightarrow 2Fe_3O_4 + H_2O \quad (2.4)$$

$$CH_4 + CO_2 \rightarrow 2H_2 + 2CO \quad (2.5)$$

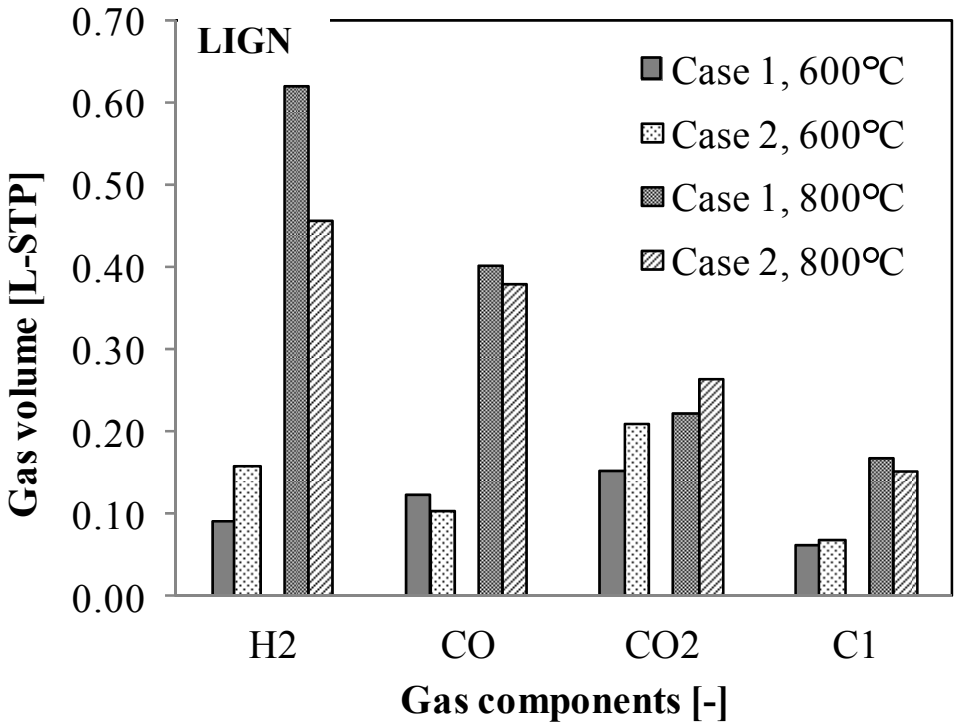

Fig. 2-10 The gas composition produced during the pyrolysis of lignite coal (LIGN) at different temperatures. Case 1: no iron ore; case 2: 3 g of iron ore.

The main reaction in each condition could be predicted based on gas composition. It was apparent that all gases increased as introduction of iron ore (case 2) except CO at 600 ^{o}C; tar decomposition that produced gases such as H_2, CO_2, CO and CH_4 was main reaction compared to indirect reaction and gas reforming. Small indirect reduction also happened simultaneously and reduced the amount of CO. At 800^{o}C, each gas lessened as effect of iron ore except CO_2, indirect reduction was predominant in this condition by converting CO and H_2 to CO_2 and H_2O. The decreasing of CH_4 denoted that gas reforming occurred as second main reaction.

It was well known that the pyrolysis product such as tar amount and gas were strongly affected by temperature. Fig. 2-11 shows the effect of temperature on pyrolysis tar amount and deposited carbon for LIGN fuel.

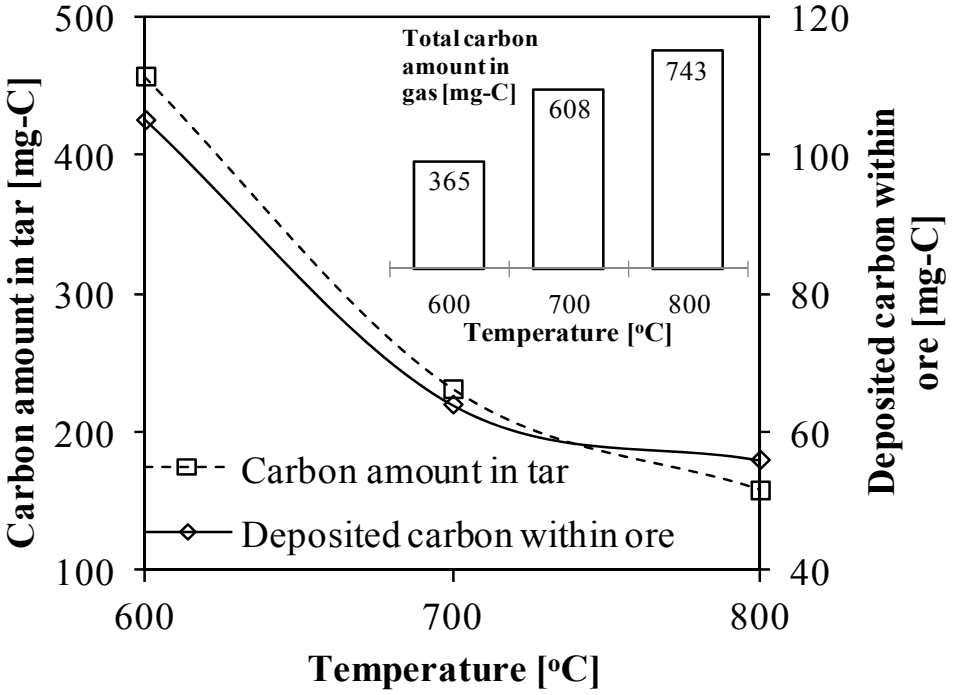

Fig. 2-11 Effect of temperatures on the tar amount and total gas volume in the pyrolysis of low-grade lignite coal, LIGN.

At high temperature, tar amount decreased and converted to gas product. Thermal cracking, decarboxylation, and depolymerization were preferred at high temperatures. It was also obviously that carbon deposition within ore pores declined at high temperature. The limited amount of tar from pyrolysis process affected small tar conversion so that deposited carbon also decreased. The tar components were more active and easier to decompose into gas phase. Therefore, total deposited carbon was proportional with the tar amount which was produced by pyrolysis. Interestingly, tar carbon was preferable to deposit within pore ore at high temperature. The pore volume was still vacant at high temperature due to small tar decomposition and carbon deposition

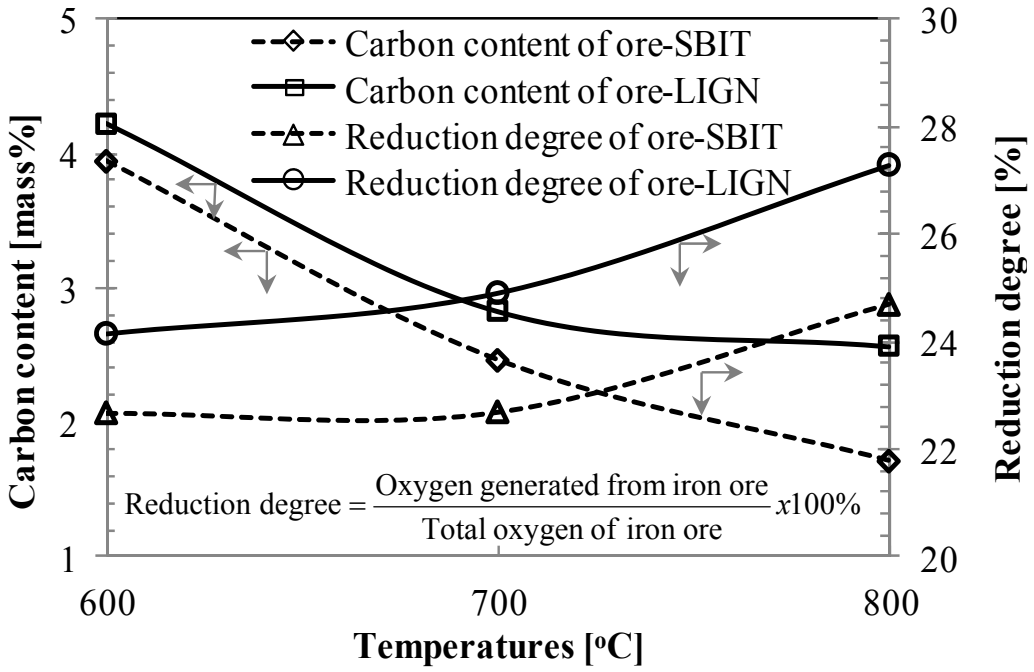

Fig. 2-12 Dependence of carbon deposited within iron ore and degree of reduction of iron ore on temperature, showed similar tendency: with increasing temperature, carbon content decreased and degree of reduction increased.

Fig. 2-12 shows the effect of temperature on deposited carbon within the pores and the degree of reduction of iron ore. As explained in the previous section, the amount of deposited tar carbon decreased at high temperatures due to the high activity of tar components during the decomposition reaction. Thus, the carbon content and degree of reduction showed an opposite behavior for both of the low-grade coals. It is well known that coal pyrolysis also generates gas products such as H_2, CO, CO_2, and CH_4. The concentration of each gas was strongly dependent on the pyrolysis conditions such as temperature, gas flow rate, and type of catalyst [33-35]. Besides the pyrolysis product, tar decomposition also produced several gas components as listed in reaction (2.1). The indirect reaction of iron ore with gas components such as CO and H_2 occurred simultaneously with carbon deposition. At high temperatures, coal pyrolysis and tar decomposition resulted in a larger amount of gas products; hence, the degree of reduction of iron ore increased at higher temperatures.

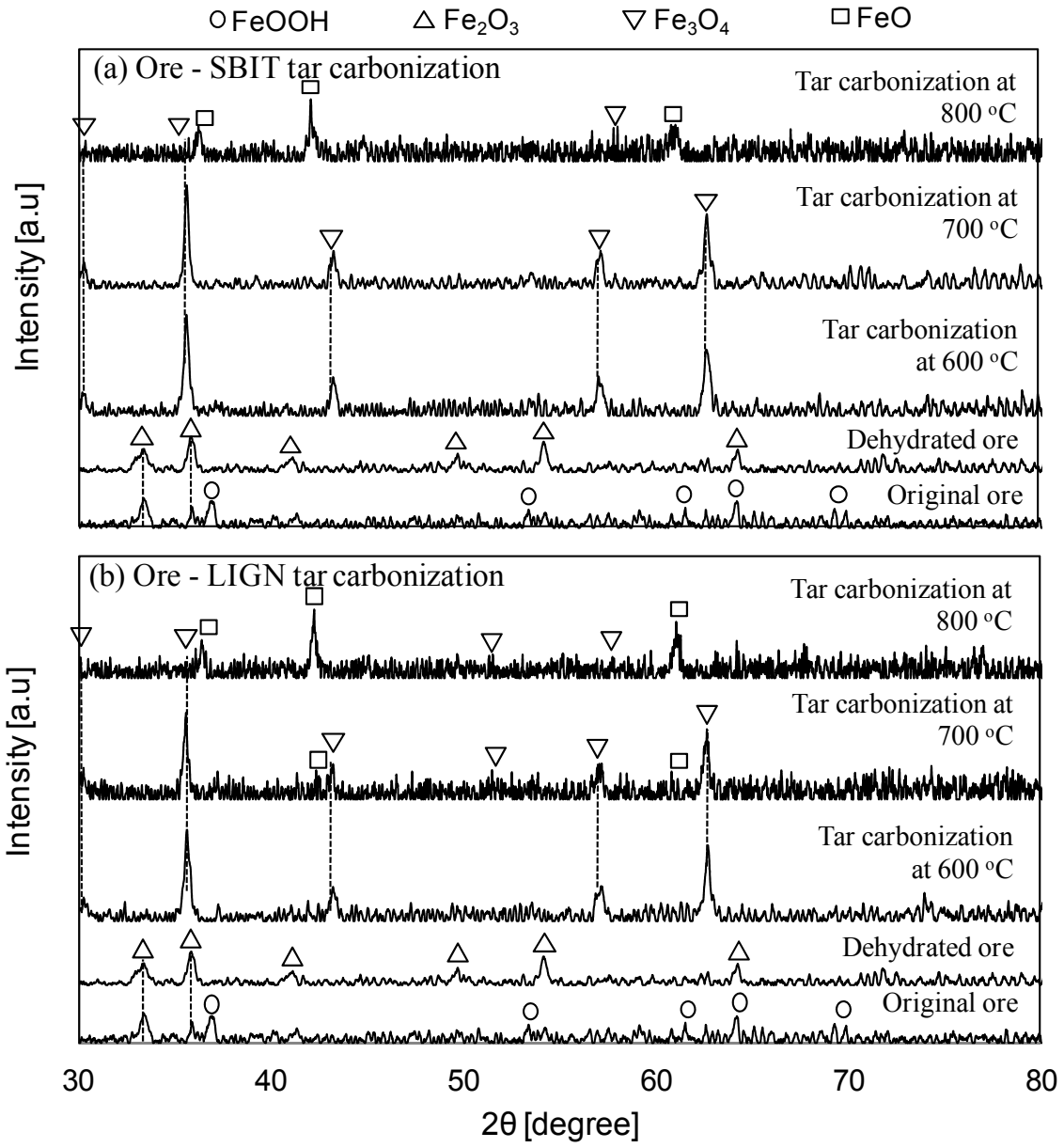

Fig. 2-13 XRD patterns of iron ore, dehydrated ore, and ore after tar carbonization at different temperatures, showed that dehydration enhanced FeOOH → Fe_2O_3 conversion and tar carbonization caused reduction of iron ore to magnetite and wustite at higher temperatures. SBIT: Indonesian Subbituminous Coal, LIGN: Australian Lignite Coal.

XRD analysis was performed to clarify the changing of iron compounds during tar decomposition and ore reduction. Fig. 2-13 shows that both the low-grade coals showed similar results. In the iron ore preparation, dehydration of CW changed the iron compound by reaction (2.2). FeOOH was never found in the material after dehydration, and this indicated that complete dehydration occurred at 450°C. Hematite in the ore was reduced by indirect reduction during the tar carbonization process. Wustite was never found after tar carbonization at low temperatures because the amount of reduced gas, such as CO and H_2, was insufficient for reduction to wustite. These XRD results agreed with the calculated degree of reduction and the phase diagram plot.

2.3.3.2 The reactivity of CVI ore in reduction reaction

Fig. 2-3-6 shows the variation in the weight change ratio with the temperature during heating, at a rate of 50°C/min with an argon flow rate of 500 NmL/min for the carbonized ore and the reference, which was a mixture of Fe_3O_4 and metallurgical coke. The weight change ratio indicated the reduction of iron ore. The minimum theoretical temperature of direct reduction of iron was 575°C, calculated by HSC Chemistry 7 Simulation [36] based on the following reaction:

$$Fe_3O_4 + 4C(A) \rightarrow 3Fe + 4CO(g) \qquad (2.6)$$

The type of deposited carbon within iron ore was amorphous [37]. The CO product was directly derived by high flow rate of Ar, thus boudouard reaction, $CO_2(g) + C(A) \rightarrow 2CO(g)$ never occurred.

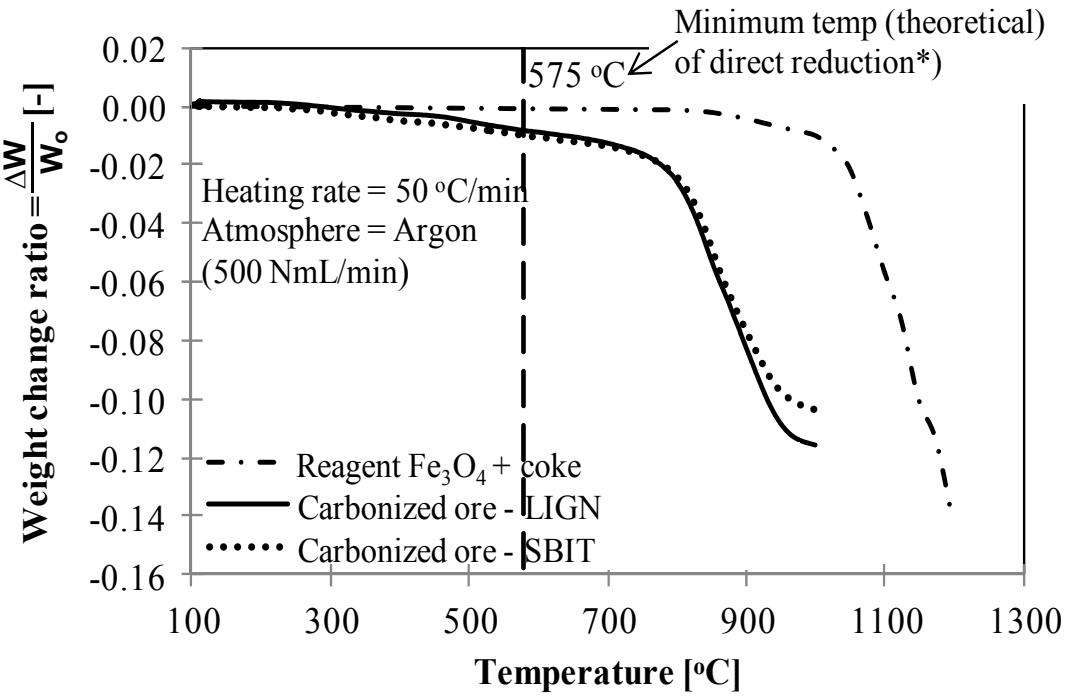

Fig. 2-14 Reduction reaction of carbon-deposited ore with low-grade coal showing that the direct reduction of the carbon-deposited ore began at 750°C, while that of the reference mixture of Fe_3O_4 and coke began at 1100°C.

The reduction of carbonized ore began at 750°C, while that of the reference mixture of Fe_3O_4 and coke began at 1100°C. This result indicated that the carbonized ore was more reactive than the mixture of Fe_3O_4 and coke. In the case of carbonized ore, since the carbon material infiltrated and deposited in the ore nanopores, the distance between the carbon and iron atoms was minimized. The nanoscale contact between iron ore and carbon enhanced the contacting area and resulted in the increasing reaction rate. The reduction of carbonized ore by LIGN coal was slightly faster than that of the carbon-deposited ore by SBIT coal because of the small difference in the amount of carbon deposited within the pores in the two ores. Generally, high carbon content in the carbonized ore would make it more reactive in the reduction reaction.

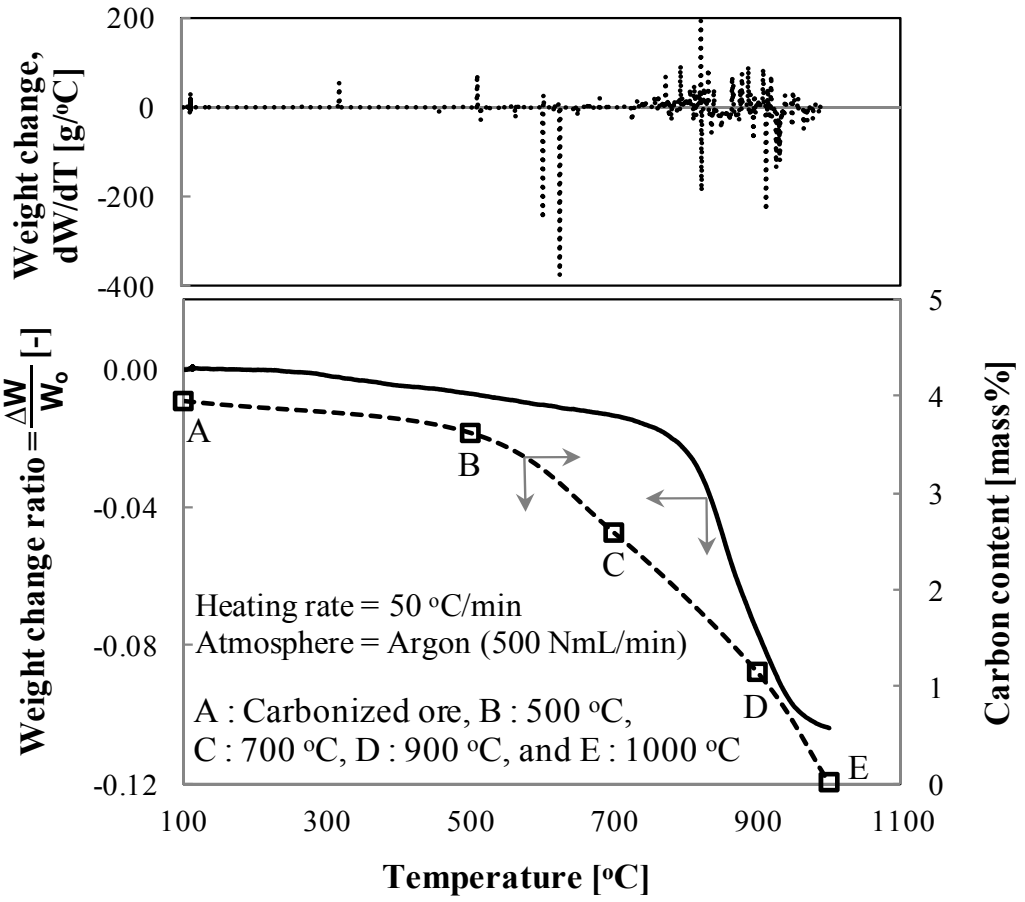

Fig. 2-15 Relationship between the reduction reaction and carbon content during direct reduction, showed that deposited carbon from tar carbonization was consumed and effective in reducing iron ore.

In order to confirm the reduction of carbonized ore, the relationship of carbon content and weight change was plotted as seen in Fig. 2-15. The weight change profile during the reduction reaction showed the following: an initial gradual decrease up to 750°C and rapid decrease at temperatures higher than 750°C. A similar tendency emerged in the case of the carbon content within the carbonized ore. By considering the tar decomposition process, the first gradual decreasing was related to re-evaporation of tar components and the second rapid decrease was the ore reduction process. When tar decomposition occurred in the porous ore,

small amounts of unreacted tar were entrapped within the pore while the temperature was decreasing. These tar components were re-evaporated at the beginning of the increase in the temperature during reduction reaction. The rapid decreasing reveals the iron ore reduction from Fe_3O_4 to FeO and Fe, seen clearly in Fig. 2-16. XRD analyses were performed for several temperatures during heating up to observe the phase change of iron ore.

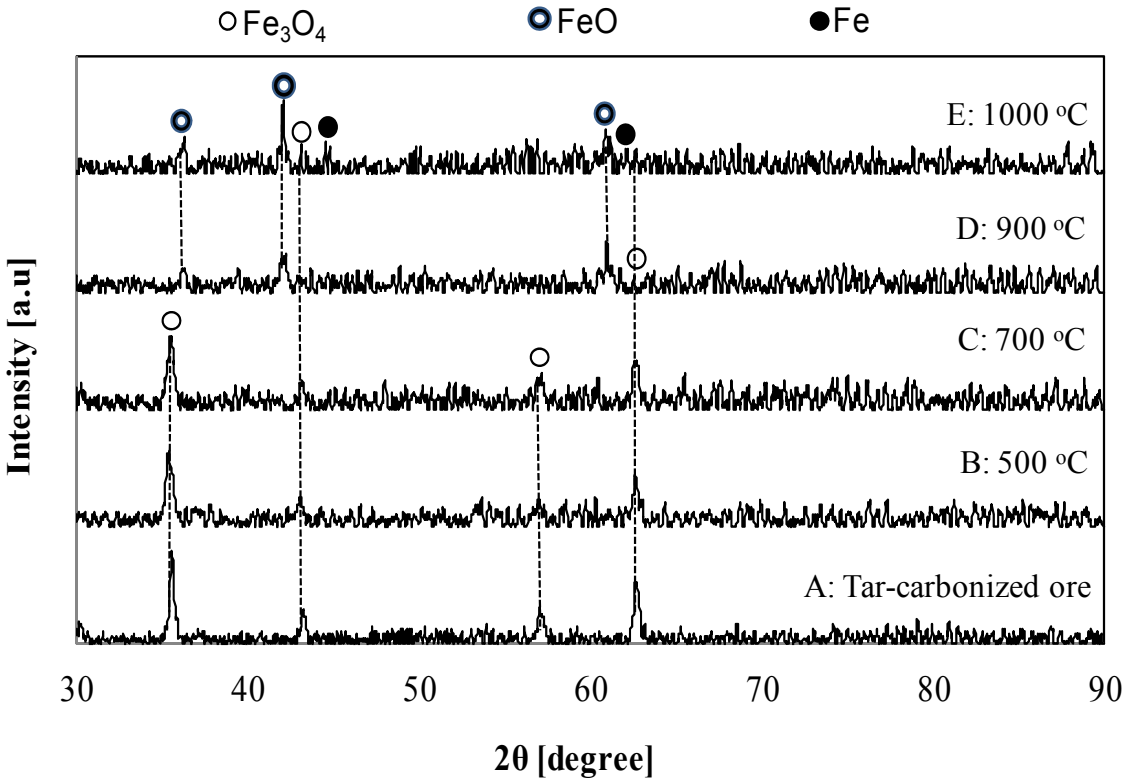

Fig. 2-16 Changes in XRD patterns of tar-carbonized iron ore during direct reduction under Ar at a flow rate of 500 NmL/min, showed that the closely contacted deposited carbon from tar carbonization was effective in reducing iron ore to wustite and metalic iron.

The XRD results showed that the patterns were similar up to 700°C, which only magnetite was found as the original of carbonized ore. It means that the ore reduction never started at this

temperature. A different XRD pattern was obtained at 900°C, which corresponded to magnetite and wustite; this indicated that ore reduction occurred at this temperature. This result also matched with the weight change ratio where a rapid decrease occurred between the temperatures of 700 and 900°C. The final product of ore reduction, an metallic iron was found at 1000°C. This was also confirmed by the decreasing rate of weight change ratio, which was almost horizontal at the end of the process.

2.3.3 Optimum temperature for maximazing carbon deposition within ore

2.3.3.1 Effect of pyrolysis temperature

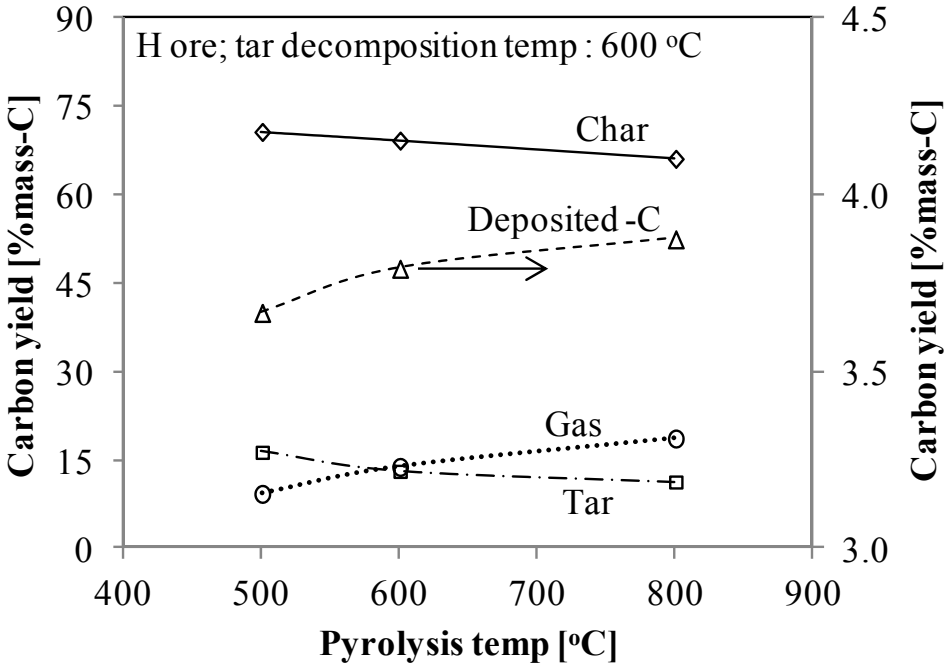

Fig. 2-17 Product distributions of integrated coal pyrolysis–tar decomposition over Hamersley (H) iron ore at different pyrolysis temperatures showed that tar decomposition occurred at elevated temperatures to produce small amounts of tar components and high amounts of deposited carbon.

Fig. 2-17 shows the effect of pyrolysis temperature on the product distribution of integrated coal pyrolysis–tar decomposition over low-grade iron H ore. When the temperature of tar decomposition process and other experimental parameters were kept constant, the amount of deposited carbon within the iron ore was affected mainly by the volatile matter (tar and gases) produced by coal pyrolysis. Tar decomposition occurred over the porous iron ore, and produced gases and deposited carbon through reaction (2.1).

A high pyrolysis temperature decreased the amount of tar and increased carbon deposition in the ore as a result of the tar decomposition process shown in Fig. 2-17. Gas production was also enhanced at high temperatures because of thermal cracking of the coal and tar decomposition. A large amount of tar promoted high conversion of tar material in the decomposition process to produce gases and deposited carbon. High carbon deposition was achieved when a large amount of tar was generated from the pyrolysis process. High-temperature pyrolysis, which produced large amounts of tar, was therefore suitable for the carbon deposition process.

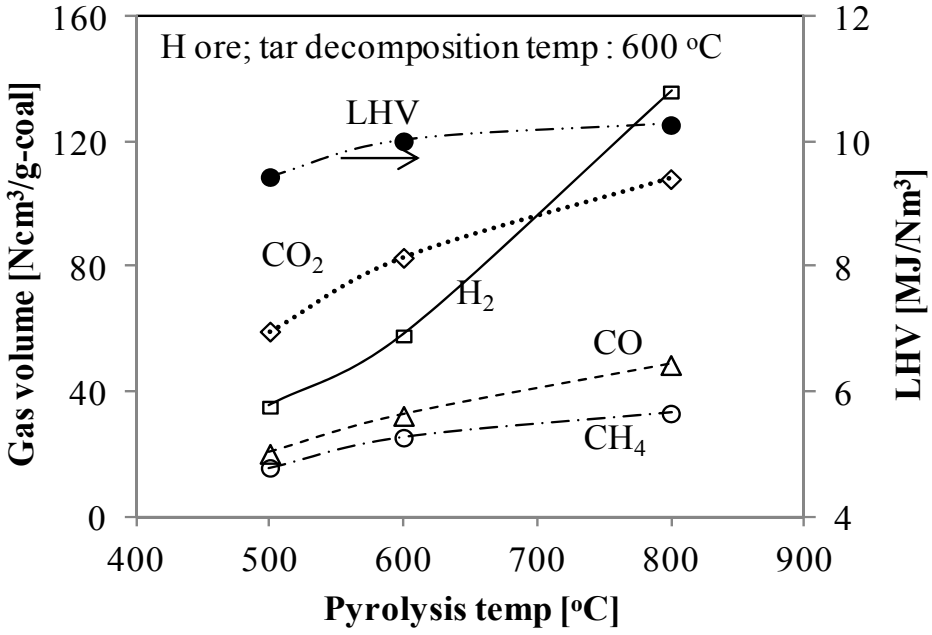

Fig. 2-18 Effect of pyrolysis temperature on gas composition and lower heating value (LHV) of integrated coal pyrolysis–tar decomposition over Hamersley iron ore; each gas volume increased at elevated temperature as a result of thermal cracking of coal and tar components.

As well as tar carbon deposition in the porous iron ore, the integrated coal pyrolysis–tar decomposition also produced several gases such as CO, CO_2, H_2, CH_4, and other light hydrocarbon. Fig. 2-18 shows the effect of pyrolysis temperature on the gas composition and

lower heating value. It can be seen that all gas components were enhanced at elevated temperatures, as a result of thermal cracking of coal and decomposition of the tar component. Thermal cracking, decarboxylation, and depolymerization of carbonaceous materials are promoted at high temperatures. In addition, the high activities of tar components at elevated temperatures increased tar conversion and made decomposition to the gas phase easier. It was also found that H_2 production at 800 °C increased rapidly compared with CO production. Gas reforming began to occur and enhanced H_2 and CO production [38]. Based on the gas reforming stoichiometry, the mole of H_2 was higher than CO in the gas reforming products. High contents of H_2 and CO at elevated temperatures also increased the heating value of the gas product. A high pyrolysis temperature therefore produced not only high carbon deposition but also increased the heating value of the gas products.

2.4.3.2 Effect of decomposition temperature (CVI process)

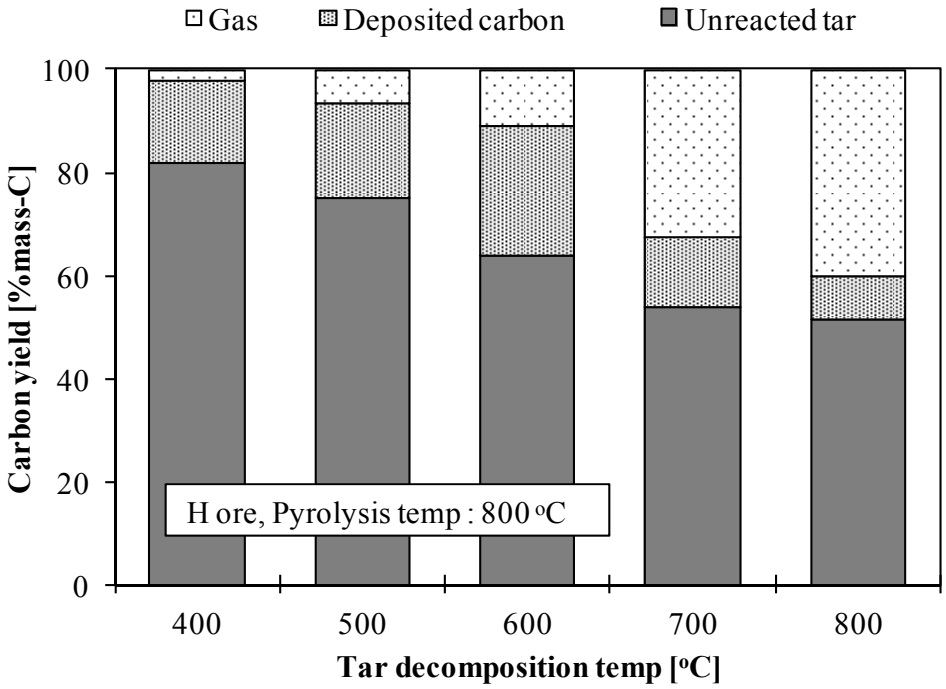

Fig. 2-19 Effect of tar decomposition temperature on tar product distribution; the tar decomposition over Hamersley ore showed that the highest carbon deposition was attained at 600°C, whereas thermal cracking was predominant to produce gases at higher temperatures (>600°C)

Based on the results of the pyrolysis experiments, tar decomposition was performed at the highest pyrolysis temperature, which generated the largest amount of deposited carbon. Fig. 2-19 shows the effect of decomposition temperature on the tar product distribution over H ore at a constant pyrolysis temperature of 800°C. The amount of unreacted tar decreased at elevated temperatures, indicating high conversion of tar components during the decomposition process. High activity of the tar component over the surface of the porous iron ore promoted decomposition to produce gases, deposited carbon, and lighter hydrocarbons. Metal oxides prevent the formation of stable chemical structures in hydrocarbons and speed up hydrocarbon

degradation by weakening the C–C bonds, decreasing the activation energy for the complex tar decomposition process [31]. The products of tar decomposition altered with tar decomposition temperature (400–800 °C). Tar carbon deposition within the porous ore, rather than formation of gas products, was predominant in the temperature range 400–600 °C. At temperatures above 600 °C, tar decomposition generated gas products rather than depositing carbon. At temperatures above 600°C, tar decomposition generated gas products rather than depositing carbon. Based on the gibbs free energy, ΔG^0, the gasification of carbon and direct reduction of iron ore through reaction (2.7) and (2.8) would be started at 698 and 651°C, respectively [36,39]. Therefore, direct reduction of iron ore and gasification of the deposited carbon took place and enhanced carbon conversion to gas products. This means that the rate of carbon deposition from tar decomposition was smaller than the rate of carbon consumption by reaction (2.7) and (2.8). The maximum carbon deposition in the porous ore was achieved at a tar decomposition temperature of 600°C. The optimum conditions of integrated coal pyrolysis–tar decomposition for producing deposited carbon in porous iron were therefore pyrolysis at 800°C and tar decomposition at 600°C.

$$Fe_2O_3(s) + 3C \leftrightarrow 2Fe(s) + 3CO(g) \quad (2.7)$$

$$C + CO_2(g) \leftrightarrow 2CO(g) \quad (2.8)$$

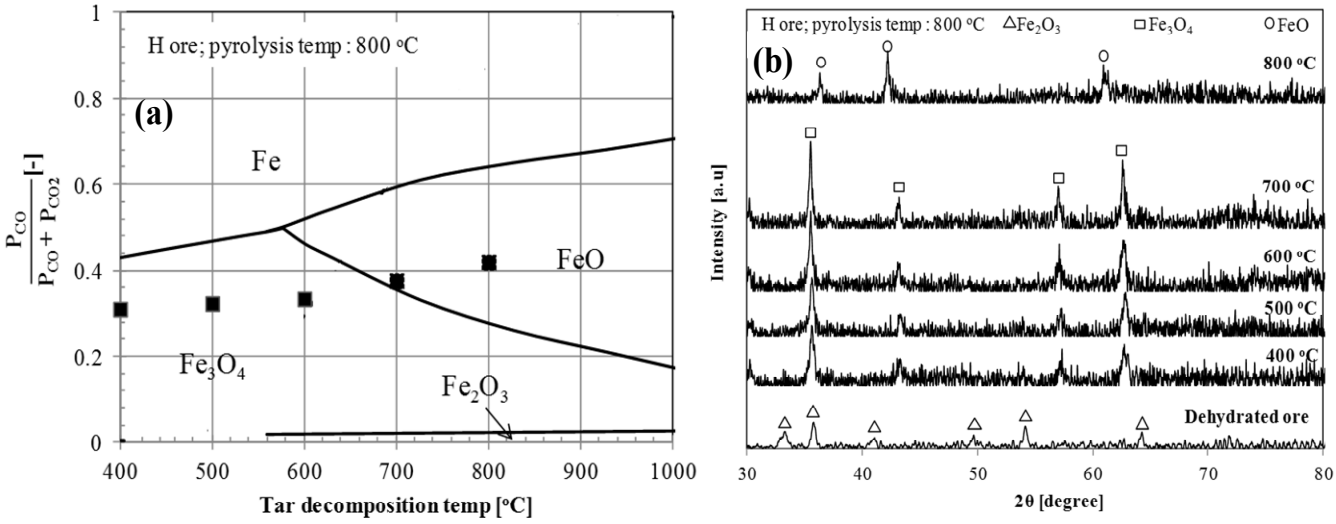

Fig. 2-20 (a) Phase diagrams for iron–wüstite–magnetite systems showed that a high temperature of tar decomposition resulted in a large reduction degree due to high amount of CO and faster reduction rate. (b) X-ray diffraction (XRD) patterns of iron ore after tar decomposition at different temperatures showed that FeO can be found at 800°C; this was consistent with the phase diagram.

The phase diagrams in Fig. 2-20a show the effect of tar decomposition temperature on the iron–wustite–magnetite system for H ore. This figure explains the indirect reduction of CO through reactions (2.9)–(2.11).

$$3Fe_2O_3(s) + CO(g) \leftrightarrow 2Fe_3O_4(s) + CO_2(g); \quad \Delta H^o = -52.86\ \text{kJ/mol} \qquad (2.9)$$

$$Fe_3O_4(s) + CO(g) \leftrightarrow 3FeO(s) + CO_2(g); \quad \Delta H^o = 36.25\ \text{kJ/mol} \qquad (2.10)$$

$$FeO(s) + CO(g) \leftrightarrow Fe(s) + CO_2(g); \quad \Delta H^o = -17.31\ \text{kJ/mol} \qquad (2.11)$$

The pyrolysis process occurred at a constant temperature and resulted in similar tar and gas products, but indirect reduction of CO generated different products. The reaction rate of iron ore reduction was higher at high temperatures, and was sufficient to produce FeO in tar decomposition at 800 °C [40]. High-temperature tar decomposition therefore resulted in a large degree of reduction, as indicated by the generation of FeO, because of the high reduction

reaction. In order to clarify the reduction degree, XRD analysis was performed for the products at different tar decomposition temperatures, as shown in Fig. 2-20b. It can be clearly seen that all Fe_2O_3 was changed into Fe_3O_4 as a result of indirect reduction by pyrolysis gases. Indirect reduction occurred simultaneously with tar decomposition and carbon deposition. This result agreed with the phase diagram, which showed that FeO was found at elevated tar decomposition temperatures because of a large amount of indirect reduction. Tar decomposition at elevated temperatures therefore produced small amounts of deposited tar carbon in the porous iron ore, but a high degree of reduction.

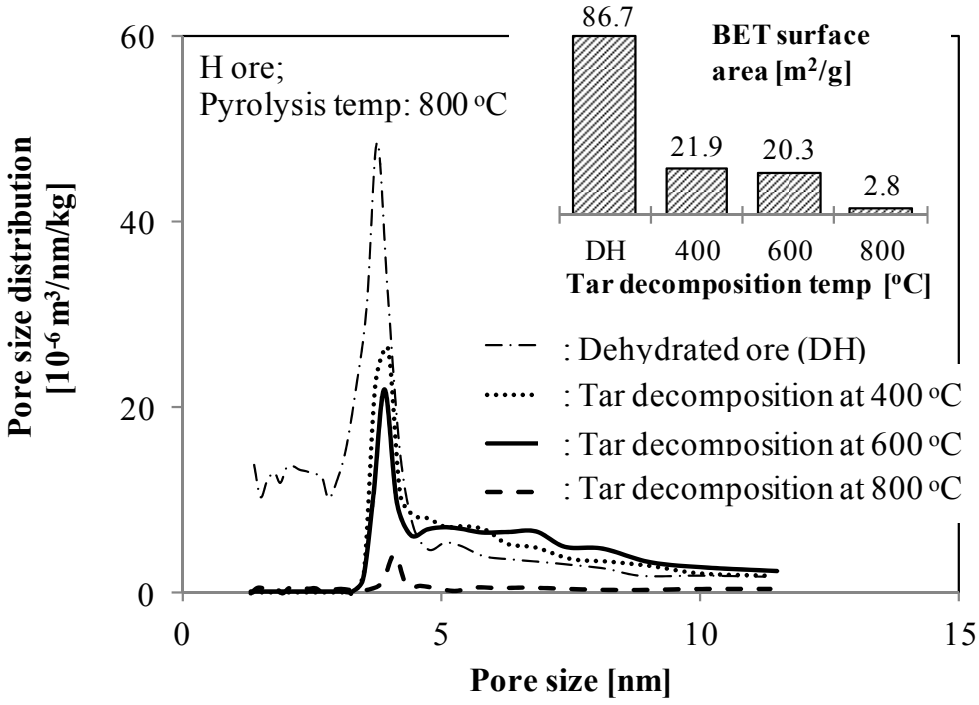

Fig. 2-21 Changes in pore size distributions and BET surface areas of Hamersley ore after tar decomposition at different carbonization temperatures showed that the BET surface area and pore size distribution at 800°C decreased significantly when the amount of deposited carbon was smallest, indicating that sintering started to occur.

Fig. 2-21 shows the changes in pore size distribution and BET surface area of H ore after tar decomposition at different temperatures. Simultaneously with tar decomposition, carbon infiltrated and was deposited in the porous iron ore, resulting in reduction in both the pore size distribution and the BET surface area. Interestingly, the carbon was only deposited in pores of size less than 4 nm because of the specific tar component. The carbon content of the porous ore was proportional to the decreases in pore size distribution and BET surface area, except in the case of tar decomposition at 800°C. The carbon content of the iron ore at 800°C was the smallest, but the decreases in pore size distribution and BET surface were higher than those under other temperature conditions. During the tar decomposition process, the iron bed was heated and kept at a constant temperature of 800°C, which was sufficiently high to promote sintering of the iron ore. The melting point of the iron ore (Fe_2O_3) was 1460°C [36]. During sintering, the pores in the iron ore joined up, resulting in a dense material. This phenomenon significantly decreased the BET surface area and pore size distribution and resulted in the lowest carbon deposition. Thus, the tar decomposition process should be performed below 800°C to produce high carbon deposition and avoid sintering.

2.4.3.3 Effect of iron ore with different combined water

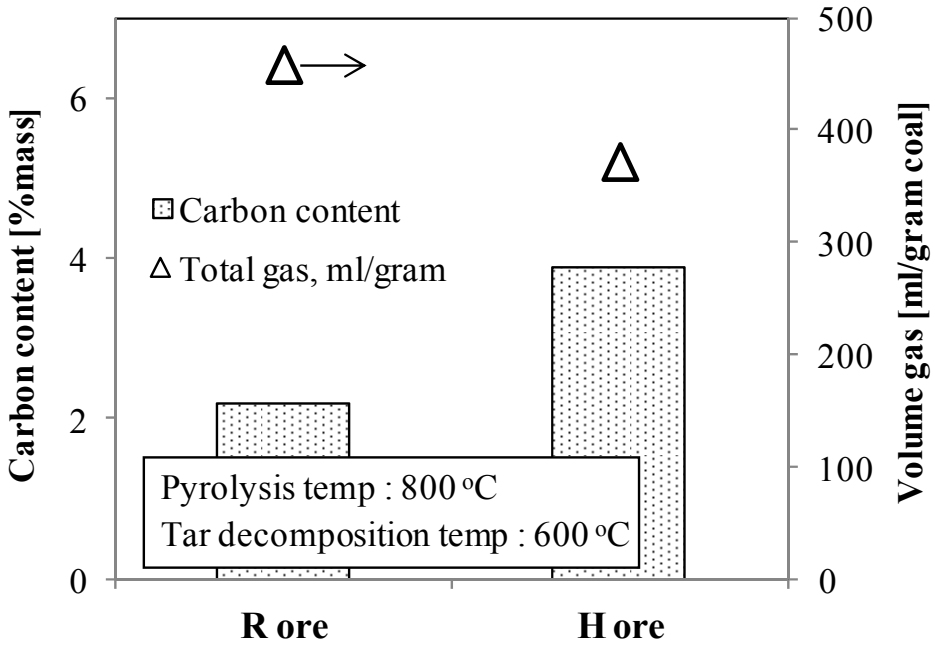

Fig. 2-22 Effect of different iron ores on deposited carbon and total gas volume showed that Hamersley (H) ore gave higher carbon deposition but a lower total gas volume compared with Robe-river (R) ore.

The results described above show that the optimum conditions for producing high carbon deposition were pyrolysis at 800 °C and tar decomposition at 600 °C. Another iron ore, the R ore, with a different CW content, was subjected to similar conditions for comparison. Fig. 2-22 shows the effect of different iron ores on the amount of deposited carbon and the total gas volume under the optimum temperature conditions. Using a similar tar component from coal pyrolysis, the H ore generated a larger carbon content but a smaller gas volume than the R ore. This indicated that the H ore had higher selectivity for carbon deposition during tar decomposition than the R ore. Decomposition of the tar component produced gases and deposited carbon in the porous ore, and the selectivity of the iron ore was established from the

ratio of these products. Generally, several factors influence the selectivity of a solid catalyst, such as surface structure, composition, surface mobility, and charge transport [41].

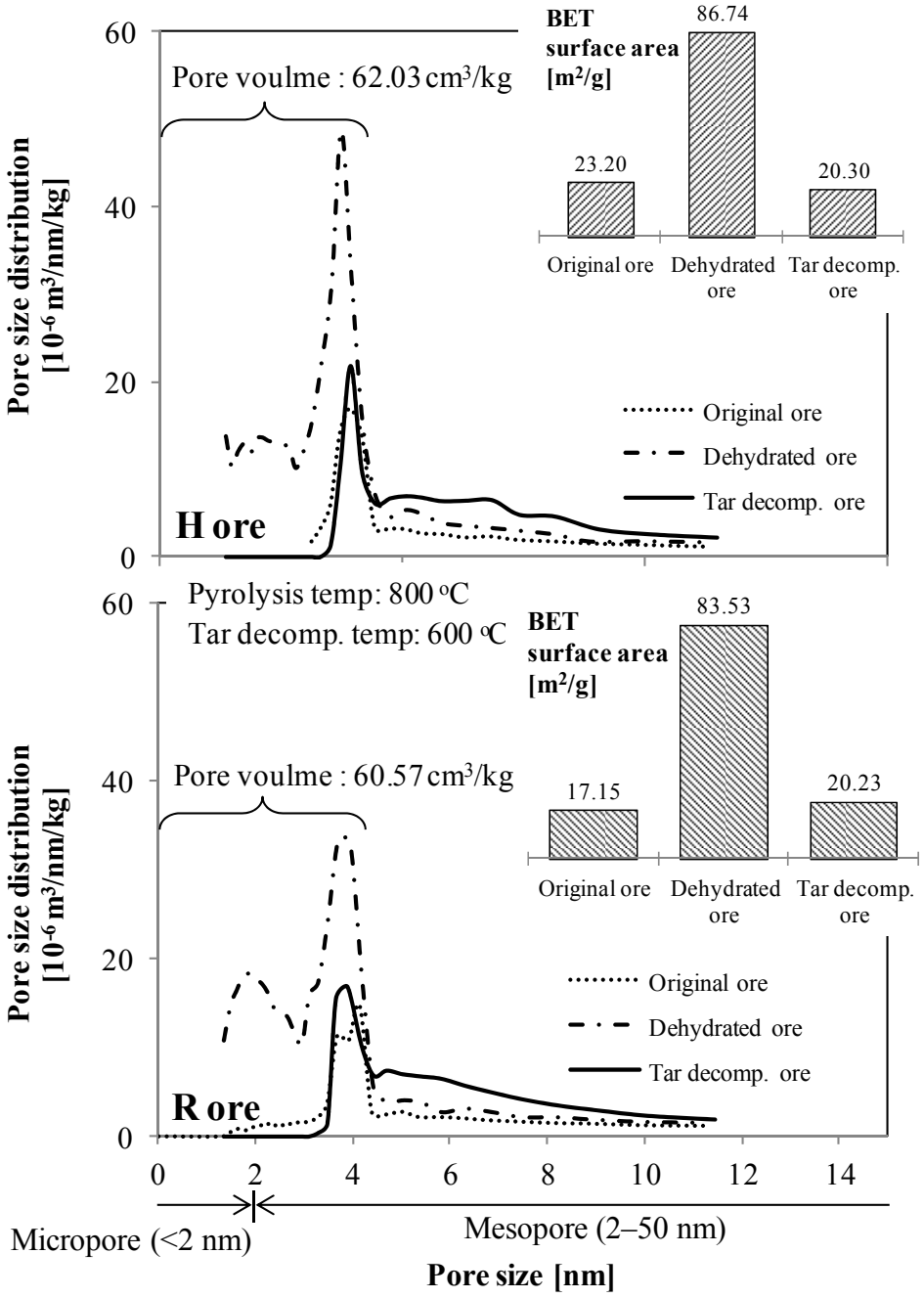

Fig. 2-23 Changes in Brunauer–Emmett–Teller (BET) surface areas and pore size distributions of two different iron ores [Hamersley (H) and Robe-river (R)] showed that larger carbon deposition in the R ore was the result of larger micropores, which were created during dehydration.

In order to investigate the factors related to the selectivity of the tar decomposition process in detail, BET analysis was performed over both H and R ores, as shown in Fig. 2-23. Dehydration of CW at 450 °C enhanced the surface area of the iron ore and created a porous ore. The surface areas of both the H and R ores after the dehydration and tar decomposition processes were similar. The surface area therefore could not explain the selectivities and different carbon contents. Different results were obtained for the pore size distributions after dehydration of CW. The H ore had larger numbers of micropores than the R ore, in particular pores of size 4 nm, although dehydration was performed under similar conditions. The tar carbon was deposited in the iron ore in pores of size less than 4 nm. These results clearly show that differences among the carbon contents were caused by the number of micropores after the dehydration process. Therefore, the pore size distribution was the dominant parameter rather than the surface area in determining the amount of deposited carbon within the iron ore.

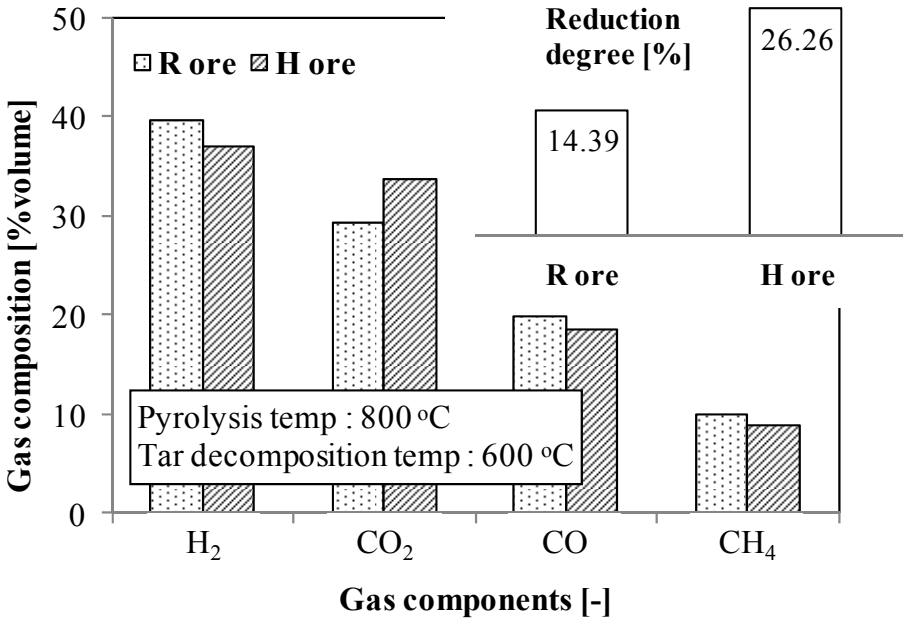

Fig. 2-24 Reduction degree of iron ore and gas composition of integrated coal pyrolysis–tar decomposition with various iron ores [Hamersley (H) and Robe-river (R)] showed that H ore produced smaller mounts of H_2 and CO, but gave higher reduction degrees, as a result of large consumption of these gases in indirect reduction

Fig. 2-24 shows the gas compositions and reduction degrees for integrated coal pyrolysis–tar decompositions, using different iron ores, under the optimum temperature conditions. As explained in the previous section, indirect reduction of the iron ore by pyrolysis gases occurred simultaneously with tar decomposition and carbon deposition. The reduction degree was estimated using the following equation:

$$\text{Reduction degree}(\%) = \frac{\text{Oxygen generated from ores}}{\text{Total removable oxygen}} \times 100\% \qquad (2.12)$$

The H ore gave a higher reduction degree than the R ore. The higher reduction degree represented large consumption of a reducing agent, CO, to produce CO_2. The gas composition shown in Fig. 2-4-7 confirmed this phenomenon, because the amount of CO gas in the H ore was

smaller than that in the R ore, because of high CO consumption in the indirect reaction. The H ore therefore produced larger amounts of deposited carbon in the porous ore and a higher reduction degree, but a smaller total volume and energy of gas products.

2.4 Conclusions

This chapter describes the proposed system, integrated pyrolysis-tar decomposition by CVI process for producing ore contained carbon, CVI ore through effective utilization of low grade coal, biomass and low grade iron ore in iron and steel industry. In section 2.3.1, the comparative study of various solid fuels as carbon source of decomposition process was performed related to tar decomposition and carbon deposition. The main results can be summarized as follows:

1 The carbon deposition was dependent on the tar amount that produced during pyrolysis process. Deposited carbon from high grade bituminous coal was higher than other solid fuels due to large tar product from pyrolysis process. Ratio of deposited carbon during tar decomposition was affected by availability of surface area. Biomass palm kernel shell, PKS resulted high ratio of deposited carbon because of small reacted tar and large vacancies of surface area.

2 The porous ore which was created through dehydration process shows promising material as carbon storage and tar decomposition. Tar carbon infiltrated and deposited effectively within ore pores which was created during the dehydration of combined water

3 Beside tar decomposition and carbon deposition, indirect reduction of iron ore by gas product (CO and H_2) simultaneously occurred and altered Fe_2O_3 to Fe_3O_4 at temperature of 600^oC.

In section 2.3.2, the study related to temperature of tar decomposition and reactivity of CVI ore in reduction process was performed more detail with the following conclusions.

1. The low grade iron ore had a significant influence on catalytic tar decomposition, and it increased the carbon content within the ore and the total amount of gas product. The

carbon deposition decreased at higher temperature due to larger gas generation in tar decomposition process.

2. At high temperatures, the reduction degree of iron ore increased, and it had a contradictory relationship with the carbon content for both of the low-grade coals. Coal pyrolysis and tar decomposition produced gas products at high temperatures, which were used in the reduction of iron ore. At high temperature, 800^{o}C, the FeO was found as a result of indirect reduction due to large gas generation.
3. The CVI ore was more reactive than the mixture of Fe_3O_4 and coke because tar carbon deposited into the nanopores; consequently, the distance between the carbon and iron atoms was minimized. The nanoscale contact between the iron ore and carbon enhanced the contacting area and resulted in the increasing of reaction rate.

In the section 2.3.3, the optimum temperature for both pyrolysis and tar decomposition were determined to obtain the maximum carbon deposition in the porous iron ore and the following conclusions were derived.

1. The pyrolysis at the highest temperature produced a large amount of carbon deposition and a clean gas product with extra heating value. Thermal cracking of the coal component increased at high temperatures and produced large amounts of gas and tar for the decomposition process.
2. Deposited carbon, rather than gas products, was predominantly produced at lower temperatures (400–600 °C), and the opposite behavior was observed in tar decomposition at higher temperatures (700–800 °C). The gasification of carbon at higher temperatures decreased the amount of carbon deposited within the porous ore. When the tar decomposition performed at 800°C, the FeO was obtained but the sintering of iron ore

was also started. The highest carbon deposition was obtained at a pyrolysis temperature of 800°C and a tar decomposition temperature of 600°C.

3. Hamersley, H ore attained higher carbon deposition but a lower amount of gaseous products compared with Robe-river, R ore, as a result of the formation of larger pores during the dehydration process. The pore size distribution was a more important factor than the BET surface area in the carbon deposition process.

These results demonstrated that the proposed system, integrated pyrolysis-tar decomposition over low-grade ores by CVI process is one of the most promising methods for the effective utilization not only low grade coal but also biomass in the iron and steel industry.

References

[1] World Coal Association. *Coal and Steel*; World Coal Association publication: Richmond, UK, 2007; p. 5.

[2] MA. Diez, R. Alvarez, C. Barriocanal, Coal for metallurgical coke production: predictors of coke quality and future requirements for cokemaking, International Journal of Coal Geology 50 (2002) 389-412.

[3] M. Kirschen, K. Badr, H. Pfeifer, Influence of direct reduced iron on the energy balance of the electric arc furnace in steel industry, Energy 36 (2011) 6146–6155.

[4] U. Srivastava, SK. Kawatra, TC. Eisele, Production of pig iron by utilizing biomass as a reducing agent, International Journal of Mineral Processing 119 (2013) 51-57.

[5] MA. Diez, R. Alvarez, JL. Cimadevilla, Briquetting of carbon-containing wastes from steelmaking for metallurgical coke production. Fuel (2012), http://dx.doi.org/10.1016/j.fuel.2012.04.018

[6] H. Shui, Y. Wu, Z. Wang, Z. Lei, C. Lin, S. Ren, C. Pan, S. Kang, Hydrothermal treatment of a sub-bituminous coal and its use in coking blends, Energy and Fuels 27 (2013) 138-144.

[7] S. Das, S. Sharma, R. Choudhury, Non-coking coal to coke: use of biomass based blending material, Energy 27 (2002) 405-414.

[8] X. Li, H. Song, Q. Wang, C. Meesri, T. Wall, J. Yu, Experimantal study on drying and moisture re-adsorption kinetics of an Indonesia low rank coal, Journal of Environmental Sciences Supplement 1 (2009) S127–S130.

[9] C. Myren, C. Hornell, E. Bjornbom, K. Sjostrom, Catalytic tar decomposition of biomass pyrolysis gas with a combination of dolomite and silica, Biomass and Bioenergy 23 (2002) 217-227.

[10] J. Srinakruang, K. Sato, T. Vitidsant, K. Fujimoto, A highly efficient catalyst for tar gasification with steam, Catalysis Communications 6 (2005) 437-440.

[11] L. Devi, KJ. Ptasinski, FJ. Janssen. A review of the primary measures for tar elimination in biomass gasification processes. Biomass and Bioenergy 4 (2003): 125–140.

[12] MM. Yung, WS. Jablonski, KA. Magrini-Bair. Review of catalytic conditioning of biomass-derived syngas. Energy and Fuels23 (2009): 1874-1887.

[13] C. Zhang, RB. Brown, A. Suby, K. Cummer. Catalytic destruction of tar in biomass derived producer gas. Energy Conversion and Management 45 (2004): 995–1014.

[14] P. Lu, Z. Yuan, C. Wu, L. Ma, Y. Chen, N. Tsubaki. Bio-syngas production from biomass catalytic gasification. Energy Conversion and Management 48 (2007): 1132–1139.

[15] PA. Simell, JO. Hepola, AO. Krause. Effects of gasification gas components on tar and ammonia decomposition over hot gas cleanup catalysts. Fuel 76 (1997): 1117–1127.

[16] A. Asadullah, T. Miyazawa, SI. Ito, K. Kunimori, M. Yamada, K. Tomishige. Gasification of different biomasses in a dual-bed gasifier system combined with novel catalysts with high energy efficiency. Appl Catal A: Gen. 267 (2004): 95–102.

[17] H. Purwanto and T. Akiyama. Hydrogen production from biogas using hot slag. International Journal of Hydrogen Energy 31 (2006): 491-495

[18] R. Coll, J. Salvado, X. Farriol, D. Montane. Steam reforming model compounds of biomass gasification tars: conversion at different operating conditions and tendency towards coke formation. Fuel Processing Technology 74 (2001): 19–31

[19] ZY. Abu El-Rub, EA. Bramer, G. Brem. Experimental comparison of biomass chars with other catalysts for tar reduction. Fuel 87 (2008): 2243-2252

[20] Y. Kashiwaya and T. Akiyama. Nanocrack formation in hematite through the dehydration of goethite and the carbon infiltration from biotar. Journal of Nanomaterials 2010, Article ID 235609.

[21] A. Uddin, H. Tsuda, S. Wu, E. Sasaoka. Catalytic decomposition of biomass tars with iron oxide catalysts. Fuel 87 (2008): 451–459.

[22] WC. Xu and A. Tomita. Effect of coal type on the flash pyrolysis of various coals. Fuel 66 (1987): 627-631

[23] K. Raveendran, A. Ganesh, KC. Khilar. Pyrolysis characteristics of biomass and biomass components. Fuel 75 (1996): 987-998.

[24] K. Raveendran, A. Ganesh. Heating value of biomass and biomass pyrolysis products. Fuel 75 (1996): 1715-1720.

[25]MM. Hagedorn, H. Bockhorn, L. Krebs. U. Muller. A comparative kinetic study on the pyrolysis of three different wood species. J. Anal. Appl. Pyrolysis 68 (2003): 231_/249

[26] PT. Williams and S. Besler. The influence of temperature and heating rate on the slow pyrolysis of biomass. Renewable energy 7 (1996): 233-250.

[27] JV. Christiansen, A. Feldthu, L. Carlsen. Flash pyrolysis of coals. Temperature-dependent product distribution. Journal of Analytical and Applied Pyrolysis 32 (1995): 51-63

[28] MV. Kok, E. Ozbas, O. Karacan, C. Hicyilmaz. Effect of particle size on coal pyrolysis. Journal of Analytical and Applied Pyrolysis 45 (1998): 103–110.

[29] WC. Xu and A. Tomita. Effect of temperature on the flash pyrolysis of various coals. Fuel 66 (1997): 632-636

[30] HY. Cai, J. Goell, IN. Chatzakis, JY. Lim, DR. Dugwell, R. Kandiyoti. Combustion reactivity and morphological change in coal chars: effect of pyrolysis temperature, heating rate and pressure. Fuel 75 (1996): 15-24.

[31] BX. Shen and L. Qin, Study on MSW catalytic combustion by TGA, Energy Conversion and Management 47 (2006) 1429–1437.

[32] C. Li, D. Hirabayashi, K. Suzuki, Development of new nickel based catalyst for biomass tar steam reforming producing H_2-rich syngas, Fuel Processing Technology 90 (2009) 790–796.

[33] MB. Folgueras, RM. Diaz, J. Xiberta, Pyrolysis of blends of different type of sewage sludge with one bituminous coal, Energy 30 (2005) 1079–1091.

[34] E. Putun, Catalytic pyrolysis of biomass: effects of pyrolysis temperature, sweeping gas flow rate and MgO catalyst, Energy 35 (2010) 2761–2766.

[35] SW. Park and CH. Jang, Effects of pyrolysis temperature on changes in fuel characteristics of biomass char, Energy 39 (2012) 187–195.

[36] A. Roine, P. Lamberg, T. Katiranta, J. Salminen, HSC Chemistry 7 Simulation. Outotec, (2009).

[37] P. Delhaes, Chemical vapor deposition and infiltration process of carbon materials, Carbon 40 (2002) 641-657

[38] J. Liu, H. Hu, L. Jin, P. Wang, S. Zhu, Integrated coal pyrolysis with CO_2 reforming of methane over Ni/MgO catalyst for improving tar yield, Fuel Processing Technology 91 (2010) 419-423.

[39] XA. Gracia, NA. Alarcon, AL. Gordon, Steam gasification of tars using a CaO catalyst, Fuel Processing Technology 58 (1999) 83-102.

[40] K. Mondal, H. Lorethova, E. Hippo, T. Wiltowski, SB. Lalvani, Reduction of iron oxide in carbon monoxide atmosphere-reaction controlled kinetics, Fuel Processing Technology 86 (2004) 33-47.

[41] GA. Somorjai, J.Y. Park, Molecular factors of catalytic selectivity, Angew. Chem., Int. Ed 47 (2008) 9212-9228.

Chapter 3

Kinetics analysis of tar decomposition over porous low grade ore

3.1 Introduction

Pyrolysis is the main process for solid fuels utilization such as biomass and coal which generate char, tar and gas product. As by-product, tar contains condensable organic material with high energy matter which may cause operational problem such as pipe blocking, condensation, and tar aerosol formation [1]. Therefore, complete decomposition of tar into a major fraction of the gaseous product that integrated with the reactor system is most essentials research subject in order to enhance the efficiency and cut the operation cost of the pyrolysis process.

It is well known that complete decomposition of tar over several metal catalysts such as Ni, Pt, Rh, and Pd are promising method [2-5]. Nickel catalysts in various types have been obtained to be highly effective for tar decomposition process in coal or biomass pyrolysis. For example, the NiMo catalyst almost removed 100% of tar material which contains mostly of methylnaphthalene hydrocarbon at 500^{o}C [6]. However, there is still very serious problem related with catalyst deactivation due to carbon deposition. Aznar et al observes that the catalyst activity of typical nickel A is drop into 54% during 35 h experiment time [7]. Beside carbon deposition, high cost for raw material and regeneration method are another problems related with the conventional metal catalyst.

In order to solve their problem, different approach was offered using certain material as catalyst that can still be used after the loss of activity. An example is the utilization of charcoal in the biomass pyrolysis for tar decomposition simultaneously and producing higher gas product [8-10]. The carbon deposition within charcoal which is resulted by tar decomposition increases total carbon content as well as heating value of charcoal. It has also been reported that iron-

oxide-based catalysts such as Fe_2O_3-Al_2O_3 could be used effectively for tar decomposition to produce hydrogen [11,12]. Natural goethite ore was useful for biomass tar decomposition to produce clean pyrolysis gas [13]. The proposed system which consisted of integrated coal pyorlysis with tar decomposition over porous low grade ore (Fe_2O_3) is a promising method to solve the problems related to tar material and catalyst development [14, 15]. In this system, the volatile matter included tar material from pyrolysis is introduced to fixed bed of porous ore for decomposition process [16]. The tar decomposition produces a high-value syngas (CO and H_2), while at the same time the carbon deposits within the porous ore and causes catalyst deactivation. Thus, the clean gas product is generated with high values of H_2 and CO which increases the energy efficiency of the pyrolysis process. In addition, the iron ore with high carbon deposition as inactive catalyst can act as reducing agent and cut the consumption of coke in ironmaking process. It's reported that the inactive catalyst exhibited high reactivity and lower temperature in reduction reaction compared to conventional process [17]. Therefore, the inactive iron ore catalyst could be excellent raw material in the ironmaking industry which contributes to address the problems about raw material, energy and environment [18]. Among those great benefits, the understanding of the proposed system was highly required such as kinetic analysis and ore reduction behaviors. The effect of carbon deposition on the activity of catalyst in decomposition process was also still questionable.

Consequently, this paper focuses on a detailed evaluation of the kinetic analysis in the proposed integrated coal pyrolysis-tar decomposition over porous iron ore. The comparison of kinetic parameters with the related experiments was also examined. In addition, the effect of carbon deposition on the catalyst activity was also discussed to further understand the lifetime of the catalyst.

3.2 The proposed of kinetic model

The kinetic model is proposed based on the decomposition of tar with the following reaction:

$$HT \xrightarrow{k} f_{LT}LT + f_{GS}GS + f_{SC}SC \qquad (3.1)$$

The heavy tar (*HT*) decomposes into gaseous product (*GS*), solid carbon (*SC*), and light tar (*LT*) over porous ore. In the case of high catalyst activity, the light tar is also possible to decompose into gases and solid carbon. The coefficients f_{LT}, f_{GS}, and f_{SC} correspond to the selectivities of light tar, gases and carbon respectively.

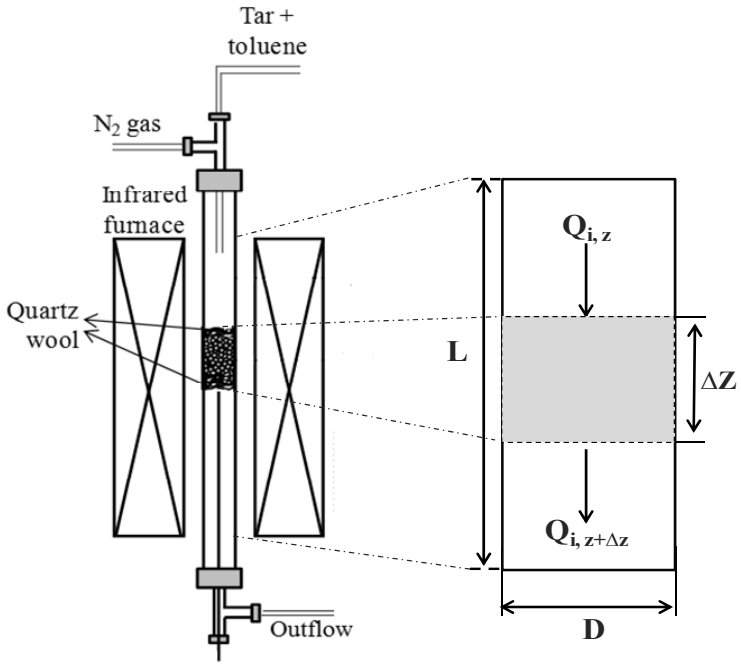

Fig. 3-1 Schematic diagram of continuous fixed bed reactor which used for development of kinetic equation model.

By assuming the reaction is first-order kinetic, the reaction rate can be expressed as follow:

$$r = -k\phi(t)C_T y_{HT} = f_{GS}k\phi(t)C_T y_{HT} = f_{SC}k\phi(t)C_T y_{HT} \qquad (3.2)$$

where C_T corresponds to total concentration of the reactant, y_{HT} denotes the mass fraction of the heavy tar material, ϕ express the catalyst deactivation due to carbon deposition. Fig. 3-1 shows the schematic fixed bed reactor which used for developing of the kinetic equations. By assumption the plug flow reactor, the mass balance of heavy tar through fixed bed reactor can be expressed with the differential equation:

$$\frac{\partial y_{HT}}{\partial t} + u\frac{\partial y_{HT}}{\partial z} = -k\phi(t)y_{HT} \tag{3.3}$$

By defining gas velocity, $u = \frac{Q}{A}$ and dimensionless variables, $x = \frac{z}{L}; \quad \theta = \frac{t}{t_R}$, where Q is volumetric gas flow rate, A indicates bed cross-section area, L represents total reactor length and t_R means total reaction time. The equation (3.3) can be modified as follow:

$$\frac{1}{t_R}\frac{\partial y_{HT}}{\partial \theta} + \frac{Q}{AL}\frac{\partial y_{HT}}{\partial x} = -k\phi(\theta)y_{HT} \tag{3.4}$$

The substitution of reactor volume, $V_R = AL$ and gas residence time, $\tau = \frac{AL}{Q}$ into equation (3.4) results the following equation:

$$\frac{\tau}{t_R}\frac{\partial y_{HT}}{\partial \theta} + \frac{\partial y_{HT}}{\partial x} = -\tau k\phi(\theta)y_{HT} \tag{3.5}$$

In case of continuous system with appropriate gas flow rate, the gas residence time is a lot of smaller than reaction time; therefore the equation (3.5) could be expressed in the simple form:

$$\frac{\partial y_{HT}}{\partial x} = -\tau k\phi(\theta)y_{HT} \tag{3.6}$$

The equation (3.6) can be solved using boundary condition (BC) in the reactor entrance, $x = 0 \rightarrow y_{HT} = 1$, thus the mass balance equation of heavy tar is defined as follow:

$$y_{HT} = \exp\left[-\tau k \phi(\theta) x\right] \tag{3.7}$$

Based on the similar method, the mass balance of gaseous product is also developed as the following form:

$$\frac{\partial y_{GS}}{\partial x} = f_{GS} \tau k \phi(\theta) y_{HT} \tag{3.8}$$

By applying equation (3.7) and BC in the reactor entrance, $x = 0 \rightarrow y_{HT} = 1 \rightarrow y_{GS} = 0$ so the equation (3.8) can be rearranged:

$$y_{GS} = f_{GS} \tau k \phi(\theta) \frac{1}{-\tau k \phi(\theta)} \exp\left[-\tau k \phi(\theta) x\right]_0^x \tag{3.9}$$

Inserting of BC in the outlet reactor, $x = 1 \rightarrow y_{GS} = y_{GS}$, the equation (3.9) can be modified in following form:

$$y_{GS} = f_{GS} \left[1 - \exp\left[-\tau k \phi(\theta)\right]\right] \tag{3.10}$$

The catalyst deactivation is assumed as first order exponential function, $\phi(\theta) = \exp(-\lambda\theta)$ where λ is deactivation factor due to carbon deposition. The equation (3.10) can be modified and rearranged in the form:

$$\ln\left[-\ln\left(1 - \frac{y_{GS}}{f_{GS}}\right)\right] = \ln(\tau k) - \lambda\theta \tag{3.11}$$

The reaction rate constant and deactivation factor could be evaluated using experimental data of tar decomposition process by simple linear correlation.

3.3 Materials and experimental methods

3.3.1 Materials

Lignite coal tar was examined as carbon sources in the tar decomposition process over porous iron ore which originated from Japan ironmaking industry. The tar was derived from Australian lignite coal (LIGN) which is similar material used in section 2.3. A low-grade iron ore, pisolite, was employed as catalyst for decomposition of tar and storage of deposited carbon. The properties of the low grade ore are also similar to Table 2-2-2.

3.3.2 Experimental methods

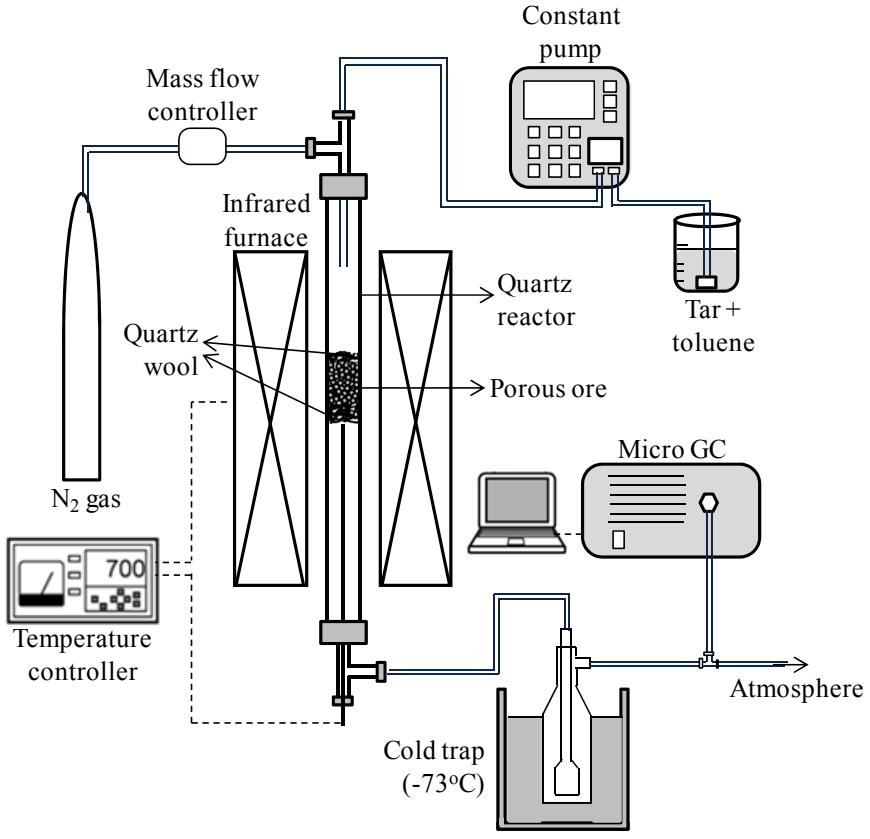

Fig. 3-2 Experimental apparatus for tar decomposition over porous ore. Total tar flow rate and porous ore were 0.25 ml/min and 250 mg , respectively. Toluene was added for tar dilution and preventing of pump problem. GC: gas chromatography.

Fig. 3-2 shows the schematic diagram of the experimental apparatus which consisted of HPLC pump, gas flow controllers, a tubular fixed-bed reactor, cold trap and micro gas chromatography (GC) for evaluating gas composition in the reactor downstream. The reactor was made from a transparent quartz tube with an inner diameter of 8mm which equipped with infrared heater and temperature controller. The fixed bed reactor was 250 mg of porous ore and supported by quartz wool for catalyst of tar decomposition and carbon deposition. The tar liquid was mixed by toluene in the certain amount to decrease the viscosity and allow for pumping system.

Table 3-1 Raw material and experiment condition in tar decomposition process

Code	Sample	Temp [^{o}C]	Catalyst weight [mg]	N_2 flow rate [mL/min]
Run 1	Toluene	600	250	50
Run 2	Lignite tar (5%) + Toluene	500	250	50
Run 3	Lignite tar (5%) + Toluene	600	250	50
Run 4	Lignite tar (5%) + Toluene	700	250	50

Experiments were performed at atmospheric pressure with a total N_2 flow rate of 50 mL/min and reactor heating rate of 10 K/min. After the reactor temperature was constant at desired temperature, the liquid tar was pumped into top of the reactor with the flow of 0.25 ml/min. The decomposition of tar occurred over porous ore to produce gas, carbon and light tar. The reduction reaction and carbon deposition within pores ore also took place simultaneously in the fixed bed reactor. The gas product and remaining tar were allowed to flow through the cold trap was maintained at –73°C for ensuring complete separation on liquid and gas product. The gas product was evaluated using micro GC to determine the amount of H_2, CO, CO_2, and light hydrocarbon gases. The characterization of iron ore was performed by XRD analysis and BET measurement. The carbon content within the iron was also examined using CHNO elemental

analysis to evaluate the tar carbon deposition. Table 3-1 lists the experimental conditions for evaluating the reactivity and kinetic constant of tar decomposition over porous iron ore.

3.4 Results and Discussion

3.4.1 Effect of reaction time on tar decomposition and carbon deposition

In the decomposition process, the tar material generated into gasses, carbon and light hydrocarbon as stated in equation (3.12). Fig. 3-3 shows the product comparison of tar decomposition for pure toluene and mixture of toluene and lignite tar.

$$\text{Tar} \rightarrow H_2 + CO + CO_2 + CH_4 + \text{other light hydrocarbon} + C \qquad (3.12)$$

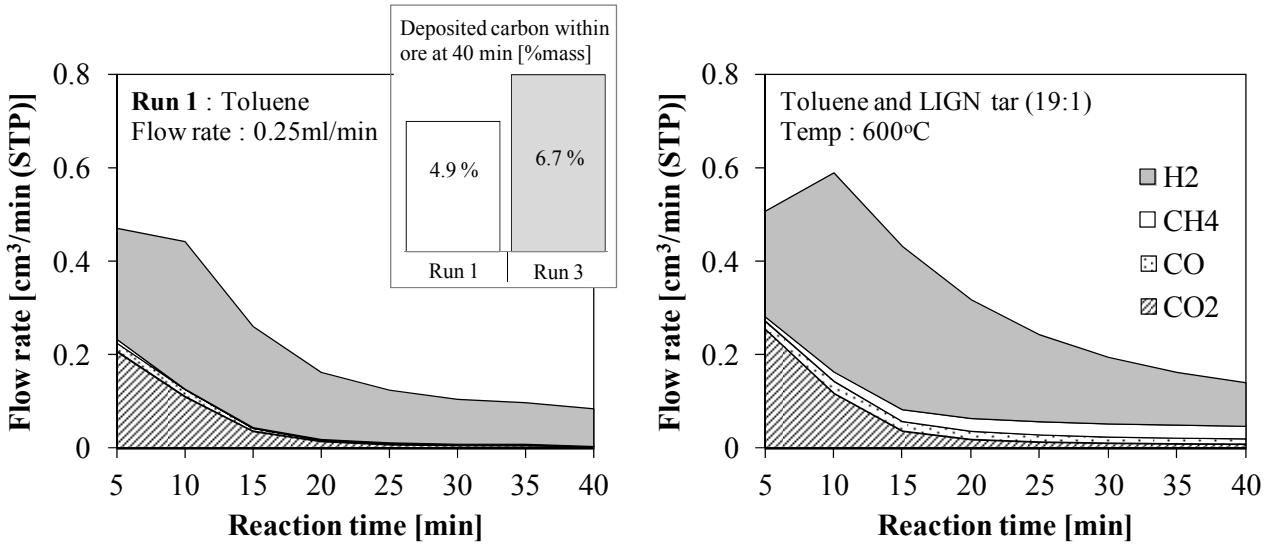

Fig. 3-3 Comparison of tar decomposition product for different raw material shows that the small addition of LIGN tar (5%mass) affected in enhancing of total gas product and carbon deposition.

The gas composition of both experiment showed similar tendency that H_2 was predominant compared to other gasses. It related to the chemical bonding which was easy to break and form H_2 from any type of hydrocarbon. Obviously, small addition of lignite tar into toluene resulted large different in gas and carbon products. The 5% of lignite tar within toluene mixture (run3) enhanced 58.65% of gas product and 36.73% of carbon deposition compared to pure toluene

(run1). In addition, the run 3 exhibited also different gas profile which rising in beginning of reaction time. It denoted that the adding of lignite tar within pure toluene caused significant improvement of hydrocarbon substance in the raw material of decomposition process. Therefore, the mixture could represent the lignite tar as raw material and utilized to evaluate the tar decomposition process and kinetic parameters.

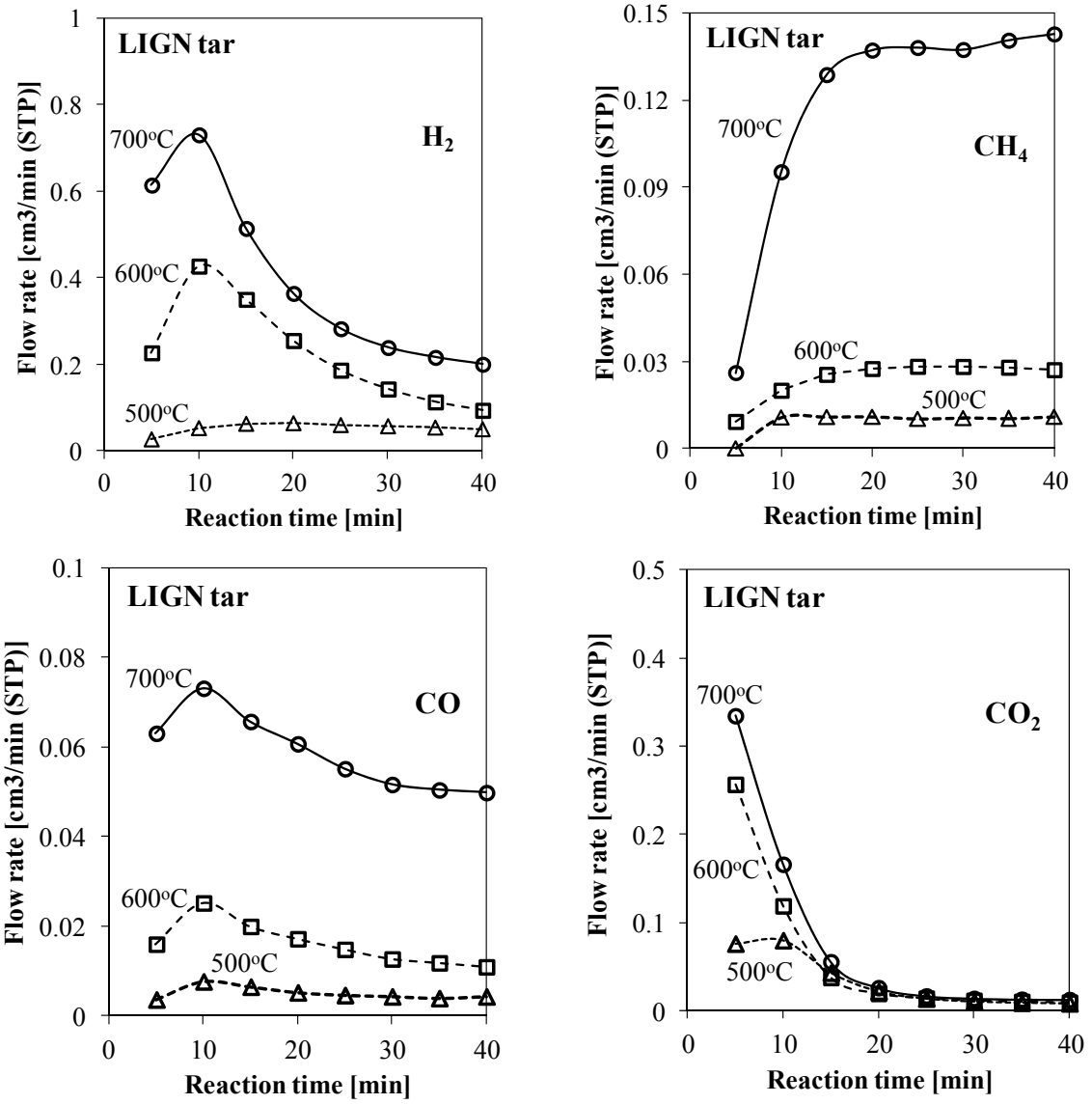

Fig. 3-4 The evolution of gas product during the experiment at various temperature shows that H_2-CO increased at the beginning step and decreased gradually till end of reaction.

Fig. 3-4 shows the evolution of each gas product during the experiments at different temperature. The H_2 and CO were generated with similar profile which was short increasing in the beginning and then smoothly decreasing till end of the reaction time. The increasing of gas product was related with the excessive activity of iron ore in the catalytic process due to large surface area and no poisoning of carbon deposition. When the carbon was deposited, the activity decreased gradually. Unlike of H_2 and CO, the profile of CH_4 was rise and steady during reaction time. As proposed mechanism of tar decomposition process by Huttinger [19], the tar material cracked into CH_4 in first step and subsequently, the H_2 and deposited carbon were formed as a resulted of CH_4 decomposition. Thus, the cracking activity of tar into CH_4 was steady but the production of H_2 and carbon was decline during the tar decomposition experiment due to unavailability of pore within iron ore. In addition, the conversion of tar material enhanced at higher temperature which indicated by huge amount of gas production. It is well known that thermal cracking, decarboxylation, and depolymerization are favored by an increasing of temperature.

Fig. 3-5 shows the changing on carbon content within porous ore at different reaction time and temperature. Apparently, the elevated temperature of tar decomposition produced large carbon content at anytime during the experiment due to excessive tar conversion. Generally, the process at elevated temperature would supplies more energy for break the chemical bonding through thermal cracking process [20]. Hence, the gas production and carbon deposition had similar tendency which large tar decomposition at elevated temperature resulted high product both gas and carbon. Generally, the changing of carbon deposition during reaction time exhibited similar profile which rising rapidly at first 10 min and then slightly increasing till end of the experiments. The rapid rising of carbon content was caused strongly by high accessible of pores

within iron ore. Furthermore, the rate of carbon deposition was decline significantly as small number of pores was available.

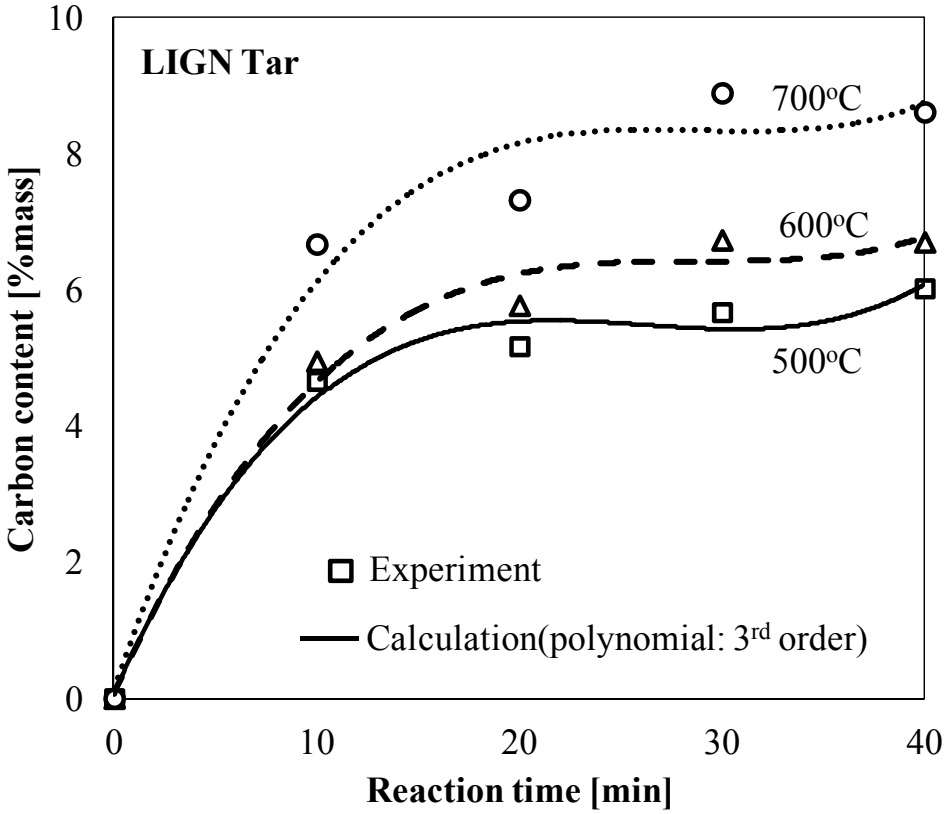

Fig. 3-5 Effect of temperature on carbon content within porous ore at different reaction time shows that high temperature attained larger carbon deposition due to large tar decomposition. Thermal hydrocarbon decomposition preferred at higher temperature.

Thus, the carbon deposition in the starting reaction time was absolutely important to control and construct dense deposition in the depth position so that the pore was still available for next deposition process. This phenomenon agreed with the gas product results as shown in the Fig. 3-4. In the end of experiment, the carbon content was near to constant due to saturated condition and unavailability of pores for deposition process. Beside carbon deposition, unavailability of

pore within iron ore caused the decreasing of catalyst activity as shown in the result of gas production.

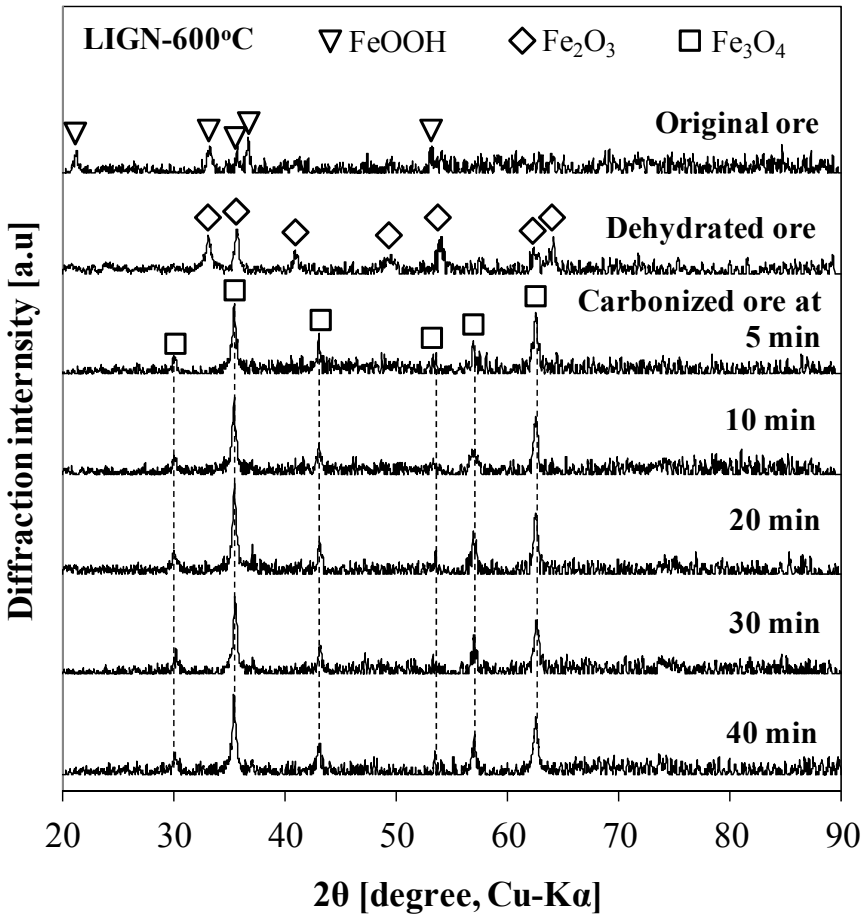

Fig. 3-6 Changing of XRD pattern at each experiment steps show that dehydration process removed OH completely while indirect reduction occurred simultaneously with decomposition process to product Fe3O4. Thermodynamic limitation caused the ore reduction reaction never proceed to FeO/Fe at longer time yet.

Fig. 3-6 shows the changing of ore phase and compound based on the XRD pattern at each experimental step. As stated in previous results [21] that the dehydration process was removed combined water (CW) completely by producing porous Fe_2O_3 from FeOOH. The

indirect reduction occurred simultaneously with decomposition process to product Fe_3O_4 through the reaction (3.13-3.14).

$$3Fe_2O_3(s) + CO(g) \leftrightarrow 2Fe_3O_4(s) + CO_2(g) \quad (3.13)$$

$$3Fe_2O_3(s) + H_2(g) \leftrightarrow 2Fe_3O_4(s) + H_2O(g) \quad (3.14)$$

However, the compound of iron ore was never changed to FeO/Fe at longer reaction time. As well known that the indirect reduction reaction is highly depend on the ratio of $H_2/(H_2O+H_2)$ and $CO/(CO_2+CO)$ at specific temperature. When the ratio was quite low, the reduction never proceeds to FeO/Fe as our experiment. In the previous report, the tar decomposition at higher temperature generates more H_2 and CO, thus the ore reduction would precede more and produce FeO/Fe [15]. Therefore, the thermodynamic limitation caused the ore reduction reaction never proceed to FeO/Fe in the decomposition process.

3.4.2 The analysis of kinetic parameters

In order to calculate the kinetic parameter using equation (3-11), the gasses conversion and selectivity were based on the experiment data and tabulated in Table 4-2.

Table 4-2 The product, gas conversion and selectivity of each experiment condition

Time [min]	Product [mg]						Selectivity [-]			Conversion [-]		
	Gas			Carbon			Gas			Gas		
	500°C	600°C	700°C	500°C	600°C	700°C	500°C	600°C	700°C	500°C	600°C	700°C
10	1.22	3.54	5.42	11.65	12.37	16.67	0.095	0.223	0.245	0.054	0.016	0.238
20	2.36	5.34	9.09	12.92	14.42	18.30	0.154	0.270	0.332	0.052	0.012	0.199
30	2.84	6.19	11.39	14.17	16.82	22.43	0.167	0.269	0.337	0.042	0.091	0.166
40	3.20	6.85	13.48	15.05	16.75	20.40	0.175	0.290	0.398	0.035	0.075	0.148

The gas selectivity was evaluated as mass ratio of total gas product and total product (gas and carbon). As the gas conversion was calculated based on the mass ratio of total gas product and raw material of tar. Based on the equation (3-11) and Table 7-2, the constant of reaction kinetic and catalytic deactivation were determined by linear correlation as shown in the Fig. 3-7.

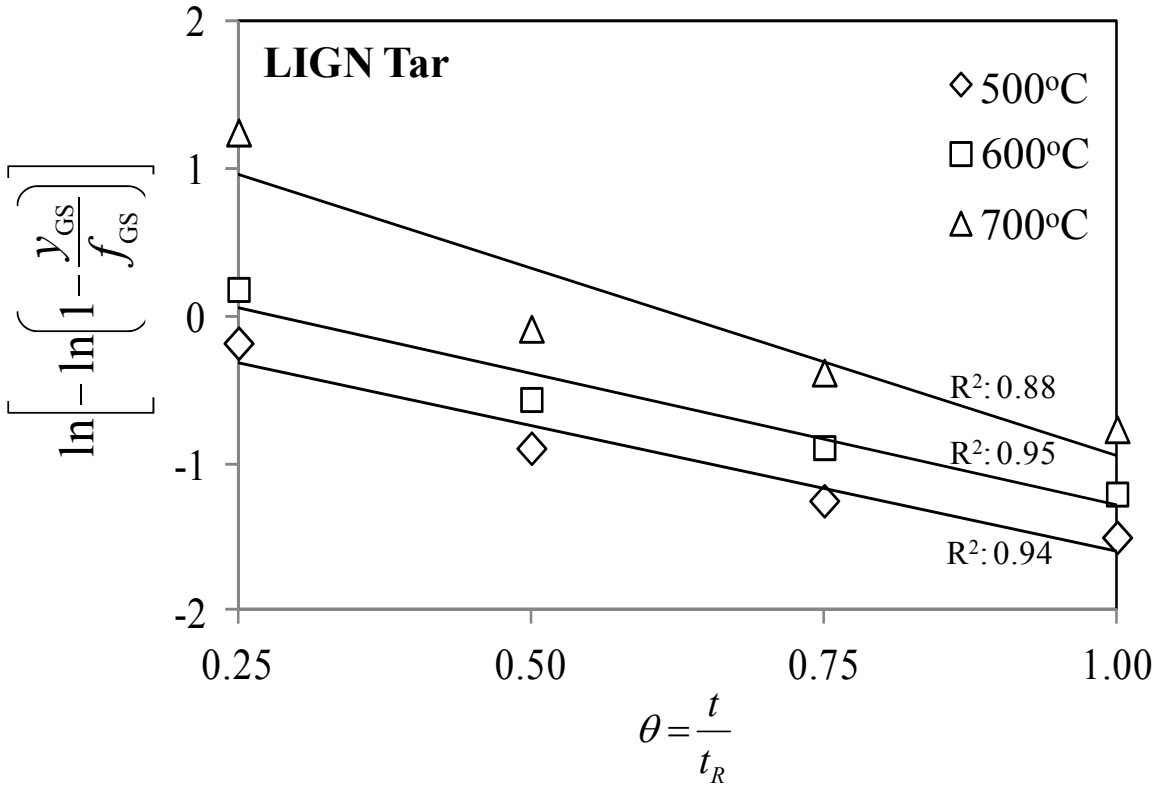

Fig. 3-7 Determination of kinetic parameters using linearization method at different experiment temperatures.

The data correlation owned linear tendency which confirmed the valid assumptions in the development the kinetic model. Using the slope (A) and intercept (B) of linearization, the reaction rate constant and deactivation factor were determined using the equations (3.15).

$$k=\frac{\exp(A)}{\tau} \text{ and } \lambda=-B \qquad (3.15)$$

The result of reaction rate constants and deactivation factors at different temperatures were presented in Table 3-3.

Table 3-3 The apparent constant of reaction rate and catalyst deactivation parameter on tar decomposition over porous ore

Code	Temp [^{o}C]	Reaction rate constant, k [s^{-1}]	Deactivation factor λ [s^{-1}]
Run 2	500	0.13	1.72
Run 3	600	0.19	1.79
Run 4	700	0.55	2.53

The result matched with general theoretical and previous explanation that the tar conversion and carbon deposition were increased at elevated temperature. Based on the Arrhenius equation, the activation energy (Ea) of the tar decomposition over iron ore was calculated using the data of reaction rate constant at different temperature.

Table 3-4 Activation energy of tar decomposition reaction over porous ore and other catalyst

Catalyst	Activation energy, Ea [kJ/mol]	Raw material	Ref
Porous ore	44.80	Coal tar (5%) + toluene	This study
Dolomite	67.41	Coal tar + pyrolysis gas	[22]
Zeolite	37.20	Simulated tar (1-MN)	[6]
CaO	32.90	Gasco coal tar	[23]

Table 3-4 shows the result of the activation energy and compared to other related experiments over various solid catalyst. It seems that the value of this experiment was comparable with other researcher even with different raw material of tar composition. In general, it well known that tar material consisted with hydrocarbon in various form such as toluene, xylene, benzene, naphthalene, phenanthrene, antrecena, aliphatic compounds and etc. Thus, the

porous iron ore was promising catalyst in the tar decomposition process with other benefits compared to conventional catalyst such as cheap, abundant natural resource and unnecessary catalyst support. In addition, the carbon deposition was no problem in this catalyst and would be advantage in the future utilization as raw material in ironmaking industry.

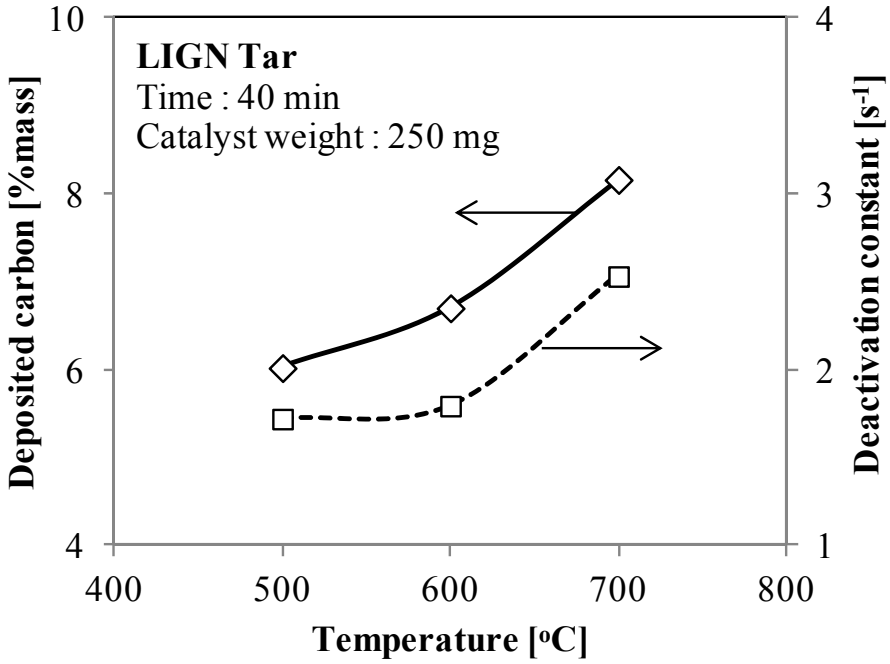

Fig. 3-8 The relationship between deposited carbon and deactivation constant at different temperature shows that the carbon deposition within ore caused deceasing of catalytic activity during tar decomposition process.

Fig. 3-8 shows the relationship between amount of carbon deposition and deactivation factor at various experiment temperature. Clearly, the both parameters showed similar tendency that larger carbon deposition resulted higher deactivation factor. It means that the carbon deposition within pores ore highly affected the decreasing of catalyst activity in the tar decomposition process. However, the high carbon content within this inactive ore catalyst would offer extra benefit in the steel production by exhibiting of high reactivity in reduction process.

3.5 Conclusions

The proposed system which consisted of integrated coal pyorlysis over porous iron ore was promising candidate for tar decomposition and offered also solution for problem related with resaource, energy and environment in ironmaking industry. The kinetic analysis and deactivation of ore catalyst was evaluated in detail using proposed model to understand fully related with the system. The main findings of this study can be summarized as follows

1. The generation of both H_2 and CO gasses had similar profile which was short rising and then declining smoothly till the end of experiment. In the starting experiment, the catalyst iron ore owned high activity in tar decomposition due to large surface area and no poisoning of carbon deposition. Beside decompsoition process, the indirect reduction occured simultaneaously to produce Fe_3O_4. However, thermodynamic limitation caused the ore reduction never proceed to FeO/Fe.
2. The reaction rate constant, *k* and deactivation factor, λ were calculated successfully using the proposed model with the range of 0.13 – 0.55 s^{-1} and 1.72 – 2.53 s^{-1}, respectively at 500-700^{o}C. Based on the Arrhenious plot, the activation energy, Ea was around 44.86 kJ/mol. It seems that the kinetic parameters of this experiment were comparable with other researchers.
3. Obiously, the deactivation factor exhibited similar tendency with amount of carbon deposition within pores iron ore. It means that the carbon depsoition highly affected to the catalyts deactivation during the tar decompistion process. The carbon deposition raised rapidly at the beginning process due to high accessible in pores within iron ore. Furthermore, the rate of carbon depsoition diminished significantly as small number of pore available.

These results represent the important data and knowledge related with the proposed system of integrated coal pyrolysis and tar decomposition over natural and cheap calaytst of porous iron ore.

References

[1] A. Ziebik, K. Lampert, M. Szega. Energy analysis of blast-furnace system operating with the Corex process and CO_2 removal. Energy 33 (2008): 199-205.

[2] R. Zhang, RB. Brown, A. Suby, K. Cummer. Catalytic destruction of tar in biomass derived producer gas. Energy Conversion and Management 45(2004): 995–1014.

[3] P. Lu, Z. Yuan, C. Wu, L. Ma, Y. Chen, N. Tsubaki. Bio-syngas production from biomass catalytic gasification. Energy Conversion and Management 48 (2007): 1132–1139.

[4] PA. Simell, JO. Hepola, AO. Krause. Effects of gasification gas components on tar and ammonia decomposition over hot gas cleanup catalysts. Fuel 76 (1997): 1117–1127.

[5] M. Asadullah, T. Miyazawa, SI. Ito, K. Kunimori, M. Yamada, K. Tomishige. Gasification of different biomasses in a dual-bed gasifier system combined with novel catalysts with high energy efficiency. Appl Catal A: Gen. 267 (2004): 95–102.

[6] B. Dou, J. Gao, X. Sha, SW. Baek. Catalytic cracking of tar component from high temperature fuel gas. Applied Thermal Engineering 23 (2003): 2229-2239.

[7] MP. Aznar, MA. Caballero, J. Gil, JA. Martin, J. Corella. Commercial steam reforming catalysts to improve biomass gasification with steam-oxygen mixtures: 2. Catalytic tar removal. Ind. Eng. Chem. Res 37(1998): 2668-2680.

[8] ZY. Abu El-Rub, EA. Bramer, G. Brem. Experimental comparison of biomass chars with other catalysts for tar reduction. Fuel 87(2008): 2243–2252.

[9] S. Hosokai, K. Kumabe, M. Ohshita, K. Norinaga, CZ. Li, JI. Hayashi. Mechanism of decomposition of aromatics over charcoal and necessary condition for maintaining its activity. Fuel 87 (2008): 2914–2922.

[10] T. Kimura, M. Nakano, S. Hosokai, K. Norinaga, CZ. Li, JI. Hayashi. Steam reforming of biomass tar over charcoal in a coke-deposition/steam-reforming sequence. Proceedings of CHEMECA 2009, Perth, CD-ROM Edition; 2009.

[11] M. Barati, S. Esfahani, TA. Utigard. Energy recovery from high temperature slags. Energy 36 (2011): 5440–5449.

[12] A. Uddin, H. Tsuda, S. Wu, E. Sasaoka. Catalytic decomposition of biomass tars with iron oxide catalysts. Fuel 87 (2008): 451–459.

[13] S. Kudo, K. Sugiyama, K. Norinaga, CI. Li, T. Akiyama, JI. Hayashi. Coproduction of clean syngas and iron from woody biomass and natural goethite ore. Fuel 2011. doi:10.1016/j.fuel.2011.06.074.

[14] RB. Cahyono, AN. Rozhan, N. Yasuda, T. Nomura, S. Hosokai, Y. Kashiwaya, T. Akiyama. Integrated coal-pyrolysis tar reforming using steelmaking slag for carbon composite and hydrogen production. Fuel 109 (2013): 439 - 444.

[15] RB. Cahyono, N. Yasuda, T. Nomura, T. Akiyama. Optimum temperatures for carbon deposition during integrated coal pyrolysis–tar decomposition over low-grade iron ore for ironmaking applications. Fuel Processing Technology 119 (2014): 272-277.

[16] RB. Cahyono, AN. Rozhan, N. Yasuda, T. Nomura, S. Hosokai, Y. Kashiwaya, T. Akiyama. Catalytic coal-tar decomposition to enhance reactivity of low-grade iron ore. Fuel Processing Technology 113 (2013): 84-89.

[17] S. Hosokai, K. Matsui, N. Okinaka, K. Ohno, M. Shimizu, T. Akiyama. Kinetic study on the reduction reaction of biomass-tar-infiltrated iron ore. Energy and Fuels 26 (2012): 7274-7279.

[18] RB. Cahyono, N. Yasuda, T. Nomura, T. Akiyama. Utilization of low grade iron ore (FeOOH) and biomass through integrated pyrolysis-tar decomposition (CVI process) in ironmaking industry: Exergy analysis and its application. ISIJ International 2014. Inpress.

[19] KJ. Huttinger. CVD in hot wall reactors: the interaction between homogeneous gas-phase and heterogenneous surface reactions. Chemical Vapor Deposition 4 (1998): 151-158.

[20] C. Li, D. Hirabayashi, K. Suzuki. Development of new nickel based catalyst for biomass tar steam reforming producing H_2-rich syngas. Fuel Processing Technology 90 (2009): 790–796.

[21] RB. Cahyono, G. Saito, N. Yasuda, T. Nomura, T. Akiyama. Porous Ore Structure and Deposited Carbon Type during Integrated Pyrolysis–Tar Decomposition. Energy and Fuels 28 (2014): 2129-2134

[22] A. Shamsi. Catalytic and thermal cracking of coal-derived liquid in a fixed bed reactor. Ind. Eng. Chem. Res. 35 (1996): 1251-1256.

[23] JM. Faundez, XA. Garcia, AL. Gordon. A kinetic approach to catalytic pyrolysis of tars. Fuel Processing Technology 69 (2001): 239-256.

Chapter 4

Porous ore structure and type of carbon deposition during CVI ironmaking

4.1 Introduction

Almost 70% of global steel is currently produced by blast furnaces that rely on metallurgical coal, otherwise known as coking coal [1]. The consumption of coking coal is therefore expected to continuously increase, as a result of the growing demand for steel in order to satisfy world economic growth. This, in turn, should result in an increase in price and limited resource availability, as well as greater competitiveness within the steelmaking industry. Consequently, alternative reducing agents need to be introduced into existing steelmaking processes, reducing their reliance on coking coal by substituting materials such as non-coking coal, wooden biomass, and carbon briquettes [2-4]. In conventional steelmaking, the coke is converted in a coke oven through pyrolysis with limited oxygen, producing an improved coke that fulfills critical roles in providing an energy source, a reducing agent, and maintaining the bed permeability in blast furnace operations [5]. In addition to coke, the coke oven also generates tar and gas, referred to as coke oven gas (COG) that contains large amounts of chemical and heat energy, and there are no significant means of energy recovery. Moreover, the tar material often causes operational problems during transportation, such as pipe plugging, condensation, and tar aerosol formation [6].

Integrating coal pyrolysis-tar decomposition over a low-grade iron ore is a promising method to address the problems related to the use of alternative reducing agents, as well as allowing energy recovery from COG and tar material [7-8]. In this process, tar material is

introduced to a porous low-grade iron ore with a pore size around of 4 nm, which is then subjected to decomposition and carbon deposition processes. The tar decomposition produces a high-value syngas (CO and H_2), while at the same time depositing carbon within the porous ore. This gas product could be utilized as an energy source in other areas of steelmaking, while the deposited carbon can act as reducing agent and diminish the consumption of coke in blast furnace operations. In addition, indirect ore reduction by CO and H_2 occurs alongside tar decomposition and carbon deposition, thus transforming Fe_2O_3 into Fe_3O_4. The proposed method also allows the effective utilization of low-grade iron ore in steelmaking, which remains an abundant and low-cost resource, and can therefore help reduce the cost of raw materials.

Carbon deposited by integrated coal pyrolysis-tar decomposition has been shown to demonstrate a high reactivity and lower temperature during reduction reaction [9]. In addition, the nanoscale contact between iron and carbon within the porous ore enhances the overall contact area, which increases the pre-exponential factor in the Arrhenius equation, and therefore the reaction rate constant [10]. The homogeneous distribution of carbon deposited within porous iron ore is a critical factor in ensuring that reduction occurs throughout the ore; however, there is currently no information regarding such distribution of deposited carbon in suitable detail. Furthermore, the study of the ore's porous microstructure is of great value in understanding the phenomena that occur during deposition. Thus, a substantive investigation into the distribution and microstructure of carbon deposited within porous ore is urgently required in order to fully understand the potential benefits of the proposed method.

The decomposition of hydrocarbons, such as tar, can result in the formation of various carbon structures ranging from amorphous to crystalline forms. All these different forms can exhibit different reactivities, with the reactivity of amorphous carbon in particular being

determined by the ratio of sp2 to sp3 in its atomic structure. The formation of carbon during the decomposition of hydrocarbons is a highly complex system involving molecular and free radial chain reactions, as well as phase changes from gas to liquid to solid [11]. Furthermore, the direct reduction of hematite differs depending on the use crystalline or amorphous carbon, with reaction starting at temperatures of 709°C and 576°C respectively [12]. Consequently, this paper focuses on a detailed evaluation of the type of carbon deposited during integrated coal pyrolysis-tar decomposition over porous iron ore, with various solid fuels used as a hydrocarbon source. The microstructure of the porous ore and distribution of deposited carbon was also examined to further understand the carbon deposition process.

4.2 Materials and experimental methods

4.2.1 Materials

The CVI ore which was produced from the previous experiments was subjected for microstructure and carbon type analysis. The carbon deposition within porous ore originated from various solid fuels such as high grade bituminous coal, low grade lignite coal and palm kernel shell biomass. In order to evaluate the effect of temperature on microstructure and carbon type, the CVI ore which was produced at different temperature was also examined.

4.2.2 Experimental methods

4.2.2.1 Microscopic analysis

The changing pore size distribution and crystalline compound of low grade iron ore during the CVI process were evaluated using BET measurement (Autosorb 6AG, Quantachrome) and XRD analysis (Miniflex, Rigaku). In order to study the evolution of the iron ore's nanoscale

microstructure, both scanning electron microscope (SEM) and transmission electron microscope (TEM) were applied over porous iron ore. SEM images and energy-dispersive X-ray spectroscopy (EDS) analysis of the samples were obtained by using a JEOL JSM-7400F. In addition, the TEM was taken by using a JEOL JEM-2010 microscope at an operating voltage of 200 kV and various magnifications. The water containing iron ore was dropped on a collodion-coated Cu microgrid (150 mesh, Nisshin EM, Tokyo, Japan), subsequent drying at 60^{o}C in the oven before TEM observation.

4.2.2.2 Raman spectroscopy

The carbon deposited within the porous iron ore was examined with a Renishaw InVia micro-Raman spectrometer (Renishaw, Wotton-under-Edge), equipped with a CCD detector. The samples were scanned using a laser excitation wavelength of 532 nm, and a 20x objective. The laser power was set below 7.5 mW (50% of maximum power), and the exposure time to 10 s, as these conditions prevented sample damage caused by laser irradiation. The spectra were measured in the range 900–2000 cm^{-1}, and after scanning were processed using WiRE 2.0 software.

4.3. Results and Discussion

4.3.1 BET measurement and TEM analysis

Fig. 4-1(a) shows the change in pore size distribution with each experimental step, ranging from the dehydration of combined water (CW) to the integrated pyrolysis-tar decomposition of various carbon sources. One of the biggest drawbacks to use of low-grade iron ore as a raw material for ironmaking is the large amount of combined water such ores typically contain, which subsequently requires additional energy for dehydration; however, this dehydration can produce a porous low-grade iron ore with a pore size of 1–4 nm.

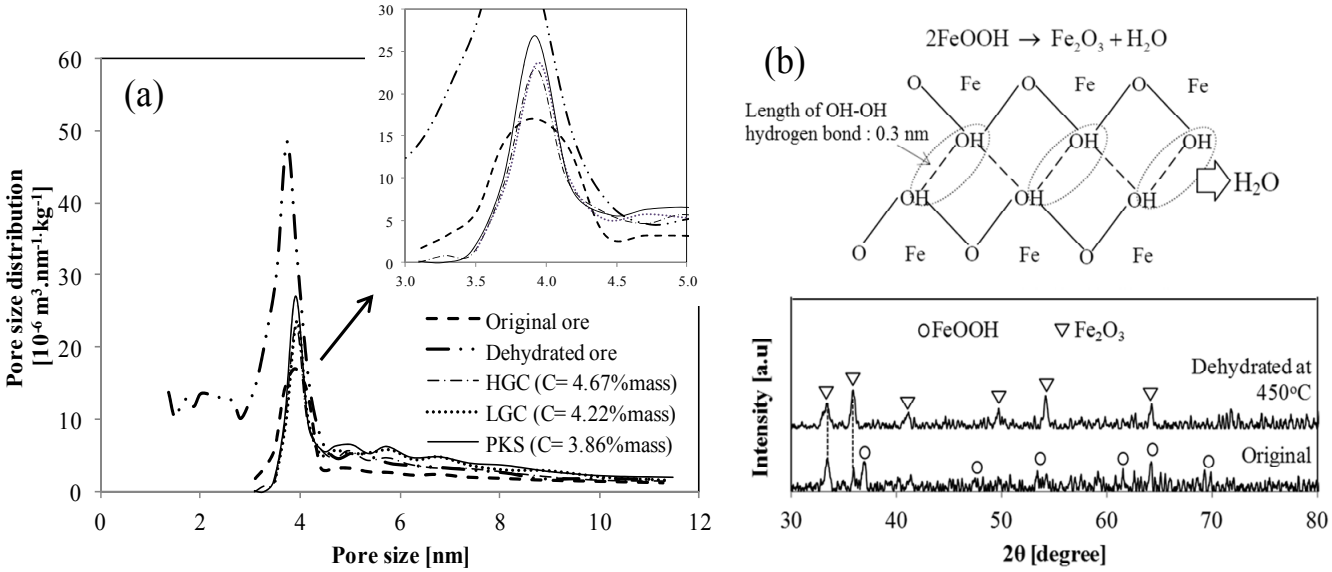

Fig. 4-1 (a) Change in pore size distribution with each experimental step; exhibiting a preference for deposition with pore sizes of less than 4 nm. (b) Effect of dehydration on the removal of the hydroxide (OH) group and the XRD pattern of the low-grade iron ore used.

As shown in Fig. 4-1(b), the removal of the OH group from FeOOH molecules by heat treatment can initiate void spaces, and thus generate a porous material which was suitable for carbon deposition. Based on the XRD results, dehydration at 450 °C was sufficient to eliminate the OH group by converting the FeOOH to Fe_2O_3. The tar material subsequently produced from the

pyrolysis of solid fuels was decomposed within this porous iron ore into gases and carbon through the following reaction:

$$\text{Tar} \rightarrow H_2 + CO + CO_2 + CH_4 + \text{other light hydrocarbons} + C \quad (4.1)$$

At the same time, this carbon infiltrated and was deposited within the pores of the iron ore, thus resulting in a decrease in pore size distribution, as shown in Fig.4-1(a). Interestingly, the amount of carbon deposition was proportional to the decrease in pore size distribution; for example, carbon deposition from HGC tar was the highest observed and caused the largest reduction in the pore size distribution. Furthermore, the carbon was deposited only in within those pores with a size of less than 4 nm, which was due to the specific nature of the tar material and dominance of Knudsen diffusion. Specifically, with a small pore diameter, the resistance of Knudsen diffusion was the dominant factor in the total rate of diffusion. This Knudsen diffusion caused a higher percentage of intermolecular collisions with the pore walls, and thus a higher carbon deposition was achieved with a smaller pore size. Consequently, the porous material generated by dehydration as allowed for effective carbon storage.

Fig. 4-2(a–c) shows TEM images at different magnifications of dehydrated iron ore at 450°C. This shows that the complete removal of combined water results in the formation of pores confirmed to be around 3 nm in size; and with a layered pore structure, as shown in Fig. 4-2(a). The formation of a large crack due to dehydration was also observed in the surface of iron ore, as shown in Fig. 4-2(b), which agrees with the results of similar work conducted by other researchers [13-14]. Interestingly, the highest magnification TEM image (Fig. 4-2(c)) explained the difference in pore size which was created during dehydration. This clearly shows that the distribution of micropores and mesopores was higher than that of macropores, and thus,

dehydration can successfully create pores of different sizes that are suitable for tar decomposition and carbon deposition.

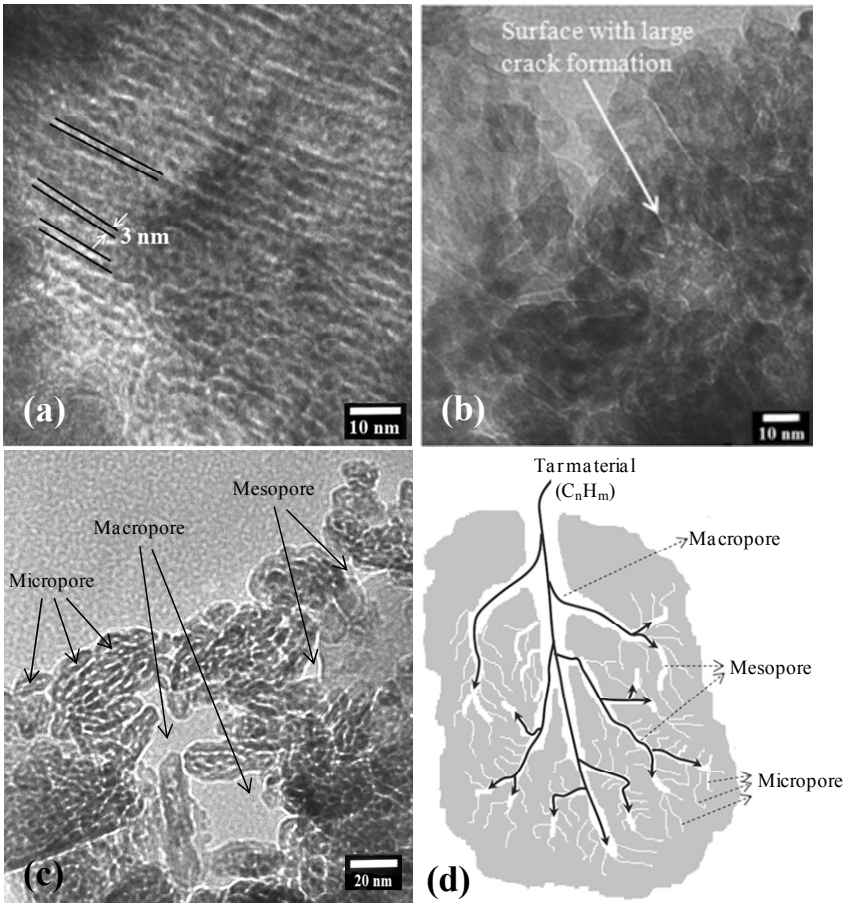

Fig. 4-2 TEM images of dehydrated iron ore at different magnifications: (a) Layered structure of dehydrated ore with a pore size of around 3 nm. (b) Large crack formation in the surface of iron ore. (c) Micropores and macropores within dehydrated iron ore. (d) Graphical representation of porous iron ore during tar decomposition and carbon deposition.

Based on the pore size distribution and TEM imaging, a model for the tar decomposition and carbon deposition in the ore was proposed, which was illustrated in Fig. 4-2(d). In this, the tar vapor penetrated through the macropores of the ore in order to reach meso/micropore. The diffusion of tar vapor occurring predominantly in the smaller pore sizes. The decomposition of

tar material occurred within the pore surface, and produces both gases and solid carbon. The gaseous products were able diffuse outward and return to the gas bulk, whereas the carbon was deposited in the pores and progressively reduce the pore size distribution.

4.3.2 SEM-EDS analysis

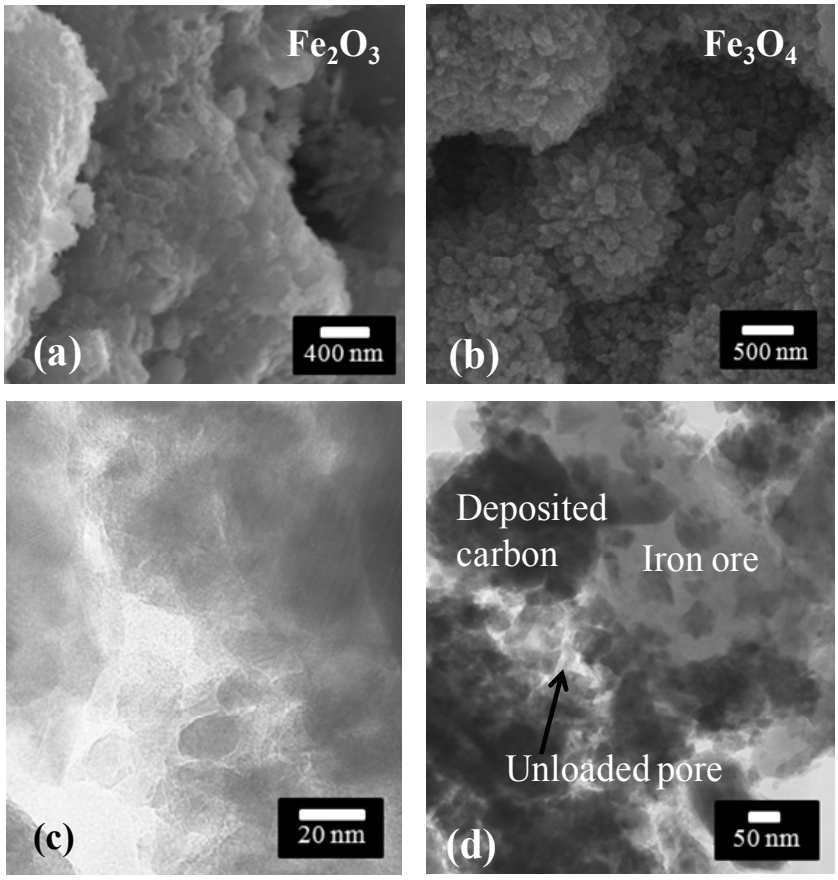

Fig. 4-3 SEM images showing change during tar decomposition: (a) untreated iron ore consisting mainly of Fe_2O_3, (b) iron ore after tar decomposition, containing Fe_3O_4 due to the indirect reduction (CO and H_2). TEM images of the iron ore after tar decomposition: (c) crack formation in the ore surface disappeared due to carbon deposition, (d) blockage of pore by deposited carbon, which caused a decrease in total carbon deposition.

The SEM images in Fig. 4-3(a–b) show the change in the dehydrated iron ore due to the tar decomposition process. Hematite (Fe_2O_3) can be seen in the original dehydrated ore, which

agrees with the XRD results. This hematite is completely transformed into magnetite (Fe_3O_4) after tar decomposition, as shown in Fig. 4-3(b). This indirect reduction that occurred simultaneously with tar decomposition was due to the presence of H_2 and CO from pyrolysis. As a product of tar decomposition, carbon infiltrated and was deposited within the iron ore, resulting in the disappearance of nanocracks from the surface that can be seen in the TEM image of Fig. 4-3(c). This phenomenon was confirmed by the reduction in the pore size distribution after tar decomposition and carbon deposition, with Fig. 4-3(d) showing the deposition of carbon with the ore in greater detail. Based on the pore size distribution, it seems unlikely that the deposited carbon completely filled the pore space of the iron ore, as a small pore volume still exists after tar decomposition. It can therefore be seen that some of the deposited carbon effectively blocks the pores, thus limiting the total carbon deposition.

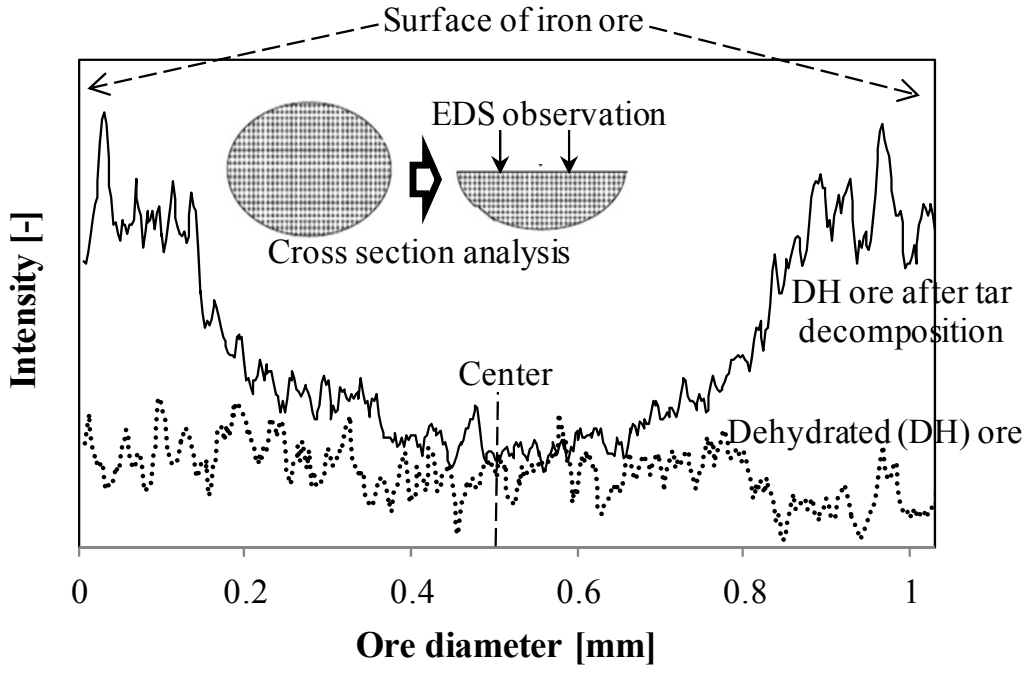

Fig. 4-4 Cross section of EDS line analysis, showing that carbon was deposited from the surface toward the center of porous dehydrated ore.

In order to determine the change in carbon distribution due to tar decomposition, an EDS line analysis was performed along the cross section of the dehydrated iron ore, as can be seen in Fig.4-4. The carbon distribution within the original dehydrated ore was found to be the lowest, and closer to a base line of carbon intensity in EDS analysis. A very different profile was observed in the dehydrated ore after tar decomposition. The carbon distribution was highest near the outer surface and decreased gradually with increasing depth in the inner section of ore. By a distance of 0.2 mm (inner diameter 1 mm) from the surface, the carbon content dropped to the base line level of carbon intensity. This indicates that the tar vapor was capable of infiltrating as far as this depth, which similarly marks the limit of decomposition and carbon deposition within the ore.

4.3.3 Raman spectrometry

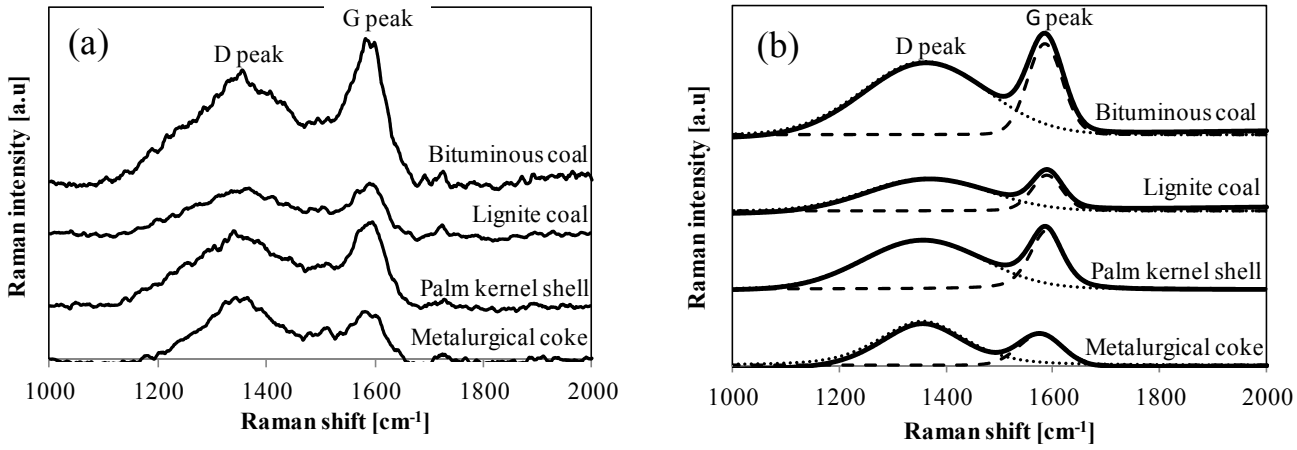

Fig. 4-5 (a) Raman spectra of metallurgical coke and carbon deposited within ore after tar decomposition from various solid fuels. (b) Curve fitting of the Raman spectra into D and G peaks, showing the differences in the intensity ratio.

Fig. 4-5 shows typical Raman spectra of carbon deposited by the decomposition of tars generated by the pyrolysis of various solid fuels. In addition, metallurgical coke was also analyzed for the purposes of comparison. The Raman spectra are all characterized by two strong main peaks: the D ("Defect or Disorder) peak at around 1350 cm^{-1}, which is affected by disorder in the graphitic lattice, and the G ("Graphite") peak at around 1580 cm^{-1}, which relates to an ideal graphitic lattice [15]. The spectrum deconvolution applied with the curve fitting offers quantitative information in an effective and rigorous way with regards to the material structure. Qualitatively, the spectra of the carbon deposited from the different solid fuels were all quite similar, suggesting that the mechanism of deposition in each instance was essentially identical. However, the metallurgical coke exhibited a different behavior, in that the intensity of the G peak was weaker than that of the D peak. This indicates that the carbon deposited through tar decomposition has a different carbon structure to that of metallurgical coke.

Based on the Raman spectra, there are several methods for evaluating the disordered structure of a material, such as peak intensity ratio, peak area ratio, G peak position, and full width at half maximum (FWHM) [16-17]. Using G peak position (ω_G), Ravikant et al proposed an equation for calculating the sp3 fraction of an amorphous carbon, as listed in (4.2) [18-19]. Moreover, the cluster diameter of the structure can also be estimated using the intensity ratio of D and G peaks (I_D/I_G) as showed in (4.3) [20].

$$\text{Sp3 fraction}\,[\text{nm}] = 0.24 - 48.9(\omega_G - 0.1580) \qquad (4.2)$$

$$\text{Cluster diamater, La}\,[\text{nm}] = 44(I_D/I_G)^{-1} \qquad (4.3)$$

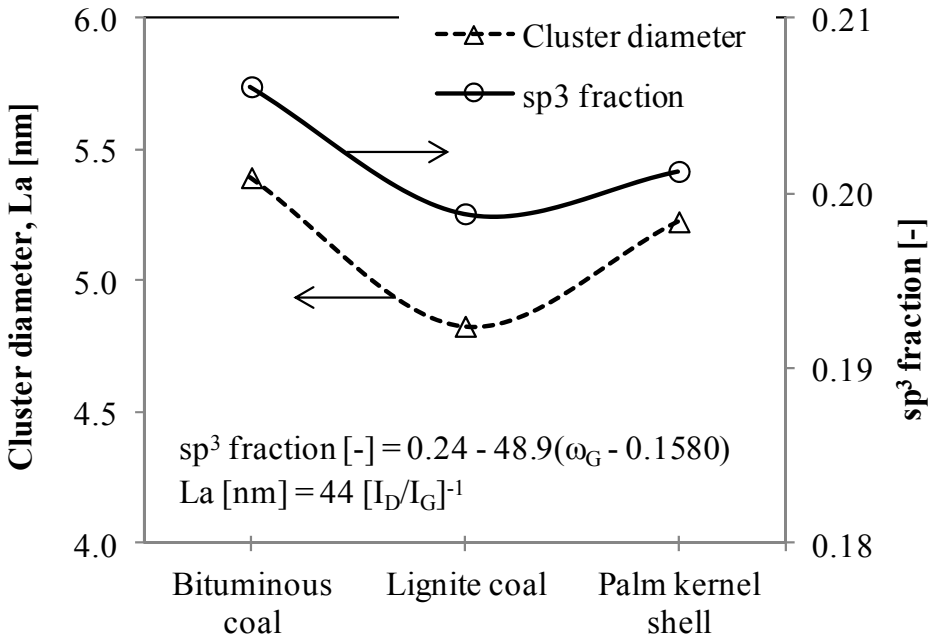

Fig. 4-6 Relationship between sp3 fraction and cluster diameter of carbon deposited from tar decomposition of various solid fuels.

Fig. 4-6 shows the results for sp3 content, as well as the cluster diameter (La), of carbon deposited by the decomposition of tar from various solid fuels. This reveals that both the sp3 content and La are highest in the case of carbon deposited from a bituminous tar; however, the difference in sp3 content between the various solid fuels was not significant, at around 0.20 (fraction). It is well known that various quality solid fuels generate slightly different tar components, and that this affects the structure of deposited carbon. The results show that the cluster diameter shows a similar tendency to sp3 content. The high disordered material that indicated with sp3 fraction was dispersive structure; hence the cluster diameter would be open up and become bigger [21]. This suggests that Raman spectroscopy could be readily used for evaluating the sp3 content and structure of deposited carbon within porous ore.

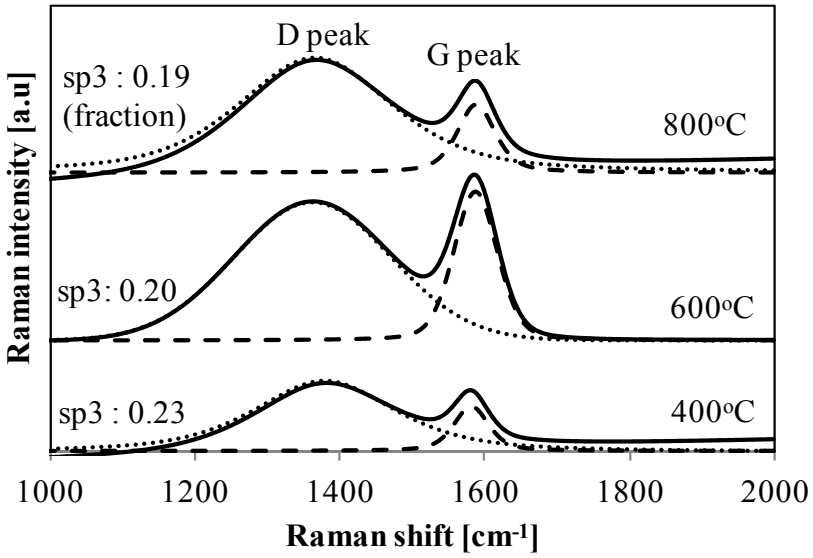

Fig. 4-7 Curve fitting of the Raman spectra and sp3 fraction of carbon deposited by tar decomposition of lignite coal at different temperatures.

Fig. 4-7 shows the effect of temperature on the Raman spectra and sp3 fraction of carbon deposited by the decomposition of tar lignite coal within porous low-grade iron ore. The slight shift observed in the G peak position indicates that the sp3 content was smaller at higher temperatures, due to a higher degree of graphitization. This increase in graphitization at higher temperatures causes the carbon structure to become more ordered, with various forms of structural defects and large carbon crystallites being created. This increased graphitization also reduces the concentration of large aromatic rings [22].

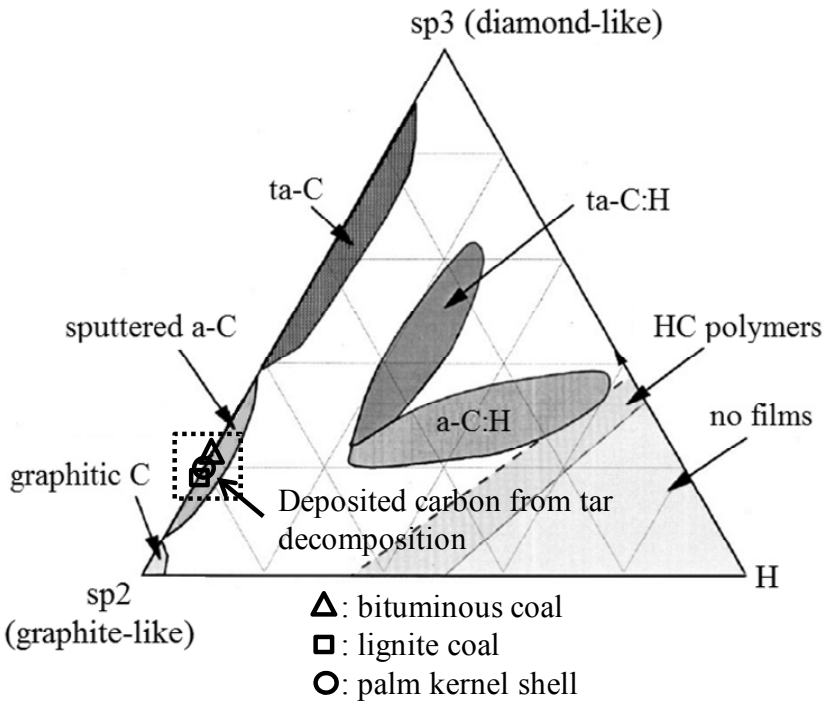

Fig. 4-8 Ternary phase diagram of carbon, showing that carbon deposited by the decomposition of tar from various solid fuels can be categorized as amorphous carbon (a:C) with an sp3 content of 19–21 %.

Fig. 4-8 shows a ternary phase diagram for the various forms of amorphous carbon films containing hydrogen (H), sp2 and sp3 carbon atoms, as proposed by Ferrari et al [21]. The three corners correspond to diamond-like (sp3), graphite-like (sp2) and hydrocarbon (H) phases. There is an excluded area present at high H concentrations, as the molecular solid cannot be formed. The amorphous carbon (a-C) film contains virtually no hydrogen and is quite soft, typically being formed at higher temperatures. Meanwhile, tetrahedral amorphous carbon (ta-C) is similarly without hydrogen, but contains a high content of sp3 bonding [23]. Based on the sp3 fraction calculation from the Raman spectrometry, the carbon deposited by tar decomposition of various solid fuels through chemical vapor infiltration (CVI) method could be categorized as amorphous carbon (a-C), with a sp3 content of 19–21%. This amorphous carbon demonstrated a

high reactivity during reduction when compared to graphite carbon. The direct reduction of iron ore by deposited carbon started at a temperature (750°C) lower than that in the case when the conventional mixture of Fe_2O_3 and coke (1100°C) is used [9]. In addition to the nanoscale contact between carbon and iron ore, the amorphous nature of the deposited carbon also contributes to a high reactivity during direct reduction.

4.4 Conclusions

Carbon deposited within porous iron ore by means of integrated pyrolysis-tar decomposition, proved to be a promising reducing agent for future ironmaking processes. The structure of the porous low-grade iron ore was evaluated in detail by SEM and TEM, in order to understand the phenomena that occur during the carbon deposition process. In addition, a detailed investigation into the carbon structure and type was conducted by Raman spectroscopy. The main findings of this study can be summarized as follows:

1. Removal of combined water (CW) by dehydration within low-grade ore was found to also remove the hydroxide (OH) group from the chemical structure and thus generated pores of around 3 nm size, with a layered structure. This process created a high volume of micro/mesopores, which were appropriate for the deposition of carbon from the decomposition of tar.
2. Not all of the pores within the low-grade iron ore were employed for carbon deposition during integrated pyrolysis-tar decomposition, as evidenced by pore size distribution data. TEM images further confirmed that some of the carbon that was deposited acts to partially block pores in the ore, which prevented complete loading by carbon. Identifying

this phenomenon offered a great opportunity to maximize the utilization of pore space in iron ore.

3. The sp3 content of carbon deposited from a number of different solid fuels was found to be similar, and exhibited similar tendencies as the cluster diameter. The Raman G peak position was found to shift slightly, indicating that the sp3 content was smaller at higher temperatures, due to a higher degree of graphitization. The carbon deposited through proposed method was categorized as being an amorphous carbon (a:C), with an sp3 content of 19–21%.

These results represent important knowledge and understanding related to the carbon deposition process, as well as to the structure of porous ores and carbon for innovative ironmaking process using integrated pyrolysis-tar decomposition over low-grade iron ores.

References

[1] World Coal Association. Coal and Steel; World Coal Association publication: Richmond, UK, 2007; pp 5.

[2] H. Shui, Y. Wu, Z. Wang, Z. Lei, C. Lin, S. Ren, C. Pan, S. Kang. Hydrothermal treatment of a sub-bituminous coal and its use in coking blends. Energy and Fuels 27 (2013):138 – 144.

[3] MA. Diez, R. Alvarez, JL. Cimadevilla. Briquetting of carbon-containing wastes from steelmaking for metallurgical coke production. Fuel 114 (2013): 216 – 223.

[4] U. Srivastava, SK. Kawatra, TC. Eisele. Production of pig iron by utilizing biomass as a reducing agent. International Journal of Mineral Processing 119 (2013): 51–57

[5] MA. Diez, R. Alvarez, C. Barriocanal. Coal for metallurgical coke production: Predictors of coke quality and future requirements for cokemaking. International Journal of Coal Geology 50 (2002): 389-412.

[6] C. Myren, C. Hornell, E. Bjornbom, K. Sjostrom. Catalytic tar decomposition of biomass pyrolysis gas with a combination of dolomite and silica. Biomass and Bioenergy 23 (2002): 217–227.

[7] RB. Cahyono, AN. Rozhan, N. Yasuda, T. Nomura, H. Purwanto, T. Akiyama. Carbon deposition using various solid fuels for ironmaking applications. Energy and Fuel 27 (2013): 2687–2692.

[8] RB. Cahyono, AN. Rozhan, N. Yasuda, T. Nomura, S. Hosokai, Y. Kashiwaya, T. Akiyama. Integrated coal-pyrolysis tar reforming using steelmaking slag for carbon composite and hydrogen production. Fuel 109 (2013): 439 - 444.

[9] RB. Cahyono, AN. Rozhan, N. Yasuda, T. Nomura, S. Hosokai, Y. Kashiwaya, T. Akiyama. Catalytic coal-tar decomposition to enhance reactivity of low-grade iron ore. Fuel Processing Technology 113 (2013): 84-89.

[10] S. Hosokai, K. Matsui, N. Okinaka, K. Ohno, M. Shimizu, T. Akiyama. Kinetic study on the reduction reaction of biomass-tar-infiltrated iron ore. Energy and Fuels 26 (2012): 7274-7279.

[11] P. Delhaes. Review: Chemical vapor deposition and infiltration processes of carbon materials. Carbon 40 (2002): 641–657.

[12] A. Roine, P. Lamberg, T. Katiranta, J. Salminen. HSC Chemistry 7 Simulation. Outotec 2009.

[13] K. Miura, K. Miyabayashi, M. Kawanari, R. Ashida. Enhancement of reduction rate of iron ore by utilizing low grade iron ore and brown coal derived carbonaceous materials. ISIJ International 51 (2011): 1234–1239.

[14] Y. Kashiwaya and T. Akiyama. Nanocrack formation in hematite through the dehydration of goethite and the carbon infiltration from biotar. Journal of Nanomaterials, Article ID 235609 (2010).

[15] Y. Kameya and K. Hanamura. Kinetic and Raman spectroscopic study on catalytic characteristics of carbon blacks in methane decomposition. Chemical Engineering Journal 173 (2011): 627–625.

[16] MA. Capano, NT. McDevitt, RK. Singh, F. Qian. Characterization of amorphous carbon thin films. Journal of Vacuum Science and Technology A: Vacuum, Surfaces, and Films 14 (1996): 431–435.

[17] M. Kawakami, T. Karato, T. Takenaka, S. Yokoyama. Structure analysis of coke, wood charcoal and bamboo charcoal by raman spectroscopy and their reaction rate with CO_2. ISIJ International 45 (2005): 1027–1034.

[18] C. Ravikant, P. Arun, S. Roy, MP. Srivastava. Deposition of Diamond-like Carbon films using Dense Plasma Focus. arXiv.org (2008). Journal ID: arXiv:0811.0162

[19] S. Zeb, M. Sadiq, A. Qayyum, G. Murtaza, M. Zakaullah. Deposition of diamond-like carbon film using dense plasma focus. Materials Chemistry and Physics 103 (2007): 235–240

[20] PK. Chu and L. Li. Characterization of amorphous and nanocrystalline carbon films. Materials Chemistry and Physics 96 (2006): 253–277.

[21] AC. Ferrari and J. Robertson. Interpretation of Raman spectra of disordered and amorphous carbon. Physical Review B 61 (2000): 14095–14107.

[22] X. Zhu and C. Sheng. Influences of carbon structure on the reactivities of lignite char reacting with CO_2 and NO. Fuel Processing Technology 91 (2010): 837–842.

[23] AC. Ferrari and J. Robertson. Raman spectroscopy of amorphous, nanostructured, diamond-like carbon, and nanodiamond. Phil. Trans. R. Soc. A 362 (2004): 2477–2512.

Chapter 5

Exergy analysis and application of CVI ironmaking

5.1 Introduction

The ironmaking industry is one of the most energy-intensive industries in the world and consumes 24 EJ/year, which constitutes around 5% of the total global energy consumption [1]. The primary energy source is fossil fuels, and such ironamking is one of the biggest contributors to CO_2 emissions, 3–4% of the total global emissions [2]. Several programs have been initiated worldwide to reduce fossil fuel utilization and CO_2 emissions, such as ULCOS in the EU, COURSE50 in Japan, and AISI in the USA [3]. In addition, a simple way to resolve emission concerns is to use biomass resources in the ironmaking industry. Pyrolysis and gasification serve as the primary steps in the utilization of biomass energy by converting it into char, tar, and gas. Tar contains highly condensable hydrocarbons and may cause issues, such as pipe plugging, condensation, and tar aerosol formation [4-5]. Several researchers have attempted to remove tar and eliminate problems such as adsorption-absorption and catalytic decomposition [6]. However, the results are still unsatisfactory because of technical and catalyst problems.

The effective utilization of low-grade ores such as goethite, FeOOH, in the modern ironmaking industry is highly required to solve the problems related to the depletion and shortages of high-grade iron ores. The drawback of low-grade ores containing goethite as a raw material is the presence of a large amount of combined water (CW) in the ores, which necessitates additional energy for the dehydration process. However, it has been reported that the dehydration of goethite at 450°C with a heating rate of 3°C/min in an air creates micropores ranging from 2 to 4 nm in size and a BET specific surface area as high as 70 m^2/g [7]. Because of

these, Miura et al [8] proposed iron ore/carbon composite (IOC) by introducing carbonaceous material into the pores to enhance the reduction rate of iron ore. The reduction rate of an IOC sample prepared using FeOOH reagent and thermoplastic carbon resin is dramatically enhanced and proceeds at temperatures as low as 700°C.

The integrated pyrolysis-tar decomposition over low-grade ores through Chemical Vapor Infiltration (CVI) is one of the most promising methods for the effective utilization of biomass and low-grade ores in the ironmaking industry. In this method, volatile matter, tar, and pyrolysis gas are introduced to a porous iron ore for a tar-decomposition process that produces highly valuable syngas (CO and H_2) and carbon materials that infiltrate and deposit within the pores of the iron ore. Under certain conditions, the conversion of tar in the decomposition process is 20–30 %mass for the pyrolysis of lignite coal and Palm Kernel Shell (PKS) biomass [9]. In addition, indirect iron ore reduction by CO and H_2 and conversion from Fe_2O_3 to Fe_3O_4, simultaneously occur during tar decomposition. Therefore, the method offers benefits such as removal of tar, effective use of low-grade ores and prereduced ores containing deposited carbon. As the main product, the ore containing deposited carbon, namely CVI ore exhibits high reactivity during the reduction reaction that started at 750°C primarily because of the nanoscale contact of iron ores and carbon [10].

To truly understand the energy efficiency and complexity of the proposed method, a specific analysis was definitely required. Exergy analysis based on the second law of thermodynamics may be the best method to assess the energy efficiency of the proposed method and to compare it with existing systems [11-12]. Therefore, an exergy analysis was performed using the developed process system diagram to evaluate the advantages of the proposed method over conventional methods. The sinter plant is the second biggest contributor of CO_2 emissions

after the blast furnace in the ironmaking process because of the utilization of coke breeze and coke oven gas (COG) [13-14]. The CO_2 is generated by combustion of coke breeze and calcinations of carbonates. The heat generated by the combustion process causes the iron ore granules to agglomerate into lump materials. Several research topics are initiated for minimizing CO_2 emission from sinter plant through fuel substitution [15-18]. In addition to fuel, combustion characteristic is also studied to lower ignition temperature and save energy [19]. The utilization of the CVI ore containing deposited carbon and a prereduced ore could be initiated in the sinter plant. The deposited carbon within the iron ore pores could serves as an energy source for the sintering process. Thus, the consumption of coke breeze in sinter plants could be minimized in order to achieve lower CO_2 emissions. The objectives of this chapter are to propose a process system diagram for the CVI process and compare its exergy analysis with conventional processes. In order to examine the feasibility of the process, the exergy analysis was processed based on previous published experimental results. In addition, a feasibility study of CVI ore utilization in sinter plants was discussed in terms of energy consumption and coke breeze utilization.

5.2. Analysis method

5.2.1 System definition

The process system diagram was developed with a strict boundary with regard to use of the energy generated from Palm Kernel Shell (PKS) biomass in the pyrolysis process. The exergy analysis comparison was carried out based on the proposed system (case 1) and conventional system (case 2), as briefly explained below.

- Case 1: Proposed integrated pyrolysis-tar decomposition (CVI process) system

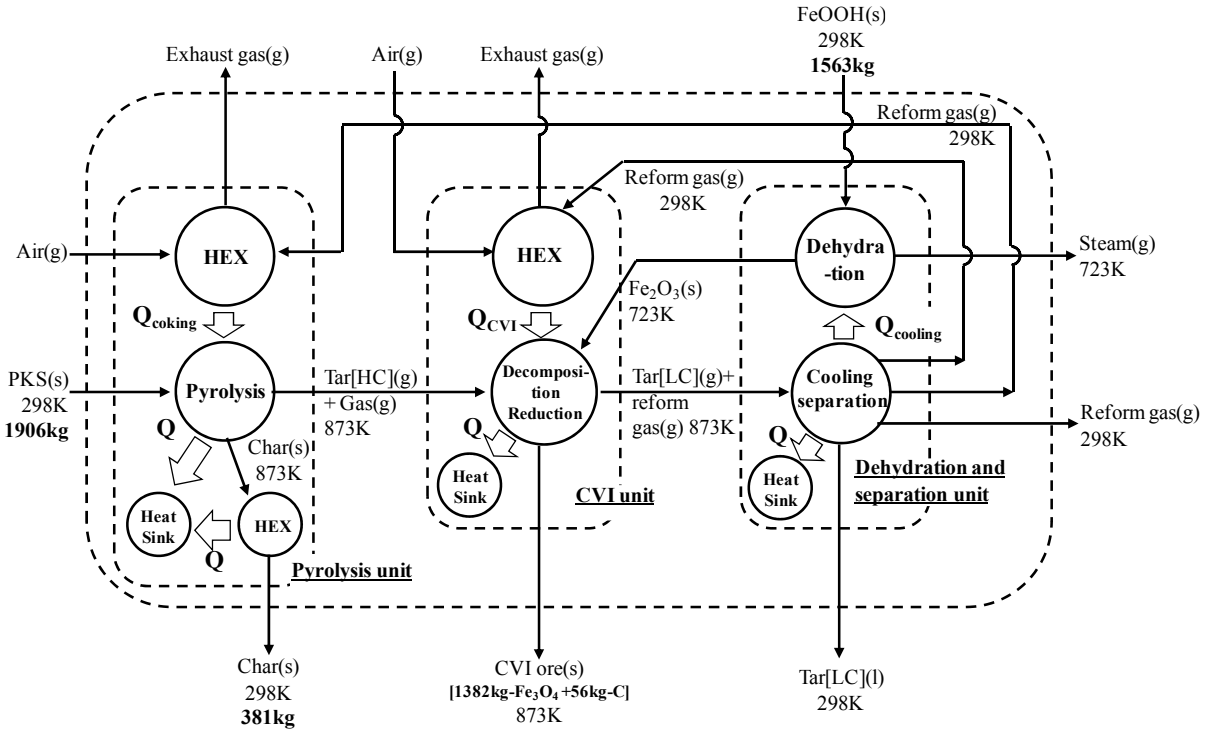

Fig. 5-1 Proposed system for utilization of PKS biomass and low grade iron ore (FeOOH) to produce 381 kg-char and 1000 kg-Fe through CVI ironmaking. PKS: Palm Kernel Shell biomass, HC: Heavy hydrocarbon, LC: Light hydrocarbon, HEX: Heat Exchanger, Heat sink means environment, and the dotted line is the boundary of system.

Fig. 5-1 shows the proposed system which was composed of integrated pyrolysis-tar decomposition for the recovery of tar energy using low-grade iron ores. This system was

composed three units, pyrolysis, CVI, and dehydration-separation. In the pyrolysis unit, PKS biomass was fed at atmospheric pressure and 873 K. As an endothermic process, the unit was supplied with heat generated through the combustion of recycled pyrolysis gas (after separation). Solid product char was taken directly from the unit and used as an energy source for combustion in another unit while the volatile matter (tar and gas) was transported to the CVI unit for tar decomposition. The low-grade ore, goethite, was dehydrated at 723 K under air to create porous ores based on the following reaction:

$$2FeOOH(s) \leftrightarrow Fe_2O_3(s) + H_2O(g); \quad \Delta H = 49.8\,kJ/mol\text{-}Fe_2O_3 \text{ at } 723\,K \qquad (5.1)$$

The dehydration energy was provided by waste heat from the cooling process of the mixture, in addition to tar and gas following the CVI process. The porous ore and volatile matter from the pyrolysis unit were delivered to the CVI unit for tar decomposition (5.2) and reduction (5.3–5.4) based on the following reaction.

$$Tar \rightarrow H_2 + CO + CO_2 + CH_4 + \text{other light hydrocarbons} + C \qquad (5.2)$$

$$3Fe_2O_3(s) + CO(g) \leftrightarrow 2Fe_3O_4(s) + CO_2(g); \quad \Delta H = -6.73\,kJ//mol\text{-}Fe_2O_3 \text{ at } 873\,K \qquad (5.3)$$

$$3Fe_2O_3(s) + H_2(g) \leftrightarrow 2Fe_3O_4(s) + H_2O(g); \quad \Delta H = 5.39\,kJ//mol\text{-}Fe_2O_3 \text{ at } 873\,K \qquad (5.4)$$

Simultaneously to the tar decomposition, the carbon product infiltrated and deposited in the porous ore to produce an iron ore containing carbon material. In addition, the indirect reduction of the iron ore (Fe_2O_3 to Fe_3O_4) also took place with the use of H_2 and CO, both of which were produced from pyrolysis and tar-decomposition. Thus, the CVI unit resulted in the prereduced iron ore containing a carbon material, CVI ore which could be sent to the next processing unit such as the sinter plant or blast furnace. After the CVI process, the mixture of unreacted tar (light hydrocarbon) and reform gas was transported into a separation unit for cooling. The amount of condensable hydrocarbon in the mixture was smaller because of the decomposition process, and it was possible to recover the heat of the mixture for iron-ore dehydration. The total carbon

content of unreacted tar was 22% less than that in the tar product obtained from the conventional system [9]. The reform gas product can be recycled as a heat source for several endothermic units such as pyrolysis, CVI, and dehydration. The remaining reform gas could be applied as an energy source in other ironmaking processes. The chemical energy of cooled un-reacted tar can be unrecovered again within the system and delivered outside of the ironmaking industry. Therefore, the proposed system offers both thermal and chemical energy recovery through CVI and separation units.

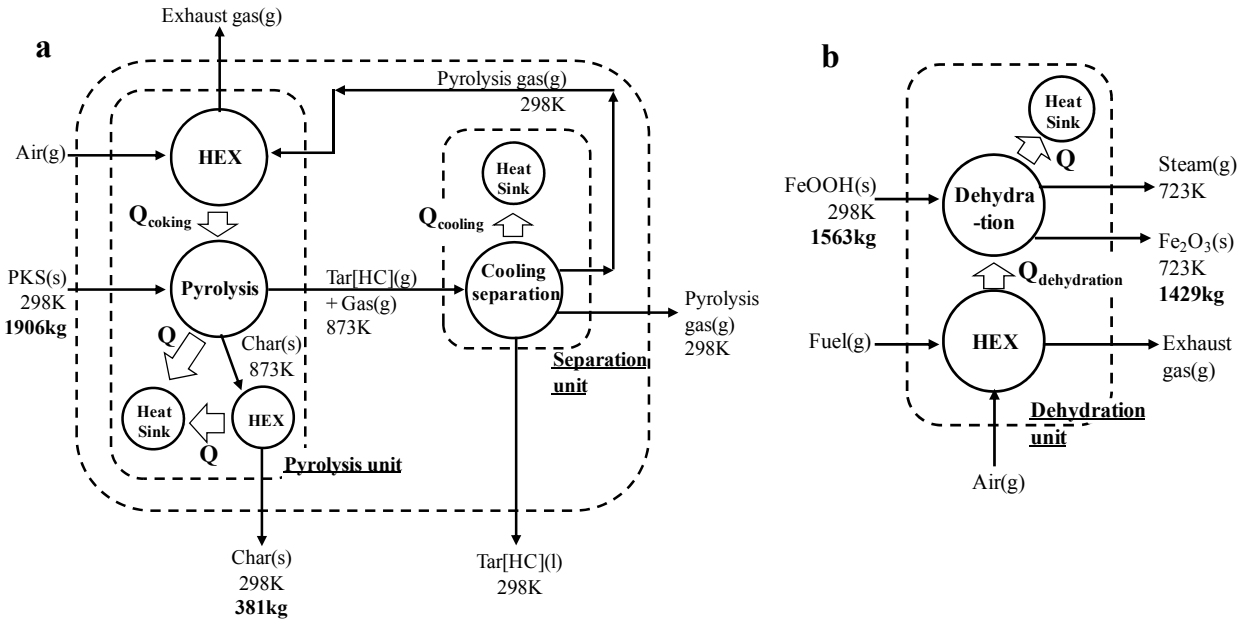

Fig. 5-2 Conventional system for (a) utilization of PKS biomass and producing of 381 kg-char through pyrolysis process and (b) dehydration process to produce 1000 kg-Fe from low grade iron ore (FeOOH) in the ironmaking industry. PKS: Palm Kernel Shell biomass, HC: Heavy hydrocarbon, LC: Light hydrocarbon, HEX: Heat Exchanger, Heat sink means environment, and the dotted line is the boundary of system

- Case 2: Conventional pyrolysis and dehydration systems

The conventional system is a common existing method for biomass pyrolysis system, which consists of pyrolysis and a separation unit, as shown in Fig. 5-2a. In order to evaluate the

exergy losses, conventional pyrolysis was carried out in a similar way to the proposed process. Unlike the proposed system, the volatile product consisting of tar and gas could not be directly utilized as an energy source because of the large amount of condensable heavy hydrocarbon. Thus, a separation process must be completed first by cooling the volatile mixture. Finally, the gas product, which was free of tar, could be used as an energy source in the pyrolysis and endothermic units. The liquid tar was collected and sent outside of the system. Therefore, the conventional system never recovered the energy of tar material because of handling and technical difficulties. In order to utilize the low grade ore (FeOOH) for ironmaking, the additional energy (gas fuel) was supplied for dehydration process as shown in Fig. 5-2b. The porous ore, Fe_2O_3 could be sent to a sinter plant or blast furnace to produce metallic Fe.

5.2.2 Exergy analysis

- Mass balance and operation data

According to the experimental data obtained under conditions [9], the material flow of both the conventional and proposed systems was calculated for producing 381 kg char and 1000 kg metallic Fe, as listed in Table 5-1. The ratio of PKS to the porous ore was similar in the experiment condition, 4:3 (mass ratio). Table 5-2 shows the operation data used in that analysis. The carbon content within the iron ore was 3.86%mass, as explained previously [9]. The high heating value (HHV) of PKS and charcoal were estimated using the Dulong equation as follows [20]:

$$\mathrm{HHV\,[kJ/kg]} = 337\mathrm{C} + 1442\left(\mathrm{H} - \frac{\mathrm{O}}{8}\right) + 93\mathrm{S} \qquad (5.5)$$

where C, H, O, and S are the percentages of carbon, hydrogen, oxygen, and sulfur.

Table 5-1 Material flow of both conventional (pyrolysis-dehydration) and proposed systems (pyrolysis-tar decomposition) in each unit. Basis: 1000 kg of metallic Fe.

Conventional	Pyrolysis process				Dehydration process	
	Pyrolysis		Separation		Dehydration	
Material [unit]	Input	Output	Input	Output	Input	Output
PKS [kg]	1906.1	0.0	0.0	0.0	0.0	0.0
Char [kg]	0.0	381.2	0.0	0.0	0.0	0.0
Tar [kg]	0.0	567.1[a)]	567.1	567.1	0.0	0.0
Pyrolysis gas[1)] [Nm^3]	291.7	909.5	909.5	909.5	0.0	0.0
Goethite ore (FeOOH) [kg]	0.0	0.0	0.0	0.0	1563.0	0.0
Porous ore (Fe_2O_3) [kg]	0.0	0.0	0.0	0.0	0.0	1429.6
Steam [Nm^3]	0.0	0.0	0.0	0.0	0.0	180.9
Fuel gas [Nm^3]	0.0	0.0	0.0	0.0	42.9	0.0
Air [Nm^3]	1002.7	0.0	0.0	0.0	251.6	0.0
Exhaust gas [Nm^3]	0.0	1203.4	0.0	0.0	0.0	284.5

Proposed	Pyrolysis		CVI		Dehydration-separation	
Material [unit]	Input	Output	Input	Output	Input	Output
PKS [kg]	1906.1	0.0	0.0	0.0	0.0	0.0
Char [kg]	0.0	381.2	0.0	0.0	0.0	0.0
Tar [kg]	0.0	567.1[a)]	567.1	478.0[b)]	478.0	478.0
Pyrolysis gas[1)] [Nm^3]	316.7	909.5	987.0	1017.8[c)]	1017.8	1017.8
Goethite ore (FeOOH) [kg]	0.0	0.0	0.0	0.0	1563.0	0.0
Porous ore (Fe_2O_3) [kg]	0.0	0.0	1429.6	0.0	0.0	1429.6
CVI ore (Fe_3O_4+C) [kg]	0.0	0.0	0.0	1438.0	0.0	0.0
Steam [Nm^3]	0.0	0.0	0.0	0.0	0.0	180.9
Air [Nm^3]	971.4	0.0	237.5	0.0	0.0	0.0
Exhaust gas [Nm^3]	0.0	1197.9	0.0	292.9	0.0	0.0

1) Input : recycling gas after separation; a) Heavy hydrocarbon; b) Light hydrocarbon; c) Reform pyrolysis gas

Table 5-2 Operation and enthalpy data which used for exergy analysis

(a) Palm Kernel Shell (PKS) and biochar elemental analysis

Material	C	H	N	O	Enthalpy [MJ/kg]
PKS	49.5	5.7	0.8	44	16.7
PKS char	79.8	3.1	0.4	15.6	28.1

(b) Composition of pyrolysis, reform pyrolysis and fuel gases [%volume]

Material	H_2	CO	CO_2	CH_4	N_2	Enthalpy [MJ/Nm3]
Pyrolysis gas	15.7	44.5	23.9	13.9	0.0	14.1
Reform pyrolysis gas	24.2	31.7	29.9	12.4	0.0	12.9
Fuel gas (COG)	53.6	6.9	2.6	29.2	5.9	20.3

(c) Material enthalpy data

Material	Enthalpy [MJ/kg]	Note
PKS tar	21.6	Cp : 4.22E-3T[kJ/kg-tar K] [21] Enthalpy of HC and LC was similar
Deposited carbon	28.1	Similar with char product
Iron ore	0.0045	Fe_2O_3 and FeOOH (CW : 8.2%mass)
Porous ore	0.35	Fe_2O_3 at 723K
CVI ore	1.01	Fe_3O_4 at 873K
Steam	3.38	Superheated steam (723K, 1 atm)

HC: Heavy hydrocarbon, LC : Light hydrocarbon

- Calculation method

Based on the material flow and operation data given above, an exergy analysis was performed to evaluate the benefit of proposed system. The exergy analysis was used to assess the feasibility of qualitatively converting the available energy into usable energy in the form of work by the following equation:

$$\Delta\varepsilon = \Delta H - T_0 \Delta S \qquad (5.6)$$

The total exergy consisted of chemical exergy (ε_C), thermal exergy (ε_T), pressure exergy (ε_P), and mixing exergy (ε_M). The detailed equations for each kind of exergy are given below:

$$\varepsilon = \varepsilon_C + \varepsilon_T + \varepsilon_P + \varepsilon_M \quad (5.7)$$

$$\varepsilon_C = \sum n_i \varepsilon_i^0 \quad (5.8)$$

$$\varepsilon_T = \left(\sum n_i C_{pi}\right)\left[T - T_0 - T_0 \ln\left(T / T_0\right)\right] \quad (5.9)$$

$$\varepsilon_P = \left(\sum n_i\right) RT_0 \sum\left[\ln\left(P / P_0\right) - \left(1 - P_0 / P\right)\right] \quad (5.10)$$

$$\varepsilon_M = RT_0 \sum\left[n_i \ln\left(n_i / \sum n_i\right)\right] \quad (5.11)$$

where ε : exergy [kJ/mol], H: enthalpy [kJ/mol], S: entropy [J/molK], n: mol of the substances [mol], Cp: specific heat at constant pressure [kJ/molK], T_0: reference temperature [K], T: actual temperature [K], P_0: reference pressure [atm], P: actual pressure [atm], and R: gas constant [J/molK]. The exergy loss (EXL) was calculated as the difference between the exergy of the input material (ε_{in}) and that of the output material (ε_{out}) in each unit of the system. The reference exergy (ε^0) was described as the chemical exergy of each substance at 298 K and 1 atm calculated based on the Gibbs free energy. The exergy calculation was made based on the following assumptions:

1. The exergy of solid fuel was equal to HHV, according to Rant's approximation [22].
2. The enthalpy of unreacted tar (LC) (after the CVI process) was identical to the tar from the pyrolysis process (HC) because of difficulties in analyzing the unreacted tar. In addition, the exergy of tar was equal to 0.975 HHV, as gleaned from Rant's approximation for liquid fuel [22].
3. The exergy of the deposited carbon was similar to char pyrolysis product.

4. Adiabatic process was done in each unit. The pressure and temperature of outflow stream in each process was assumed to be similar with the condition inside of process.
5. The requirement energy of pyrolysis, CVI, and dehydration unit were supplied by the complete combustion of the recycled gas product in each unit. Energy loss was computed and collected as a heat sink to maintain the law of energy conservation
6. To ensure complete combustion, the amount of input air exceeded 20% of the volume of the theoretical calculation.

5.3 Result and discussion

5.3.1 Exergy analysis

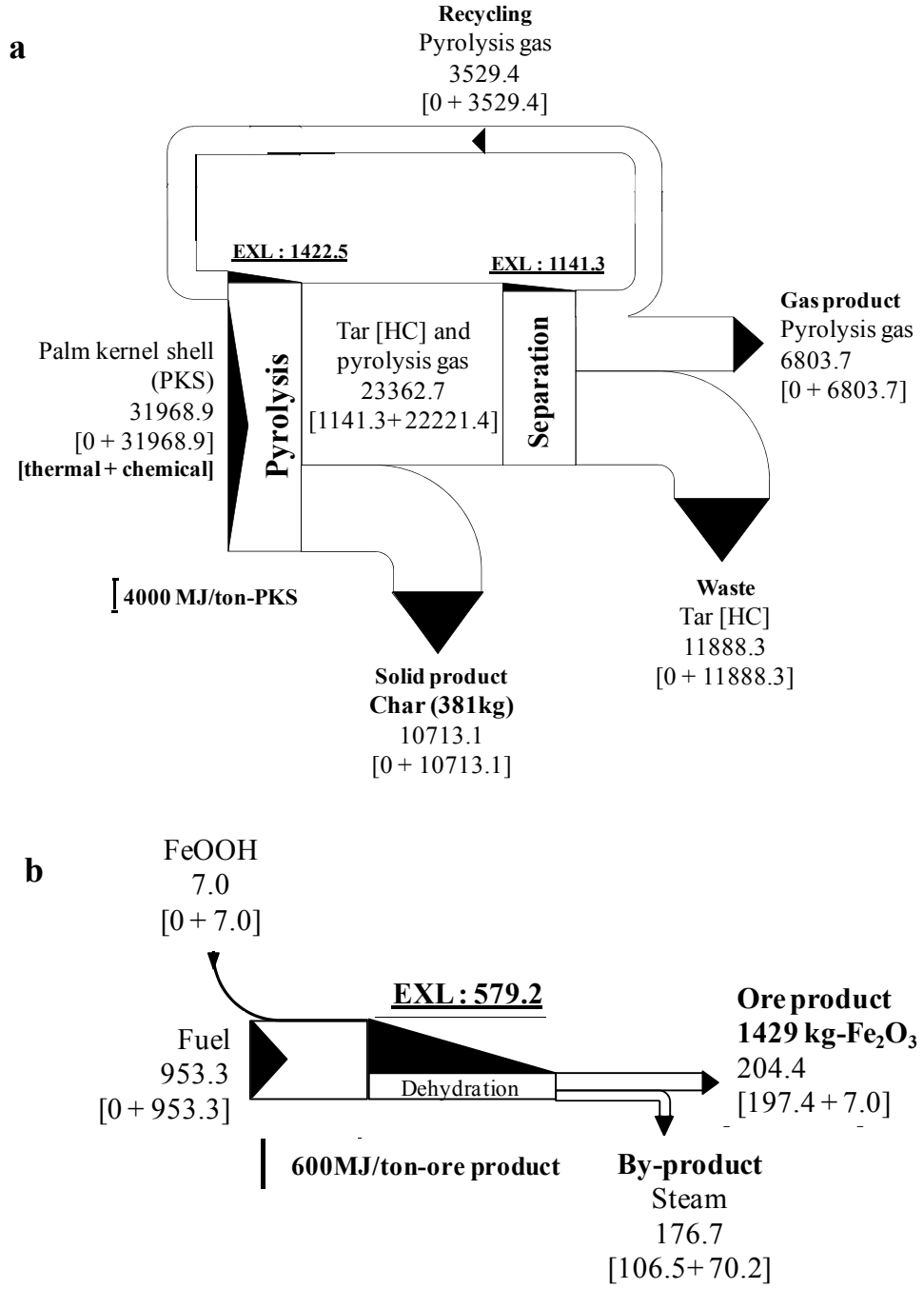

Fig. 5-3 Exergy flowchart of the conventional process (a) for producing of 381 kg-char by pyrolysis of Palm Kernel Shell (PKS) biomass and (b) for producing of 1000 kg-Fe from low grade iron ore (FeOOH) .

Fig. 5-3a shows the exergy flowchart of the conventional pyrolysis system used for producing 381 kg char. The width flow expresses the exergy quantity while the black block arrows refer to the exergy flow of each unit. It is clear that only 33.5% of PKS input exergy was converted into char exergy and could be directly utilized in the other unit. This may be related to the original composition of the biomass, which consisted of large volatile matter, around 65.4 %mass [7]. Thus, the biggest portion of PKS exergy passed directly to the separation unit. By using this unit, clean gas was recovered which contained 32.3% of the PKS exergy input. A part of this gas exergy was utilized in the pyrolysis unit while the remaining gas was delivered to another unit. It means that the tar material still comprised of 37.2% of PKS input exergy and was not utilized in the ironmaking process. The total exergy of the output material was smaller than those of the input materials in all units, indicating that each process suffered exergy losses owing to the exergy consumption required to run the process. In the pyrolysis unit, the exergy loss was 4% of the total input exergy and was mainly used for the decomposition and destruction of PKS solid fuel. Meanwhile, the exergy loss in the separation unit was 4.9% of the total input and was primarily composed of thermal exergy from cooling.

On the other hand, conventional dehydration was carried out to produce 1000 kg metallic Fe using fuel gas as shown in Fig. 5-3b. Obviously, the process consumed a significant amount of exergy which 60.3% of input exergy was lost for removing of the -OH group from the iron ore as in reaction (5.1). This process also generated steam as a byproduct which contained around 18.4% of input exergy. Therefore, the exergy flowchart illustrated that the largest amount of PKS exergy was transferred into the tar material and was not recovered in the ironmaking process. Moreover, the utilization of low grade iron ore (FeOOH) required high additional energy in the dehydration process.

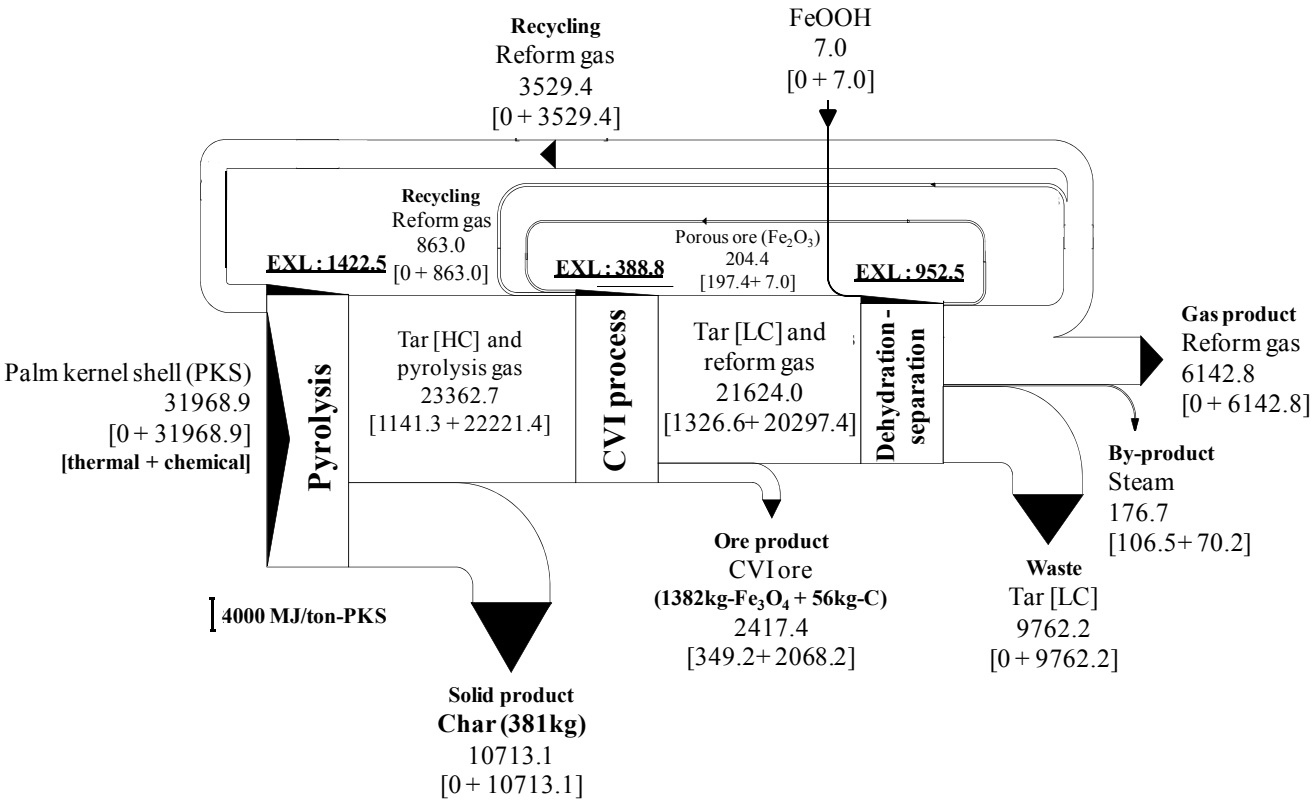

Fig. 5-4 Exergy flowchart of the proposed system for utilization of biomass and low grade iron ore (FeOOH) to produce 381 kg-char and 1000 kg-Fe through integrated pyrolysis-tar decomposition (CVI process). The integrated process showed that the CVI process increased utilization of PKS exergy by decreasing the tar exergy outflow .

Integrated pyrolysis-tar decomposition through CVI process was proposed to recover as much PKS exergy as possible using porous ores. By similar basis to conventional system, 381 kg char and 1000 kg Fe products, the exergy analysis of proposed system was conducted and the flowchart was showed in Fig. 5-4. The exergy of the pyrolysis unit was similar to the conventional system. In the proposed system, the volatile matter (tar and pyrolysis gas) was transported to the CVI unit for tar decomposition over porous ores. Unlike the conventional system, to create a porous ore, a low-grade iron ore was heated using waste heat generated from the cooling process. In addition to the porous ore, complete dehydration process resulted in

superheated steam (723 K, 1 atm) with exergy of 176.7 MJ and could be utilized in another unit as an energy source. The volatile matter was introduced with the porous ore in the CVI unit for tar decomposition, carbon deposition, and reduction. As shown in Fig. 5-4, the CVI ore exergy increased to a significantly higher value than the input exergy of the CVI unit because of due to carbon deposition and reduction reaction. The carbon material contained a large amount of exergy, while Fe_3O_4, the reduction product, released a large amount exergy during the oxidation process. The high exergy of CVI ore could be utilized to decrease the energy consumption in an ore-processing unit such as a sinter plant or blast furnace. The exergy loss in this unit was quite small, around 1.6%, compared to other units because of the limited tar conversion during the process. It is well known that the large amount of decomposition material requires a significant amount of endothermic heat and result in large exergy consumption. Therefore, the CVI unit offers an advantage in terms of tar exergy recovery by producing a CVI ore containing carbon and a pre-reduced ore, Fe_3O_4. Furthermore, the remaining exergy of the unreacted tar and gas product was delivered to the separation unit to simultaneously perform the thermal exergy recovery and cooling process. The application of waste heat for heating the iron ore allows the dehydration process of proposed system to proceed without using any external energy source. Similar to the conventional system, clean gas was recovered and utilized in the other endothermic units such as the pyrolysis, CVI, and dehydration units. The amount of the discharged tar exergy from this unit was less than the conventional system, indicating that the proposed system reutilized the tar exergy to generate a useful product.

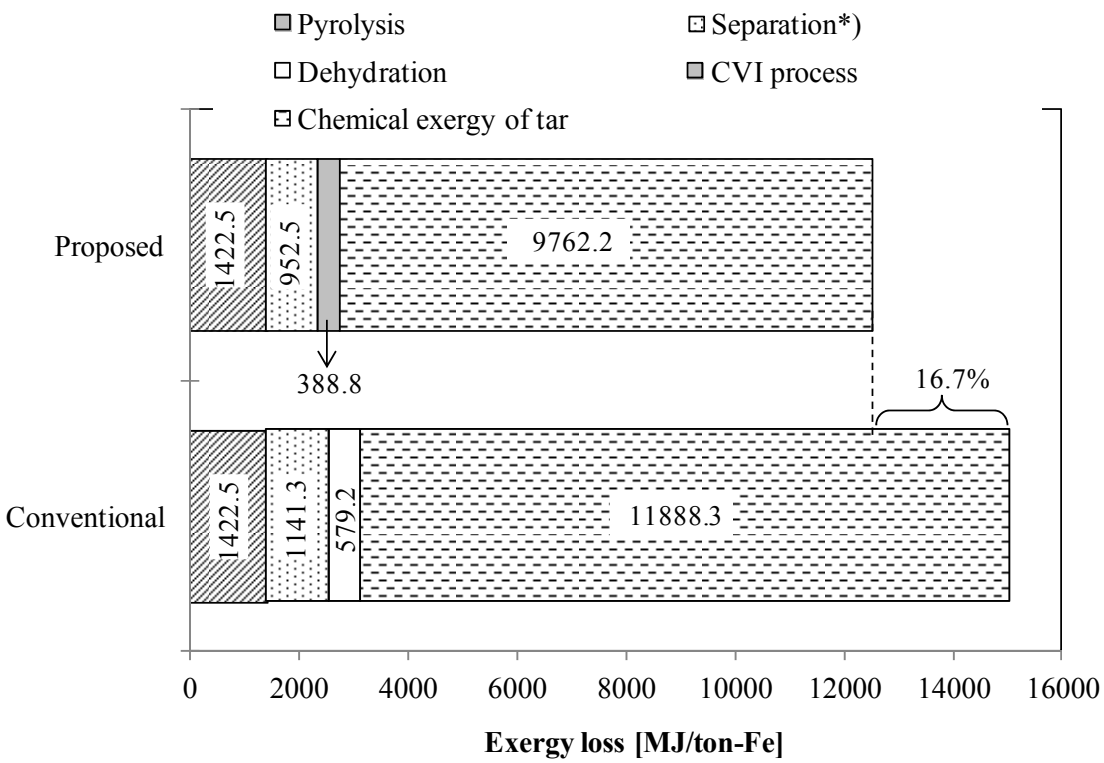

*) In the proposed system, the separation process was integrated with ore dehydration (heat recovery)

Fig. 5-5 Comparison of exergy losses showed that the proposed system decreased exergy losses compared to a conventional system by recovering both chemical and thermal exergy.

Fig. 5-5 shows a comparison of exergy losses in both a conventional and proposed system for producing 318 kg char and 1000 kg metallic Fe. The total loss which was obtained from exergy losses in each unit and outflow tar exergy can be determined by using the assumption that the exergy of char and gas product could be employed in other unit through simple conversion method. The separation process in the proposed system allowed for recovery of thermal exergy from gas and unreacted tar for the dehydration process. Obviously, the proposed system based on integrated pyrolysis-tar decomposition was effective in recovering the chemical exergy of tar using porous low-grade iron ores. In addition, the waste heat recovery in the dehydration of iron ore in the proposed system constituted a promising method to reduce the

total exergy loss. Thus, the proposed system decreased the exergy loss by around 16.7% through the recovery of both chemical and thermal tar exergy. The decomposition of the tar component into a lighter hydrocarbon and the carbon deposited in the iron-ore pores successfully decreased the total exergy losses.

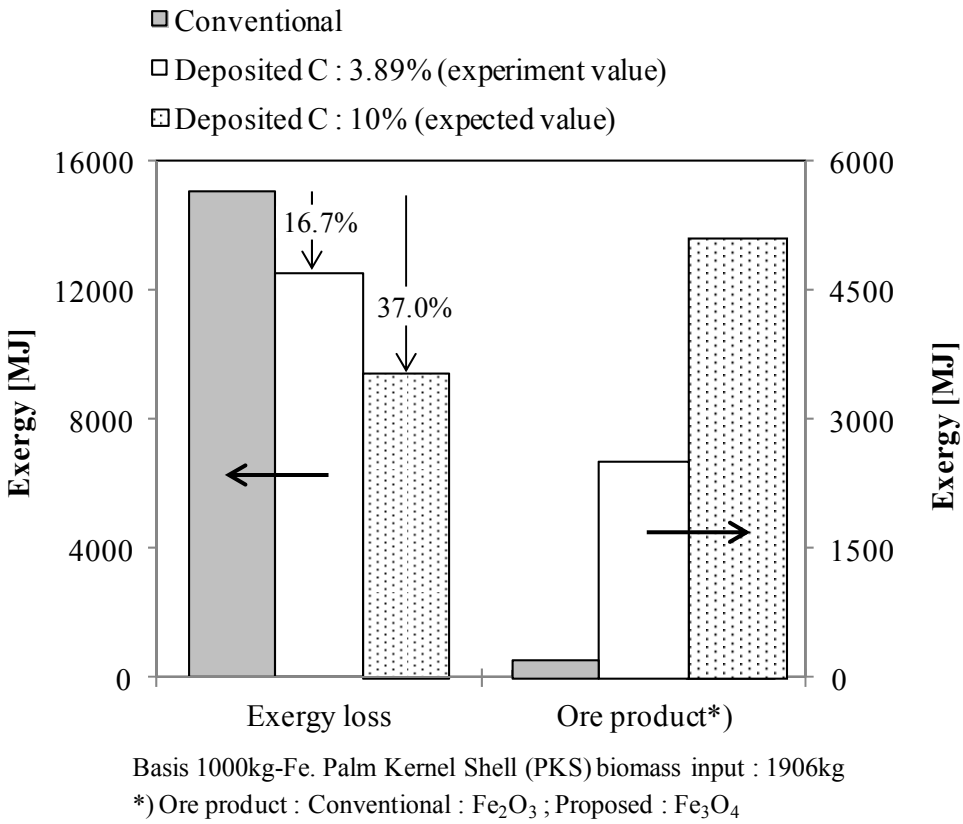

Fig. 5-6 Comparison of exergy losses and ore product for both conventional and proposed system at different amount of deposited carbon showed that the expected value of deposited carbon decreased significantly of exergy loss and enhanced dramatically of ore product exergy.

Based on the experimental values, the amount of deposited carbon within the porous ore was lower than the expected, 10%mass. This value was calculated by using the remaining pore volume of the porous ore after the carbon deposition process [7, 9]. Fig. 5-6 shows the exergy

losses and ore product for both conventional and proposed system with different amounts of deposited carbon. As the carbon deposition originated from tar decomposition, increasing the carbon deposition enhanced the ore product exergy and decreased the chemical tar exergy outflow. Therefore, the expected value of carbon deposition declined significantly of total exergy loss. In addition to exergy loss, this circumstance improved also the overall efficiency of biomass utilization in ironmaking process, meaning that a similar amount of biomass input, 1906 kg PKS resulted in higher exergy of the ore product and smaller exergy losses.

5.3.2 Application of CVI ironmaking on sinter plant

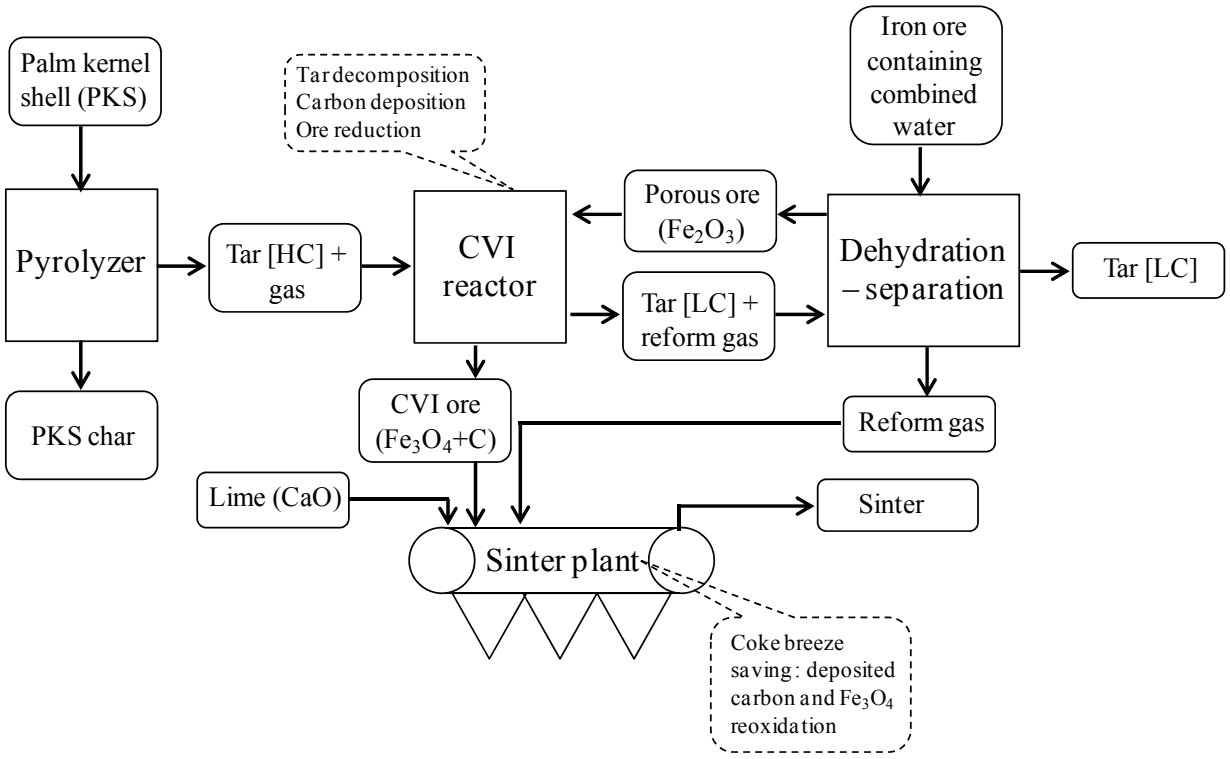

Fig. 5-7 Schematic diagram of CVI ore application in the sinter plant showed that the carbon deposited in the ore had a high potential to reduce the consumption of coke breeze in the ironmaking industry.

The main purpose of the sinter plant is to prepare an iron ore as a suitable feedstock for the blast furnace through an agglomeration process. In the existing system, this process shows high energy consumption and produces a large amount of CO_2 from the combustion of coke breeze and COG. To produce sinter, an iron ore and lime (CaO) are heated and melted at high temperatures. Therefore, the sinter plant is promising unit in the ironmaking industry to effectively utilize the CVI ore. The deposited carbon within the CVI ore could replace the coke breeze as an energy source in the sinter plant. Fig. 5-7 shows the schematic diagram of a sinter plant that utilized the CVI ore as a product of integrated pyrolysis-tar decomposition over porous iron ores. In addition to the deposited carbon, the reform pyrolysis gas could also be used as an energy source and substitute for COG. By using this system, the consumption of coke breeze and CO_2 emissions could be reduced.

The main energy source for ore agglomeration in the sinter plant comes from the combustion of solid fuel through an oxidation process. In addition to the deposited carbon, the CVI ore mainly contained prereduced iron ore, Fe_3O_4 as a result of indirect reduction in the CVI unit. Based on the Gibb's free energy, the oxidation of Fe_3O_4 into Fe_2O_3 would occur spontaneously in the sinter plant through reaction (5.12).

$$4Fe_3O_4(s) + O_2(g) \leftrightarrow Fe_2O_3(s)\,; \quad \Delta H = -495.2\,kJ \tag{5.12}$$

Using the large supply of O_2 from the input air, this reaction occurred completely without any CO_2 generation. The reaction heat of this reaction could act as additional energy for the combustion and agglomeration processes in the sinter plant. In addition to the carbon content, this represented another benefit of the CVI ore, and therefore, it could also act as an energy-storage system in the ironmaking process.

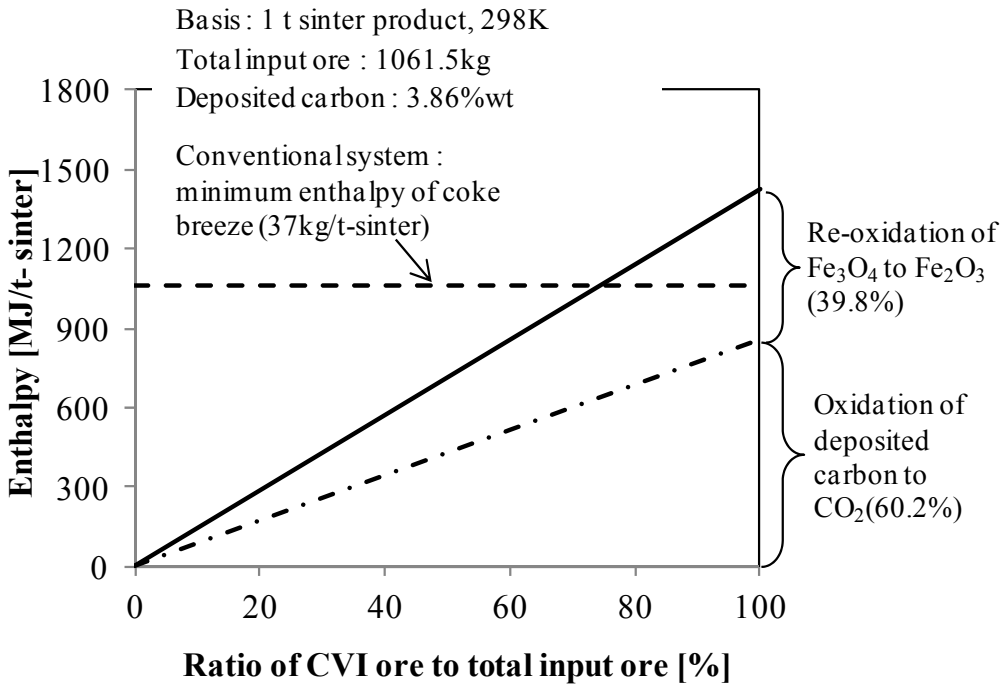

Fig. 5-8 Enthalpy content of the input iron ore in the sinter plant showed that the input enthaphy of CVI ore was higher than the minimum coke enthalpy at ratios of CVI ore above 70%.

In the existing plant, 1061 kg of the total iron ore was fed into the sinter plant with 37 kg of coke breeze as energy source to produce 1 ton of sinter. Fig. 5-8 shows the enthalpy of the CVI ore at different ratios compared to the total input ore for 1 ton of sinter product. The horizontal line indicates the minimum coke enthalpy input in the existing system. It is clear that the enthalpy of total input ore (original ore and CVI ore) was enhanced at a higher ratio of CVI ore because of the amount of deposited carbon and Fe_3O_4. The total enthalpy of CVI ore was supplied by two different sources, namely re-oxidation of Fe_3O_4 and deposited carbon with ratio of 39.8% and 60.2% respectively. The enthalpy of total input ore became more than the minimum coke enthalpy when the CVI ore content was above 70% of the total input ore. This indicated that the CVI ore enthalpy was sufficient for the sintering process without the addition

of any coke breeze. Accordingly, the oxidation enthalpy of Fe_3O_4 also had a significant effect on the total enthalpy of the CVI ore.

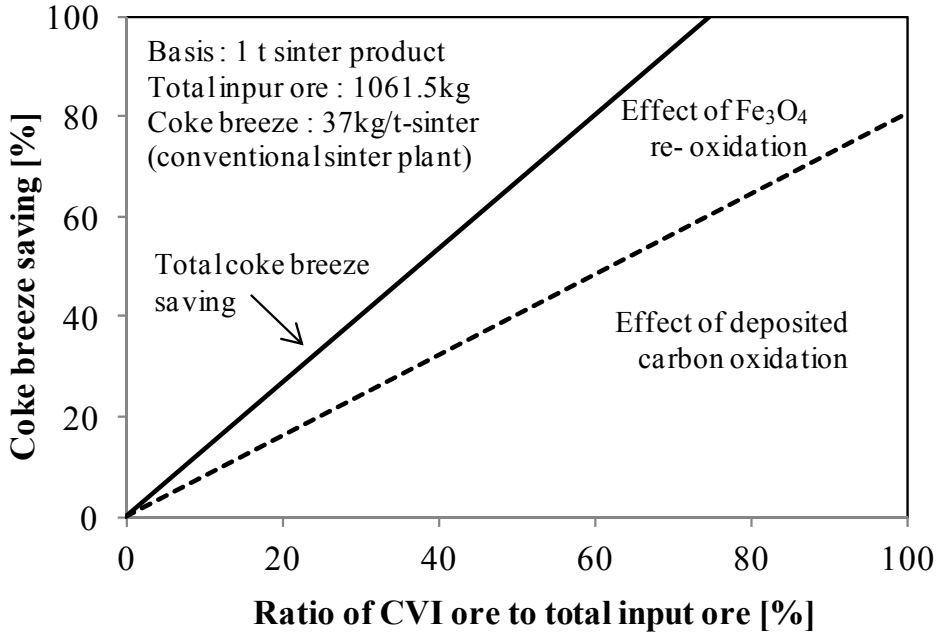

Fig. 5-9 Effect of CVI ore utilization on the consumption of coke breeze in sinter plant showed that the proposed system offered an extensive amount of coke breeze savings.

Based on the enthalpy content of the input ore, the amount of coke breeze was estimated at different ratios of the CVI ore, as shown in Fig. 5-9. The amount of coke breeze saving had a linear correlation with the CVI ore input to the sinter plant, and a larger coke saving was achieved at a higher ratio of the CVI ore to the total input ore. When the ratio of the CVI ore was 40%, the consumption of coke breeze in the sinter plant decreased to 14.4 kg, and more than 60% was saved as compared to the existing system. The coke breeze saving could become 100% when the CVI ore content was above 70% of the total input ore, meaning that the sinter plant could proceed without addition of coke breeze. Based on these results, the application of the CVI

ore in a sinter plant led to extensive decreases in coke breeze and CO_2 emissions in the ironmaking process.

5.4 Conclusions

The exergy analysis was performed to assess the benefit of CVI process and the application of CVI ore in the sinter plant was also discussed for decreasing the CO_2 emission. Several conclusions could be obtained as follow:

1. A process system diagram of the integrated pyrolysis-tar decomposition through CVI process was successfully constructed which consisted of three units: pyrolysis, CVI, and dehydration-separation. The iron ore was utilized for energy storage in this system through deposited carbon within the pores of the ore and Fe_3O_4. The energy requirements of this system were sufficiently supplied via the recycling of pyrolysis gas.
2. The exergy of CVI ore enhanced drastically in the CVI unit because of the reduction reaction and carbon deposition as a result of tar decomposition. The total exergy losses decreased by 16.7% compared to a conventional system by recovering the chemical and thermal tar exergy. When the carbon deposition reached the expected value (10%mass), the total exergy losses declined significantly to around 37.0% compared to a conventional. Thus, the proposed system is a promising method for recovery chemical and thermal tar exergy using porous low-grade iron ores.
3. In the sinter plant, the amount of the deposited carbon was sufficient to completely replace coke breeze when the CVI ore content was above 70% of the total input ore. The total enthalpy of CVI ore was sourced by re-oxidation of Fe_3O_4 and deposited carbon with the ratio of 39.8% and 60.2% respectively. The application of the CVI ore in a sinter plant

resulted in an extensive decrease in the coke breeze and CO_2 emissions in the ironmaking industry.

References

[1] C. Xu and C. Da-qiang. A brief overview of low CO2 emission technologies for iron and steelmaking. Journal of Iron and Steel Research International 17 (2010): 01-07.

[2] M. Yelliashetty, PG. Ranjith, and A. Tharumarajah. Iron ore and steel production trends and material flows in the world: Is this really sustainable? Resources, Conservation and Recycling, 54 (2010): 1084.

[3] J. Fu, G. Tang, R. Zhao, and W. Hwang. Carbon reduction programs and key technologies in global steel industry. Journal of Iron and Steel Research International 21 (2014): 275.

[4] L. Devi, K. J. Ptasinski, and FJ. Janssen. A review of the primary measures for tar elimination in biomass gasification processes. Biomass and Bioenergy 24 (2003): 125.

[5] J. Han and H. Kim. The reduction and control technology of tar during biomass gasification/pyrolysis: An overview. Renewable and sustainable energy reviews 12 (2008): 397-416

[6] C. Myren, C. Hornell, E. Bjornbom, K. Sjostrom. Catalytic tar decomposition of biomass pyrolysis gas with a combination of dolomite and silica, Biomass and Bioenergy 23 (2002): 217–227.

[7] RB. Cahyono, N. Yasuda, T. Nomura, and T. Akiyama. Optimum temperatures for carbon deposition during integrated coal pyrolysis–tar decomposition over low-grade iron ore for ironmaking applications. Fuel Processing Technology 119 (2014): 272.

[8] K. Miura, K. Miyabayashi, M. Kawanari, and R. Ashida. Enhancement of reduction rate of iron ore by utilizing low grade iron ore and brown coal derived carbonaceous materials. ISIJ International 51 (2011): 1234.

[9] RB. Cahyono, AN. Rozhan, N. Yasuda, T. Nomura, H. Purwanto, and T. Akiyama. Carbon deposition using various solid fuels for ironmaking applications. Energy and Fuels 27 (2013): 2687.

[10] S. Hosokai, K. Matsui, N. Okinaka, K. Ohno, M. Shimizu, and T. Akiyama. Kinetic study on the reduction reaction of biomass-tar-infiltrated iron ore. Energy and Fuels 26 (2012): 7274.

[11] T. Hiraki and T. Akiyama. Exergetic life cycle assessment of new waste aluminium treatment system with co-production of pressurized hydrogen and aluminium hydroxide. International Journal of Hydrogen Energy 34 (2009): 153.

[12] Y. Shudo, T. Ohkubo, Y. Hideshima, and T. Akiyama. Exergy analysis of the demonstration plant for co-production of hydrogen and benzene from biogas. International Journal of Hydrogen Energy 34 (2009): 4500.

[13] TC. Ooi, E. Aries, BC. Ewan, D. Thompson, DR. Anderson, R. Fisher, T. Fray, D. Tognarelli. The study of sunflower seed husks as a fuel in the iron ore sintering process. Minerals Engineering 21 (2008): 167–177

[14] H. Yabe and Y. Takamoto. Reduction of CO2 Emissions by Use of Pre-reduced Iron Ore as Sinter Raw Material. ISIJ International 53 (2013): 1625.

[15] A. Cores, A. Babichi, M. Muniz, S. Ferreira, J. Mochon. The influence of different iron ores mixtures composition on the quality of sinter. ISIJ International 50 (2010): 1089–1098

[16] M. Zandi, MM. Pacheco, TA. Fray. Biomass for iron ore sintering. Minerals Engineering 23 (2010): 1139–1145

[17] RR. Lovel, KR. Vining, MD. Amico. The influence of fuel reactivity on iron ore sintering. ISIJ International 49 (2009): 195–202

[18] N. Oyama, Y. Iwami, T. Yamamoto, S. Machida, T. Higuchi, H. Sato, M. Sato, K. Takeda, Y. Watanabe, M. Shimizu, K. Nishioka. Development of secondary-fuel injection technology for energy reduction in the iron ore sintering process. ISIJ International 51 (2011): 913–921

[19] W. Yang, S. Choi, ES. Choi, DW. Ri, S. Kim. Combustion characteristics in an iron ore sintering bed—evaluation of fuel substitution. Combustion and Flame 145 (2006): 447–463

[20] S. Kathiravale, MN. Yunus, K. Sopian, AH. Samsuddin, and RA. Rahman. Modeling the heating value of Municipal Solid Waste. Fuel 82 (2003): 1119.

[21] C. Li and K. Suzuki. Tar property, analysis, decomposition mechanism and model for biomass gasification—an overview. Renewable and Sustainable Energy Review 13 (2003): 594.

[22] N. Yasuda, T. Tsuchiya, N. Okinaka, and T. Akiyama. Exergy analysis of self-ignition combustion synthesis for producing rare-earth-basedhydrogen storage alloy. International Journal of Hydrogen Energy 37 (2012): 9706.

Chapter 6

General Conclusions

As a main industry in the world, the iron and steel industry is facing serious problem related to limited resources and expensive price of high grade iron ore used to produce good quality of iron and steel. The industry is also one of the second most energy-intensive industries in the world which contribute to almost 5% of world energy consumption. In addition, excessive utilization of fossil fuel causes this industry as biggest contributor to global CO2 emission. The proposed process, CVI ironmaking offered solution of the problem related to resource, energy and environment simultaneously. The proposed process consists of three main steps as follow: (1) production of porous material, (2) production of iron/carbon composite, (3) Oxidation/reduction of CVI ore. This thesis focused on the second step which is critical and controls the process to produce CVI ore. This step consists of integrated pyrolysis-tar decomposition over low grade ore. The dehydrated of low grade ore which porous material was utilized as carbon storage and catalyst of tar decomposition. This method presented several benefits such as effective utilization of low-grade iron ore and low rank coal/biomass, close arrangement of carbon and iron ore which gives fast iron reduction reaction. Several important parameters were discussed in this study such as various porous material, different carbon source, optimum temperature, and microstructure as well as exergy analysis. A summary of each chapter is given below.

Chapter 1 provided the general introduction and a description of the purpose of this thesis.

Chapter 2 describes detail evaluation of CVI ironmaking process using low grade ore as carbon storage and catalyst of tar decomposition. The low grade ore shows significant effect on tar decomposition process to enhance carbon deposition and total gas product. The tar amount from pyrolysis was strongly affected on carbon deposition which bituminous, high grade coal produced highest carbon deposition due to large tar product. Beside tar amount, surface area and pore volume also played important role in this process. The Hamersley ore which possess larger combined water obtained higher content of deposited carbon compared to Robe-river ore. Larger combined water created more pore size less than 4 nm, which was suitable for carbon deposition. The carbon infiltrated and deposited effectively within nanopores which was formed during the dehydration of combined water. The amount of carbon deposition was proportional with the decreasing of surface area and pore volume.

High-temperature pyrolysis generated large amounts of volatile matter (tar and gases), which caused high tar decomposition and produced large amounts of carbon deposition and gases. The deposited carbon was the major product of tar decomposition at lower temperatures (400–600 °C), whereas gases were mainly produced at higher temperatures (700–800°C), due to carbon gasification. However, sintering started at 800°C, and it significantly diminished the BET surface area and pore size distribution. The highest amount of deposited carbon was obtained at pyrolysis temperature of 800°C and a tar decomposition temperature of 600°C. In addition to decomposition process, the indirect reduction of iron ore simultaneaously happened to produce Fe_3O_4 at 600^oC and FeO at 800^oC. As product of CVI process, the reduction of CVI ore began at 750°C, while that of the reference mixture of Fe_3O_4 and coke started at 1100°C. The material exhibited higher reactive due to nanoscale contact between iron ore and carbon.

In the chapter 3, the kinetic analysis and carbon deposition phenomenon of tar decomposition over low grade ore were evaluated to understand the CVI process. Both kinetic constant and deactivation factor were evaluated successfully using simple proposed model with range of 0.13 – 0.55 s^{-1} and 1.72 – 2.53 s^{-1}, respectively at 500-700^{o}C with the activation energy of 44.86 kJ/mol. The deactivation factor exhibited similar tendency to amount of carbon deposition within pores iron ore. In the experiment, the decomposition of lignite tar exhibited similar profiles of H_2 and CO generation which was rising shortly after starting the experiment because ore catalyst still owned high activity and no carbon poisoning. However, the excessive carbon deposition was also simultaneously occurred in the beginning of experiment and caused deactivation of ore catalyst.

Chapter 4 studies the characteristic of the CVI product related with the microstructure of porous ore and distribution of carbon deposition. Based on the TEM images, a layered structure about 3-nm-diameter pores was observed after dehydration, due to removal of the hydroxide (OH) group from FeOOH. This pore size was deemed to be appropriate for tar decomposition and resultant carbon deposition. However, it was found that not all pores were filled with carbon. Some deposited carbon partially blocks the pores, which negatively affects the carbon deposition process. In addition to ore structure, the type of carbon deposited was also successfully evaluated using Raman spectroscopy. The position of G peak was found to shift slightly, indicating that the sp3 content was reduced at elevated temperatures due to a greater degree of graphitization. The carbon deposition by CVI process over low-grade ore was categorized as amorphous carbon (a:C), with an sp3 content of 19–21%. These results can also be explained by high reactivity of the deposited carbon, which was improved not only by nanoscale contact between iron and carbon but also by specific molecule bonding and arrangement of amorphous carbon.

Chapter 5 describes exergy analysis and feasibility study on the application of CVI process in the ironmaking industry. The CVI process was significantly increased exergy content of iron ore by tar decomposition and carbon deposition. In the basis of 3.86%mass carbon deposition (experimental value) and producing of 1000 kg metallic Fe, the exergy loss of the proposed system was found to decrease by about 16.7% compared to that of conventional systems by the recovery of both chemical and thermal tar exergy. The exergy loss drastically decreased to 37.0% when the expected carbon deposition was attained (10%mass). The CVI ore offered great chance to replace the coke breeze as a heat source in sinter plant. Regarding to experimental value, the sinter plant could be operated without using additional coke breeze when the CVI ore content was 70% to total input ore. The total enthalpy of CVI ore consisted of the oxidation of deposited carbon and Fe_3O_4 in the ratio of 60.2% and 39.8%, respectively.

Acknowledgements

This research had been carried out under the supervision of Prof. Tomohiro Akiyama, director of the Center for Advanced Research of Energy and Materials, Hokkaido University. First, I would like to express my sincere gratitude for his continuous and practical guidance and positive encouragements throughout this research. I really appreciate that he has always provided great opportunities for me to make professional progress.

I also would like to extend my gratitude to each committee, Prof. Kazuhiko Iwai and Prof. Mikito Ueda who reviewed this doctor thesis, for his valuable comments and helpful advice.

I appreciate Gadjah Mada University (UGM) and ASEAN University Network (AUN) - JICA for providing the chance and scholarship for my study in Hokkaido University, Japan.

I am grateful to my co-researchers: Dr. Sou Hosokai, Dr. Yuuki Mochizuki, Dr. Takahiro Nomura, Dr. Naoto Yasuda, Dr. Genki Saito, Ms. Alya Nail Rozhan, Ms. Othman Nur Ezzah Faezah. I would never have carried out all this study without their kind help and valuable discussion. I also wish to express my thanks to all the members in the laboratory for kind help and encouragement.

Finally, I would like to express my sincere thanks to my wife, Hetty Purwaningrum and beloved son, Putra Rabbani Cahyono as well as members of my family who have always provided spiritual support to me.